MODELING, SIMULATION, AND CONTROL OF GAS TURBINES

by

ALBERT LEE MARKUNAS

B.S., Illinois Institute of Technology
(1969)

SUBMITTED IN PARTIAL FULFILLMENT

OF THE REQUIREMENTS FOR THE

DEGREE OF MASTER OF

SCIENCE

at the

MASSACHUSETTS INSTITUTE OF TECHNOLOGY

June, 1972

Signature of Author.. .....
Department of Mechanical Engineering
May 11, 1972

Certified by.. .....
Thesis Supervisor

Accepted by.....
Chairman, Departmental Committee on Graduate Students

MODELING, SIMULATION, AND CONTROL OF GAS TURBINES

by

ALBERT LEE MARKUNAS

Submitted to the Department of Mechanical Engineering on May 12, 1972 in partial fulfillment of the requirements for the degree of Master of Science.

ABSTRACT

A textbook type treatment of the mathematical modeling of gas turbines is presented. This treatment starts from basic physical principles to develop a modeling technique that can be used to model any type of gas turbine to almost any practical degree of complexity desired.

A simple engine configuration is modeled and used to investigate some of the problems associated with the computer simulation of gas turbines. In particular, a crude, first-cut hybrid simulation is developed within the limits of the Mechanical Engineering IBM 1130-EAI 680 computer facility.

Some basic concepts of gas turbine fuel control philosophy are discussed and are used to design a fuel control for the gas turbine configuration analyzed. This control is used to close the fundamental speed control loop of the engine and allows the closed loop dynamic behavior of a single shaft, simple cycle gas turbine to be explored.

Thesis Supervisor: Henry M. Paynter
Title: Professor of Mechanical Engineering

ACKNOWLEDGEMENTS

The author wishes to express his appreciation to Professor Henry M. Paynter, who served as thesis supervisor. Professor Paynter proved to be a source of constant inspiration, a source of expert guidance, and a seemingly never ending source of knowledge and information.

Special appreciation goes to my wife, Sue, whose love and understanding made the successful completion of this thesis possible.

TABLE OF CONTENTS

NOMENCLATURE

a	local sonic velocity
A	cross sectional flow area
A_s	effective heat transfer area
A_w	wall energy storage volume per unit length
c_p	specific heat at constant pressure
c_v	specific heat at constant volume
c_w	specific heat of wall material
C	fluid mechanical capacitance
C_T	fluid thermal and general thermal capacitance
C_{TW}	wall thermal capacitance
C_w	wall fluid mechanical capacitance
C_i , $i=1,\cdots,6$	full scale turbomachinery coefficients
D	linear dimension of turbomachine
F_{ij}	linear gas turbine state matrix element
f	general function operator
g	acceleration of gravity
g_c	gravitation conversion constant
G_{ij}	linear gas turbine input matrix element
h	overall heat transfer coefficient
h	static enthalpy
h_o	total enthalpy

$h_{L.HV}$	lower heating value of fuel
H_o	total fluid head
j	square root of -1
I_R	rotary inertia
I_F	fluid inertance
k_i , $i=1,\cdots,s$	fuel control parameter
L	length of flow passage
$\dot{m}$	mass flow
M	Mach number
n	polytropic constant
N	rotational speed
$N_{G\ set}$	fuel control speed setting
p	static pressure
p_o	total pressure
P_F	fluid power transfer
P_M	mechanical power transfer
P_T	thermal power transfer
q	heat flow
R	gas constant
R_{TW}	overall wall thermal resistance
R_W	fluid resistance to wall storage
s	Laplacian operator
t	time
T	static temperature
T_o	total temperature

Te	propagation operator
U	internal energy
V_x	axial velocity
V	velocity
$Vol.$	lumped parameter fluid volume
X	axial dimension
XNC	scaled compressor corrected speed
XNT	scaled turbine corrected speed
XTQC	scaled compressor corrected torque
XTQT	scaled turbine corrected torque
XWC	scaled compressor corrected flow
XWT	scaled turbine corrected flow
Z	height above datum
Z_c	characteristic impedance
β	variable geometry parameter
γ	ratio of specific heats
Δ	perturbation operator
μ	absolute viscosity
ϕ, ψ, μ	linear turbomachine coefficients
ρ	static density
σ	ratio of wall to fluid stream thermal energy storage per unit length
τ	torque
τ_1, τ_2	wall energy storage constants
ω	radian frequency

LIST OF FIGURES

TO MY MOTHER AND TO THE

MEMORY OF MY FATHER

CHAPTER I. INTRODUCTION

Gas turbines today represent a significant percentage of prime movers used as a source of power and propulsion. Due to the inherently more efficient nature of the combustion processes associated with gas turbines and their relatively high power to weight ratio this percentage could increase rapidly in the near future. In moderation of these rather marked advantages gas turbines have some very distinct disadvantages associated with them, which must be improved before they are to find more universal acceptance as prime movers. Foremost among these disadvantages are the high costs associated with the design and development of gas turbines and the associated control systems.

The design of gas turbines of necessity entails considerable expenditures of both time and money. The larger the power output and the more demanding the performance specifications become the larger are the expenditures. Performance evaluation and control systems development represent a large portion of the overall investment and require the dynamic performance characteristics of the engine for successful execution. Due to the complex nature and long lead times associated with engine development it is not practical or desirable to wait until a prototype engine is ready for testing

to obtain dynamic performance information. Parallel operation of performance evaluation and control systems development with the overall design process is a necessity.

Modern day gas turbine control systems are suffering from an abundance of ills. Increasing engine complexity and performance specifications are placing an ever increasing demand on the performance of state of the art fuel controls that were conceptually developed more than twenty years ago. High performance gas turbines are being designed closer to safe operating limits and when something goes wrong the control hardware is sure to be blamed. Fuel control design and development is typically carried out by a separate company using specifications dictated by the engine manufacturer. This tends to isolate the control engineers from the dynamic operating characteristics of the engine and the gas turbine performance engineers from the dynamic operating characteristics of the control, resulting in a rather inefficient approach to solving the gas turbine control problems. In addition to this the cost of the fuel control represents an ever increasing portion of the overall engine cost as the engine size is decreased. In the low power engines the cost of the fuel control can approach and

sometimes exceed one-third of the overall cost. It seems rather obvious that a better understanding of the operating characteristics of gas turbines and the gas turbine-control systems interactions is necessary to enable the development of more efficient, low cost control systems.

Mathematical modeling and computer simulation of gas turbine performance can prove invaluable in obtaining solutions to the problems stated. An improved understanding of engine dynamics and control problems is possible without endangering a valuable engine. Use of this information allows performance evaluation and control systems development to be carried out in parallel with the overall design process, resulting in savings in both time and money. If enough attention is paid to detail in the mathematical modeling of the gas turbine the resulting model could provide new insights into the basic control problem, possibly leading to simpler and more efficient control systems.

Any attempt to read the literature on the subject will disclose a multitude of reasons and statements supporting the use of modeling and simulation of gas turbine performance in engine and control systems design and development. The value has been previously established and need not be further developed.

A. Brief Review of Past Work

Modeling and simulation of gas turbines is far from being new, with work existing as early as 1949 (3) and probably earlier. Although no attempt was made at a complete literature search, some general trends and classifications are evident.

Just as with other physical systems, the dynamic modeling of gas turbines can be grouped into two distinct groups. Functional modeling treats the gas turbine as a black box and uses engine response data to develop a transfer function description of the engine in terms of a few selected variables of interest, typically fuel flow, rotational speed, and output torque or power. Physical modeling starts from the actual engine characteristics and using simplified physical principles develops a mathematical description of the engine.

The work of Oldenburger(4) and Ahlbeck(5) illustrates the classical transfer function approach to system modeling. This black box type of description of gas turbine dynamics is of necessity limited to small perturbations about some steady state operating point. While such a model can be very useful in control and

Numbers in parentheses refer to references listed in the Bibliography.

stability studies of the gas turbine system it has serious shortcomings when applied to large scale engine transients and studies of more than one engine. While some qualitative trends can be distinguished in the transfer function parameters, these parameters must in general be determined experimentally for each new engine to be studied.

The physical modeling of gas turbines can be subdivided into linear or perturbation modeling and nonlinear modeling. The types of physical models also vary considerably in the degree of aerodynamic and thermal transient effects considered. The minimum dynamic model of any gas turbine includes rotor dynamics only.

Marscher(6) presents a fairly extensive study of linear gas turbine dynamics completely neglecting all dynamics except the rotor dynamics. Sarantsev(7) includes aerodynamic and thermal dynamics in a somewhat brief description of a perturbation model. These perturbation models are again very useful for stability and control studies.

Larrowe and Spencer(8) present a study of nonlinear gas turbine dynamics which can be used for large scale transients. Only rotor dynamics are included in the analog simulation. The necessary nonlinear character-

istics are implemented using bi-variant function generators. Saravanamuttoo and Fawke(9) also present a nonlinear model of gas turbine dynamics. Minimal gas dynamic effects are included in their digital simulation as a means of avoiding algebraic loops. The analog simulation considers only rotor dynamics. All nonlinear characteristics are implemented digitally by table look-up and analog wise by means of diode function generators.

Paynter(2) presents a fairly thorough study of gas turbine dynamics that includes both nonlinear and gas dynamic effects. The nonlinear characteristics are linearized in intervals and the results used to digitally implement a stepwise linear model of the system. Such a model can be used to predict steady state operation and large scale transients in addition to control and stability studies. The stepwise linear characteristics are obtained from a table look-up.

Willoh and Seldner(10) use a very sophisticated analog computer facility to implement a model of an axial flow compressor. Nonlinear characteristics are represented on a per stage basis using diode function generators. Aerodynamic effects are also included on a per stage basis. Such a model provides an extremely good description of axial flow compressor dynamics.

This compressor model is used as part of a complete engine model used by Seldner and Gold(11) in their study of a low cost fuel control for a jet engine.

Physical models have been used almost exclusively in recent studies of gas turbine dynamics. This is due to the fact that the parameters used in physical models are defined in terms of actual engine parameters and steady state operating characteristics. Thus, a given model or simulation can be very easily modified to account for changes in a particular engine as its development progresses, or for general studies of a given type of gas turbine.

B. Problem Statement

In consideration of Paynter's work (2) and the work of Willoh and Seldner (10) it is evident that modeling and simulation of gas turbine dynamics has reached a fairly advanced state. However, work such as that of Rubis and Bodnaruk (12) as recently as 1970 points out the lack of general competence and understanding in good modeling techniques and/or the inability to implement the computer simulations of the resulting models. Clearly, work must be done to further the understanding of the above mentioned modeling techniques and an effort must be made to discover new and improved methods of computer simulation.

Mathematical modeling of gas turbine dynamic performance has to follow some fairly rigid guidelines in order to provide useful models.

i) The model must be capable of predicting steady state performance. Not much confidence should be placed in dynamic performance predicted from a model that can't predict steady state results within reasonable limits.

ii) The model should be as simple as possible and still be able to describe the dynamic operation of interest. Increasing model complexity without providing an attendant increase in engine description is worthless.

iii) The model should be derived from basic physical principles. Since a valid model can't defy these basic principles it seems logical, if not necessary, to start from basic principles.

iv) The model should be easily adaptable to account for design and engine changes.

v) The modeling techniques should be such that almost any degree of engine description is readily achievable.

In a similar manner the computer simulation techniques should be constrained to provide more useful results. Because the modeling and simulation problems

are directly coupled, the simulation method, techniques, speed, and cost are more or less dictated by the particular model used. Nevertheless, any computer simulation should try to follow some general guidelines.

i) The simulation should be as efficient as possible in terms of time and money. As model complexity is increased the amount of computer hardware required (either digital or analog) increases fantastically. Seemingly small savings can be amplified greatly.

ii) The simulation results should be accurate and repeatable.

iii) The simulation techniques and hardware used should not be so sophisticated as to preclude general applicability.

The rather nebulous guidelines proposed are certainly not the governing factors in every case. Particular circumstances will almost surely dictate to a certain degree what simulation techniques are to be used and the resulting model complexity attainable.

C. Scope of Thesis

This thesis in a very limited manner was designed to address the previously stated problems. The scope of this thesis is threefold. First of all, a textbook type treatment of the modeling of gas turbine dynamics

is presented. This treatment starts from first principles to develop a modeling technique that can be used to model any type of gas turbine to almost any practical degree of complexity desired. The development closely follows that of Paynter (2) in many ways.

Secondly, a very simple engine configuration is modeled and used to explore some of the problems associated with the computer simulation of such a system. In particular, a fairly crude hybrid computer simulation is developed within the limits of the MIT Mechanical Engineering computer facility.

Thirdly, some aspects of gas turbine control philosophy and methods of implementation are discussed and the computer simulation mentioned above is used to explore the closed loop response characteristics of a simple cycle, single shaft gas turbine.

CHAPTER II. MODELING

A. General

1. Assumptions

The gas turbine engine is a very complex thermal-fluid-mechanical system. Even the simplest imaginable engine configuration is so complex that any attempt at finding a global description of the operation of such a system is doomed to failure. Obviously, simplifying assumptions have to be made and only significant overall behavior can be considered.

In this analysis the major underlying simplifications are the following:

i) The gas flow in the engine is assumed to be one-dimensional. All two-dimensional effects such as inlet distortion and compressor rotating stall are ignored.

ii) The distributed nature of the gas turbine is approximated by lumped parameter elements.

iii) The perfect gas assumption is carried throughout the analysis.

iv) The gas turbine is subdivided into its basic components and each of these is treated as a separate thermodynamic system.

v) The steady state thermodynamic performance of each component is assumed to be instantaneous.

vi) All dynamic effects are accounted for through the use of idealized dynamic lumped parameter elements.

Further, less significant assumptions are introduced as the development progresses.

2. Components

The concept of subdividing the gas turbine into its basic components is more or less fundamental in developing a generalized modeling technique. Irregardless of complexity all gas turbines may be subdivided into a limited number of components. These components can be imagined as physical building blocks from which any engine configuration may be constructed. In a similar manner the models of these components are mathematical building blocks from which the model of any gas turbine can be constructed.

One possible selection of basic components might be as follows:

i) Turbomachines

ii) Fuel Burners

iii) Diffusers, Ducts, and Nozzles

iv) Heat Exchangers

This is not the only selection possible, and it is certainly questionable if it is the best. Paynter (1) describes thermal-fluid components in terms of the umit

process involved: transduction, modulation, transmission, and exchange. The component selection listed above is used since it seems to define a natural division of the engine.

An example of this can be seen in figure 1, in which the simple cycle, single shaft gas turbine shown schematically is subdivided into its basic components. The classification of the components listed into the four basic groups is obvious.

3. Power Transfer

Since all gas turbines are energetic systems any attempt to describe the operation of such a system must start from energy considerations. The energy flow or power transfer associated with the various gas turbine components may be classified into three main groups:

i) Mechanical Power Transfer

ii) Pure Thermal Power Transfer

iii) Fluid Power Transfer

Mechanical power transfer is associated with the shafts connecting the various rotating components and any inputs and outputs that may be present. Mechanical power transfer is defined as:

$$P_M = \left(\frac{30}{\pi}\right) \cdot \tau \cdot N \qquad 1)$$

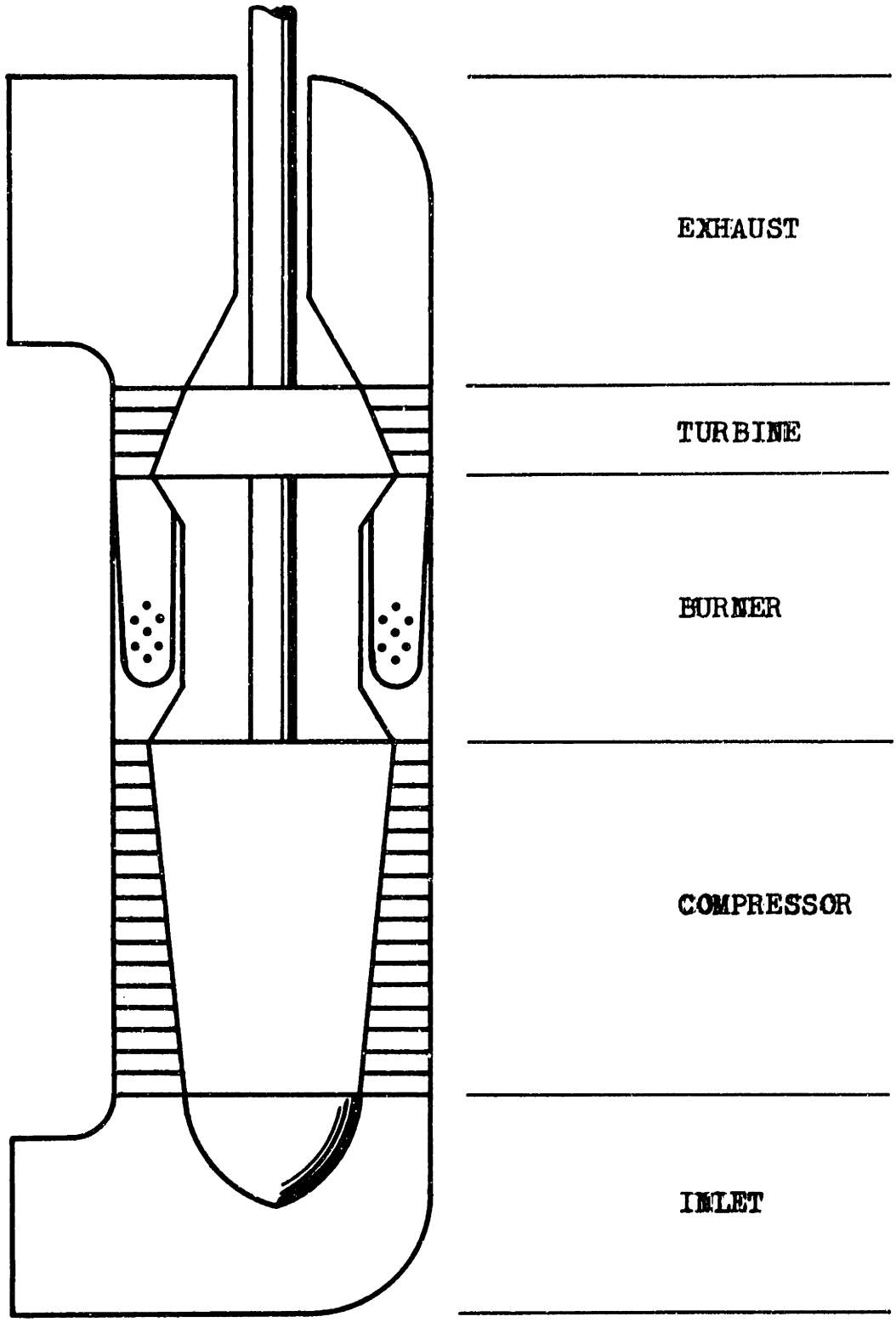

Figure 1.

where,

P_M = mechanical power transfer in ft-lbf/sec

τ = torque carried by shaft in ft-lbf

N = rotational speed of shaft in rpm's

A convenient representation for this power transfer is provided by the bond graph structure in the form of the single, acausal power bond shown. (See reference 13 for a discussion of bond graphs)

$$\frac{\tau}{N}$$

Pure thermal power transfer is simply the heat flow into and out of the various fluid streams and any metal parts present.

$$P_T = q = \left(\frac{q}{T}\right) \cdot T \qquad 2)$$

where,

P_T = thermal power transfer in ft-lbf/sec

q = heat flow in ft-lbf/sec

T = absolute temperature in °R

This may be represented by the following bond graph structure:

$$\frac{T}{q}$$

The variables ϕ and T do not strictly represent power variables, but it is useful to associate them as a pair.

Fluid power transfer is associated with the main gas stream, the fuel flow, and any secondary fluid streams present.

$$P_F = \dot{m} \cdot H_o \qquad 3)$$

where,

P_F = fluid power transfer in ft-lbf/sec

$\dot{m}$ = mass flow of fluid stream in lbm/sec

H_o = total head of fluid stream in ft-lbf/lbm

This may be further developed by considering the content of H_o.

$$H_o = u + \frac{p}{\rho} + \frac{v^2}{2g_c} + z \cdot \frac{g}{g_c} = h_o + z \cdot \frac{g}{g_c} \qquad 4)$$

where,

h_o = total enthalpy in ft-lbf/lbm

u = internal energy in ft-lbf/lbm

p = static pressure in lbf/ft^2

ρ = static density in lbm/ft^3

v = mean velocity in ft/sec

z = height above some datum in ft

g = acceleration of gravity in ft/sec^2

g_c = conversion factor $\cong$ 32.2 ft-lbm/lbf-sec^2

For most practical cases of gas turbine analysis the effects of height changes are negligible. By imposing a suitable equation of state and flow continuity, and assuming that internal energy is a point function of temperature the expression may be further simplified.

$$h_o = f_1(p, \dot{m}, T) \qquad 5)$$

Thus, the fluid power transfer may be expressed as (1):

$$P_F = \dot{m} \cdot f_1(p, \dot{m}, T) = f_2(p, \dot{m}, T) \qquad 6)$$

Since turbomachinery is defined in terms of total fluid properties, a description of fluid power transfer in terms of total fluid properties is desirable.

$$p_o = f_3(p, \dot{m}, T) \qquad 7)$$

$$T_o = f_4(p, \dot{m}, T) \qquad 8)$$

Thus,

$$P_F = f(p_o, \dot{m}, T_o) \qquad 9)$$

where,

p_o = total pressure in lbf/ft^2

T_o = total temperature in $^\circ R$

Fluid power transfer may be represented in bond graph form by means of the double, acausal power bond shown.

$$\frac{p_o}{\dot{m}}$$

$$\frac{}{T_o}$$

Again the variables indicated on the bond graph do not strictly represent power variables, but the association is useful.

The variables p_o and $\dot{m}$ primarily determine the fluid-mechanical power transfer, while the variables $\dot{m}$ and T_o primarily determine the fluid-thermal power transfer. In general there is coupling between the two processes.

Using this bond graph notation a gas turbine can be represented by its basic components and the different types of power transfer associated with the components. This is done in figure 2 for the gas turbine of figure 1. The boxes represent the overall thermodynamic performance of the components, and include dynamic as

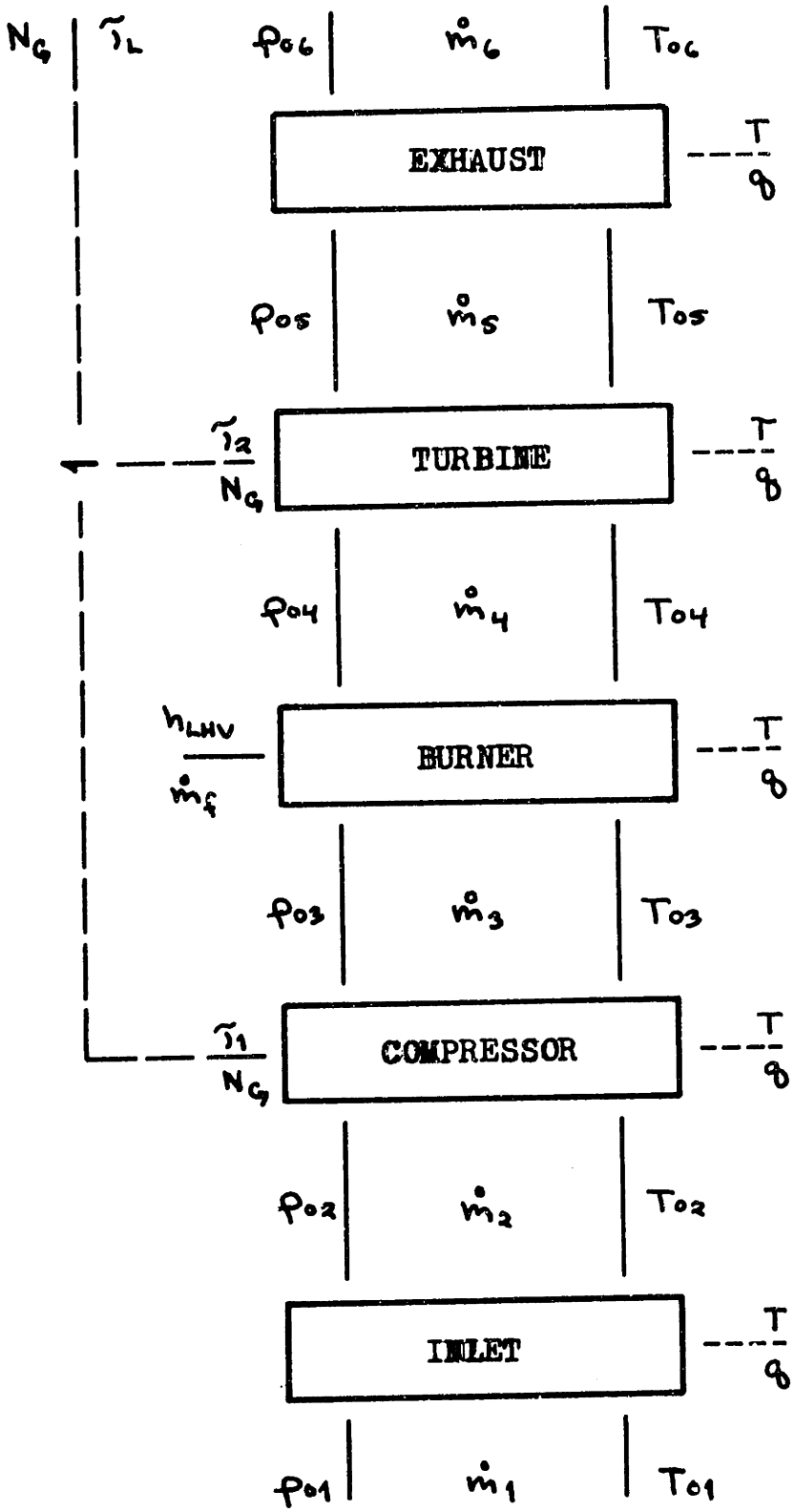
N_G
τ_L
p_{o6}
$\dot{m}_6$
T_{o6}
EXHAUST
$\frac{T}{q}$
p_{o5}
$\dot{m}_5$
T_{o5}
$\frac{\tau_2}{N_G}$
TURBINE
$\frac{T}{q}$
p_{o4}
$\dot{m}_4$
T_{o4}
$\frac{h_{LHV}}{\dot{m}_f}$
BURNER
$\frac{T}{q}$
p_{o3}
$\dot{m}_3$
T_{o3}
$\frac{\tau_1}{N_G}$
COMPRESSOR
$\frac{T}{q}$
p_{o2}
$\dot{m}_2$
T_{o2}
INLET
$\frac{T}{q}$
p_{o1}
$\dot{m}_1$
T_{o1}

Figure 2.

well as steady state behavior.

4. Generalized Element

A generalized component may be represented by means of the acausal bond graph of figure 3. In this component all three types of power transfer are present as well as the single steady state characteristic and the three simplified dynamic elements. If nothing else, this type of structure forces the model to accurately describe steady state performance when all dynamic effects die away.

The accuracy with which this model represents the actual component depends, in general, on the operating frequency range of interest. As the frequency is increased the steady state characteristics of the component have to be subdivided with an attendant increase in dynamic elements. By making the model sufficiently granulated it is possible to represent the performance of any component to any practical degree of accuracy desired. Thus, it would be more appropriate to consider the structure of figure 3 as a generalized element, where the number of elements contained in the model of a component is dependent on the frequency range of interest. Clearly, the simplest model of a component would contain only one element and would be applicable for low frequency operation only.

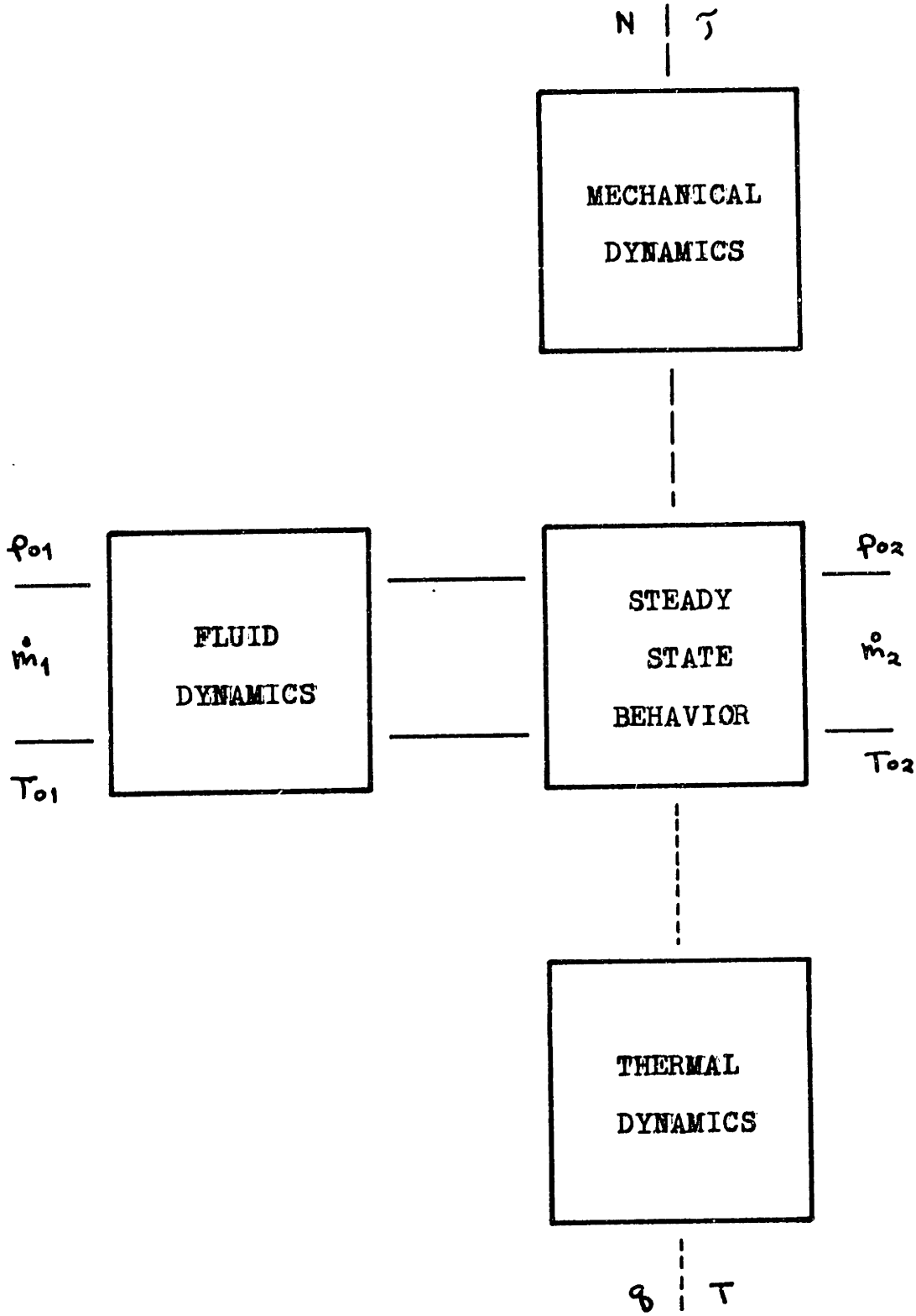
N | τ
MECHANICAL DYNAMICS
p_{o1}
$\dot{m}_1$
T_{o1}
FLUID DYNAMICS
STEADY STATE BEHAVIOR
p_{o2}
$\dot{m}_2$
T_{o2}
THERMAL DYNAMICS
q | T

Figure 3.

B. Steady State Performance

1. Turbomachines

a. Nondimensional Representation

In describing the steady state performance of a turbomachine it is generally assumed that transverse heat losses are negligible, which is substantiated in practice. Applying similitude constraints or using dimensional analysis, and assuming the causality shown,

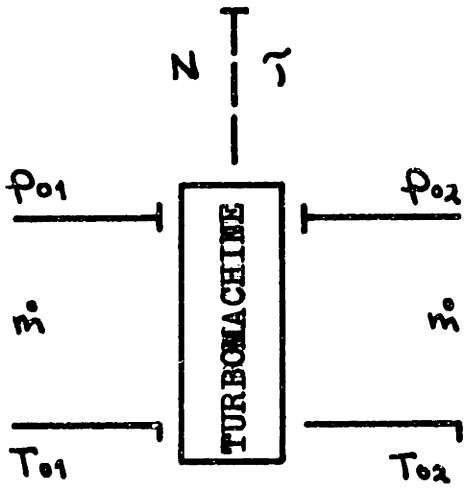

the steady state performance of any turbomachine passing a compressible fluid can be described by the following functions of dimensionless groups (14):

$$\frac{\dot{m}\sqrt{g_c R T_{o1}}}{p_{o1} D^2} = f_4\left(\frac{p_{o2}}{p_{o1}}, \frac{ND}{\sqrt{g_c R T_{o1}}}, \frac{\dot{m}}{\mu D}, \gamma, \beta\right) \quad 10)$$

$$\frac{T_{o2}}{T_{o1}} = f_5\left(\frac{p_{o2}}{p_{o1}}, \frac{N \cdot D}{\sqrt{g_c R T_{o1}}}, \frac{\dot{m}}{\mu D}, \gamma, \beta\right) \quad 11)$$

$$\frac{\tau}{p_{o1} \cdot D^3} = f_6\left(\frac{p_{o2}}{p_{o1}}, \frac{N \cdot D}{\sqrt{g_c R T_{o1}}}, \frac{\dot{m}}{\mu D}, \gamma, \beta\right) \quad 12)$$

where,

$\dot{m}$ = mass flow through the turbomachine in lbm/sec

p_{o1} = inlet total pressure in lbf/ft^2

p_{o2} = outlet total pressure in lbf/ft^2

T_{o1} = inlet total temperature in °R

T_{o2} = outlet total temperature in °R

τ = output torque of turbomachine in ft-lbf

N = speed of rotation in rpm's

D = characteristic linear dimension in ft

R = gas constant in ft-lbf/lbm-°R

μ = absolute viscosity in lbm/ft-sec

$\frac{\dot{m}}{\mu D}$ = a Reynolds number

γ = ratio of specific heats

β = variable geometry parameter

If the gas is specified, and the particular machine is specified, and all variable geometries are operating on their normal schedules, and the Reynolds number is above some critical value the above representation may be simplified to the following functions of dimensionless and pseudodimensionless groups:

$$\frac{\dot{m}\sqrt{T_{o1}}}{p_{o1}} = f_1\left(\frac{p_{o2}}{p_{o1}}, \frac{N}{\sqrt{T_{o1}}}\right) \quad 13)$$

$$\frac{T_{02}}{T_{01}} = f_2\left(\frac{p_{02}}{p_{01}}, \frac{N}{\sqrt{T_{01}}}\right) \qquad 14)$$

$$\frac{\tau}{p_{01}} = f_3\left(\frac{p_{02}}{p_{01}}, \frac{N}{\sqrt{T_{01}}}\right) \qquad 15)$$

where,

$\frac{\dot{m}\sqrt{T_{01}}}{p_{01}}$ = corrected mass flow through the turbomachime

$\frac{T_{02}}{T_{01}}$ = total temperature ratio across the turbomachine

$\frac{\tau}{p_{01}}$ = corrected torque output of the turbomachime

$\frac{p_{02}}{p_{01}}$ = total pressure ratio across the turbomachine

$\frac{N}{\sqrt{T_{01}}}$ = corrected speed of rotation of the turbomachine

The above functions have to be determined experimentally and are usually supplied by the engine manufacturer in the form of performance maps or in tabular form. In addition the form of the functions as supplied by the manufacturer may be inverted or may use different dimensionless groups, such as isentropic efficiency. The transformation to the above form is straightforward.

A steady state energy balance through the turbo-

machine with positive signs corresponding to normal turbine operation results in:

$$\dot{m}\cdot(h_{o1}-h_{o2}) = \left(\frac{\pi}{30}\right)\cdot\tau\cdot N \qquad 16)$$

where h_o is the total enthalpy of the fluid stream in ft-lbf/lbm. This says that any two of the three previously given functions are sufficient to describe the steady state performance of a turbomachine. Choosing the corrected torque as dependent results in:

$$\frac{\tau}{p_{o1}} = \left(\frac{30\,c_p}{\pi}\right)\frac{\left(\frac{\dot{m}\sqrt{T_{o1}}}{p_{o1}}\right)\cdot\left(1-\frac{T_{o2}}{T_{o1}}\right)}{\left(\frac{N}{\sqrt{T_{o1}}}\right)} \qquad 17)$$

where c_p is the mean specific heat at constant pressure of the gas in ft-lbf/lbm- R.

Care must be exercised in applying the above result since limit problems can occur as the rotational speed approaches zero. For situations where starting torque is important the corrected torque characteristic must be defined explicitly. In view of this it might be more reasonable to take corrected torque as an independent variable instead of total temperature

ratio. This would solve the limit problem for turbines and might also prove to be a better representation for compressors.

b. Compressors

A typical compressor corrected flow characteristic is shown in figure 4. An inspection of this characteristic reveals the existence of what is commonly called the surge line or surge limit. This line defines the steady state limit between stable and unstable compressor operation. Any attempt to operate in the unstable region usually results in disaster.

This surge line only strictly applies in the limit of steady state operation. For dynamic operation (with time varying inputs to the compressor) the surge line departs from the steady state value (15). To provide an accurate description of the stability limit for high frequency inputs requires dividing the compressor into a number of elements each with its steady state characteristics and appropriate lumped parameter dynamics. Carried to the limit this process would yield one element for each compressor stage (10). This model would allow the prediction of compressor dynamics and instabilities for a wide range of inputs, such as diffuser buzz or possibly a shock wave.

Such a model would be far too complex to be

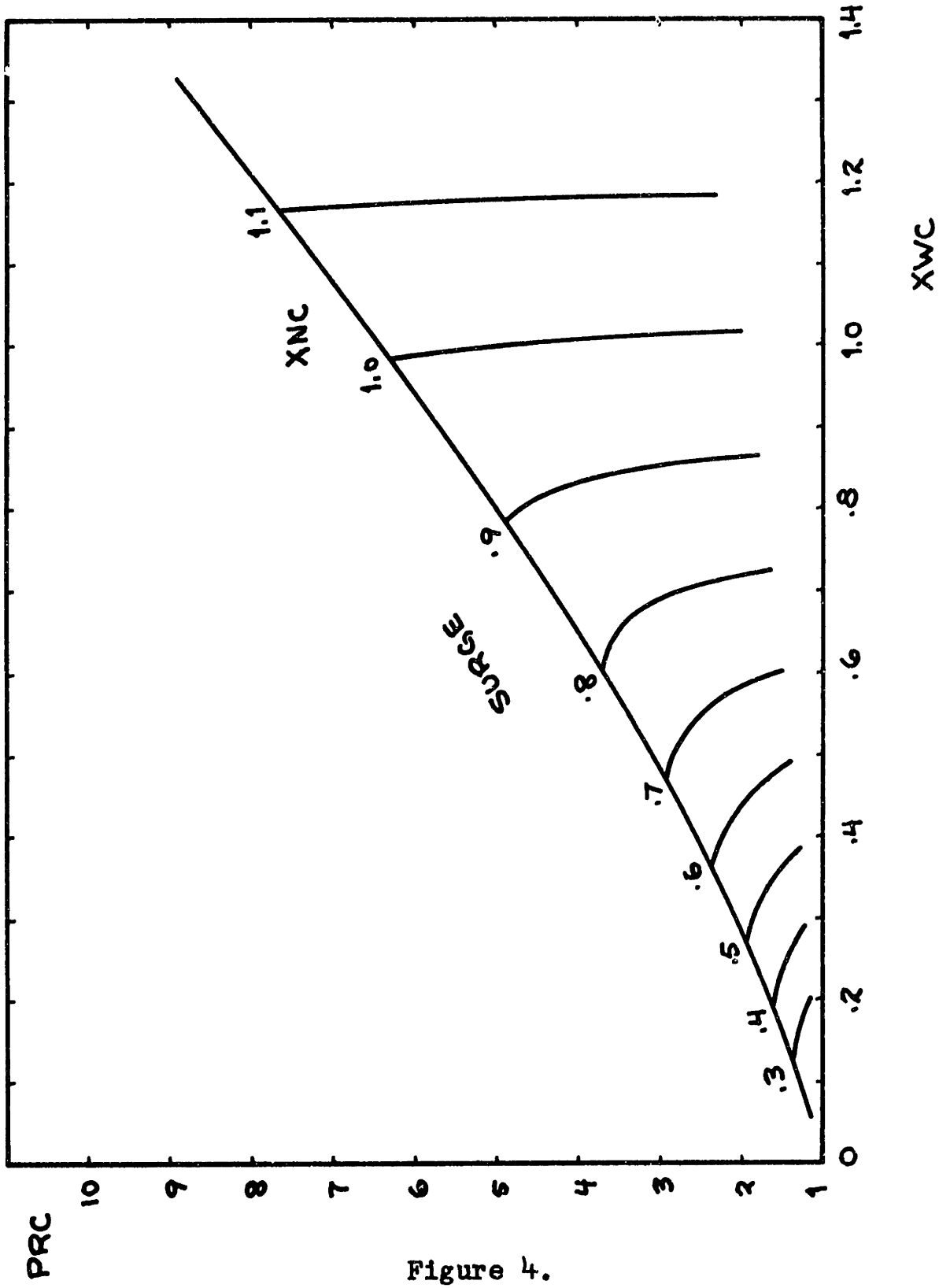

Figure 4.

useful in the overall model of a gas turbine, except for those cases with access to an extremely sophisticated computer facility. Fortunately, compressor operation is much more tolerant of rapidly changing inputs than of quasi-steady inputs, resulting in the steady state surge line being more critical than dynamic surge lines (15). This enables most problems to be adequately handled using the steady state stability limit, eliminating much of the complexity.

The above discussion completely neglects all two-dimensional effects in regards to compressor surge. Inlet distortion is probably the greatest single cause of compressor surge encountered in practice. A treatment of this phenomenon is beyond the scope of this thesis, but provides an area of possible future work.

The temperature ratio characteristic and the corrected torque characteristic of a typical compressor are shown in figures 5 and 6 respectively. The surge line is also present in both of these characteristics. The positive slopes of the corrected torque vrs. corrected speed curves can be used along with the corresponding slopes of the turbine corrected torque vrs. corrected speed curves to give some insight into the speed stability characteristics of the single shaft gas turbine.

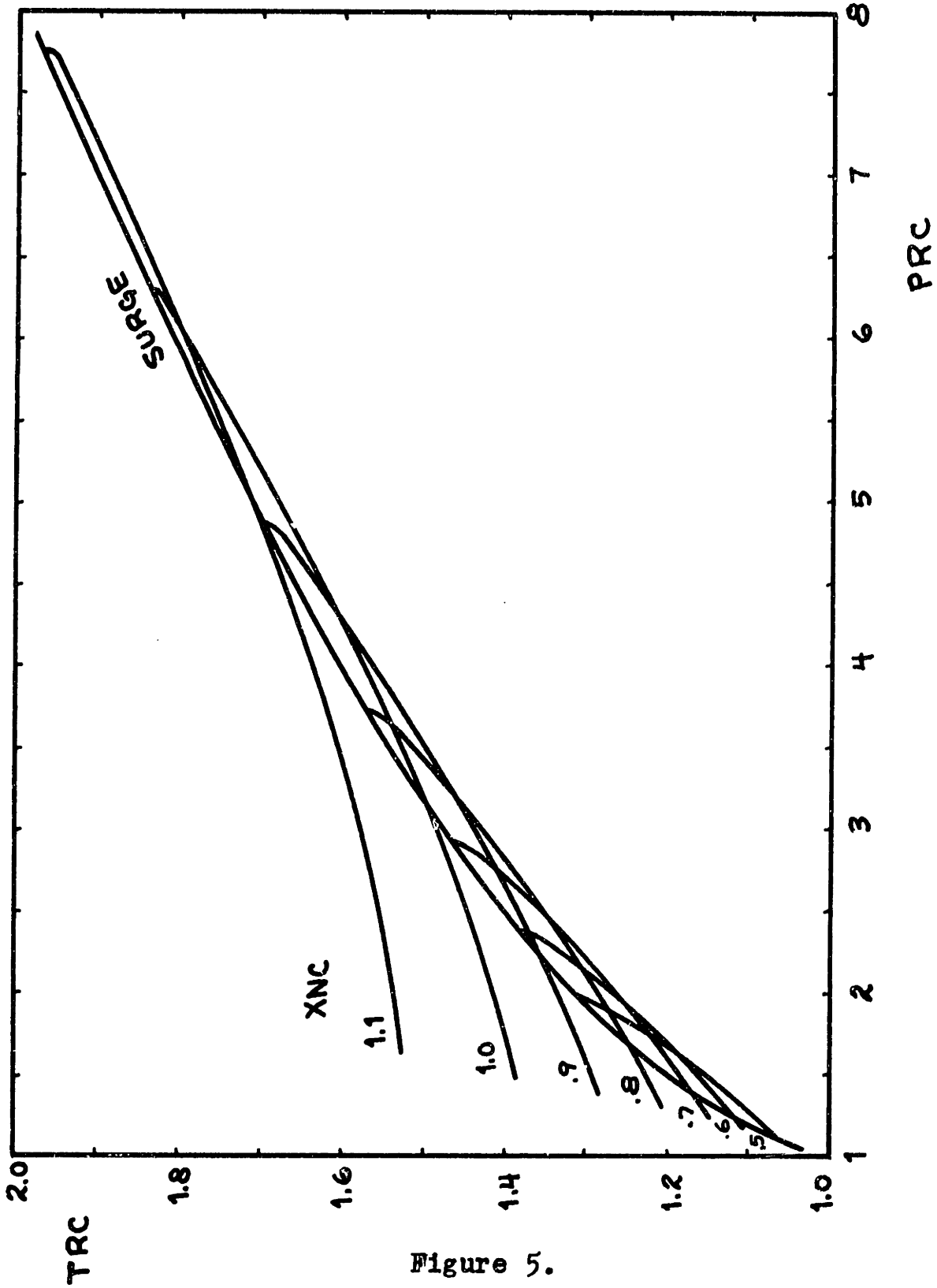

Figure 5.

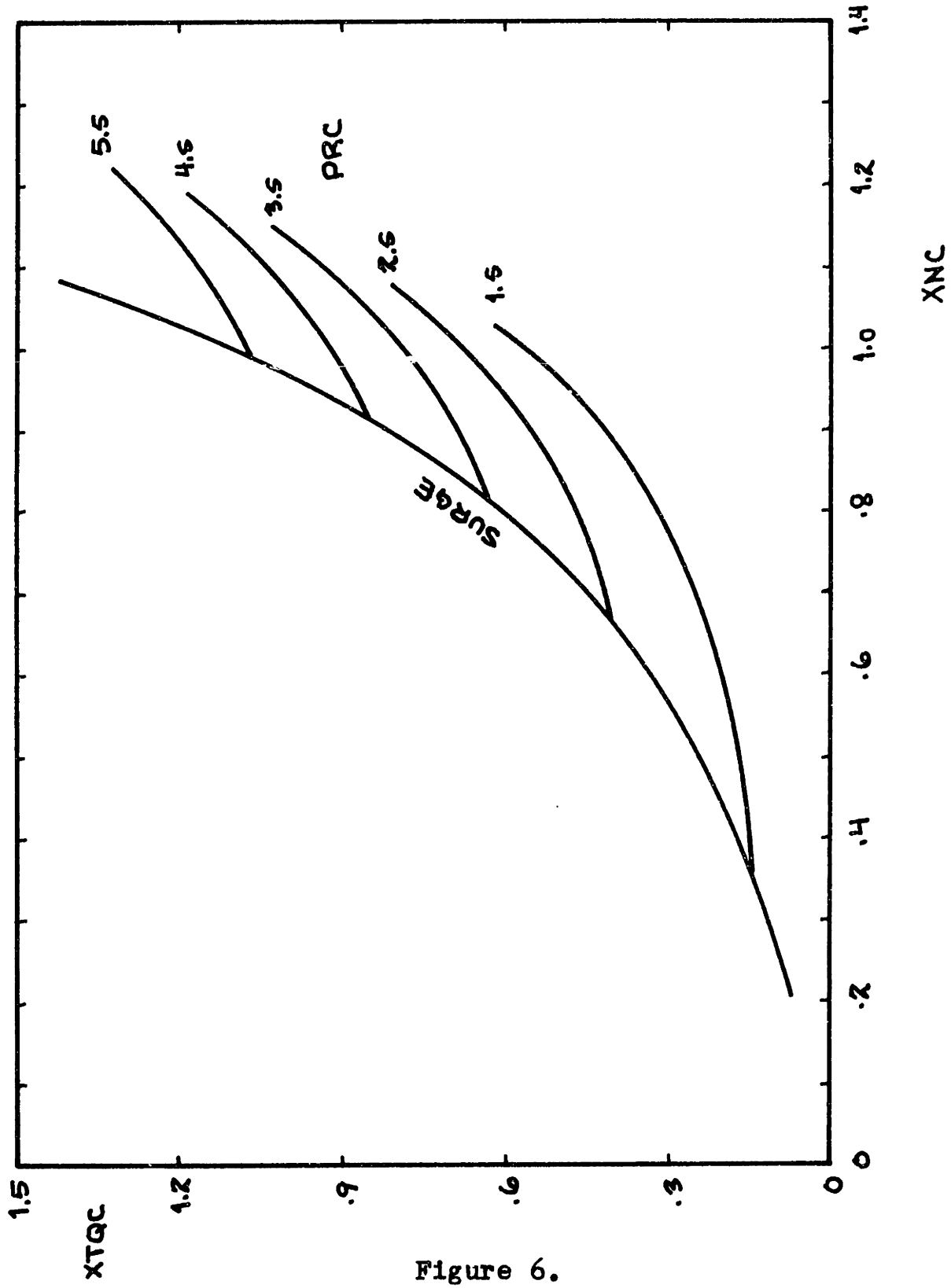

Figure 6.

c. Turbines

A typical turbine corrected flow characteristic is shown in figure 7. It is evident that the flow characteristics of a turbine are essentially those of the turbine nozzles. The flow chokes at low pressure ratios and the corrected flow vrs. pressure ratio curves have a very mild dependence on corrected speed. This result is sometimes used to provide a very simple model of a turbine in which the corrected speed has no effect on the flow characteristics.

One such simplified relation is commonly referred to as the "ellipse law" and can be expressed as (16):

$$\frac{\dot{m}\sqrt{T_{01}}}{p_{01}} = \text{const.}\sqrt{1-\left(\frac{p_{02}}{p_{01}}\right)^2} \qquad 18)$$

This relationship has its ancestry in steam turbine analysis and is more applicable there than in gas turbine analysis due to the lower pressure ratios typical of steam turbines.

The operation of a turbine does not have a stability or surge limit as does the compressor. The only dangers to safe turbine operation are excessive turbine inlet temperatures and excessive rotational speeds.

The typical temperature ratio and corrected torque characteristics of a turbine are shown in figures 8

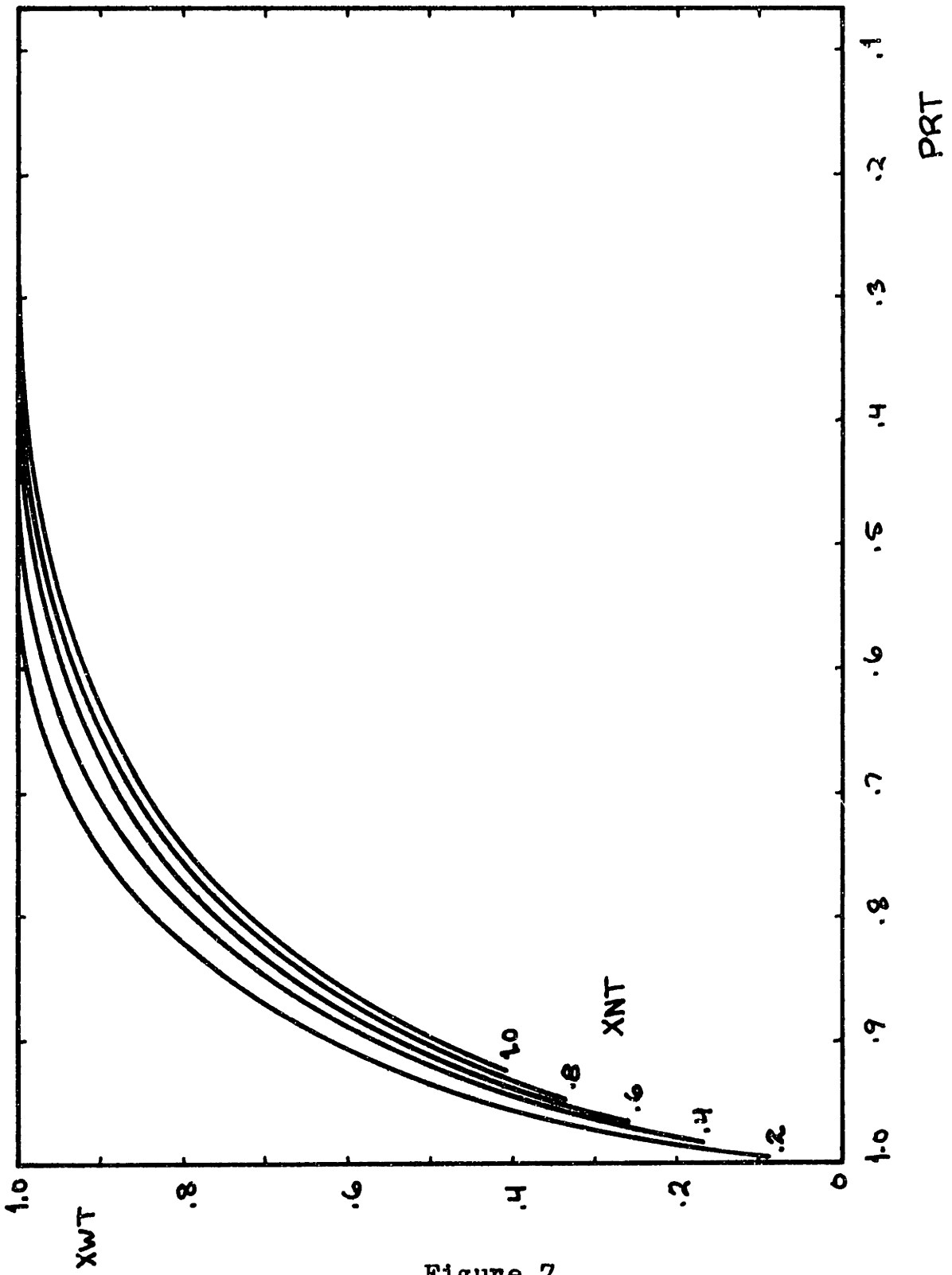

Figure 7.

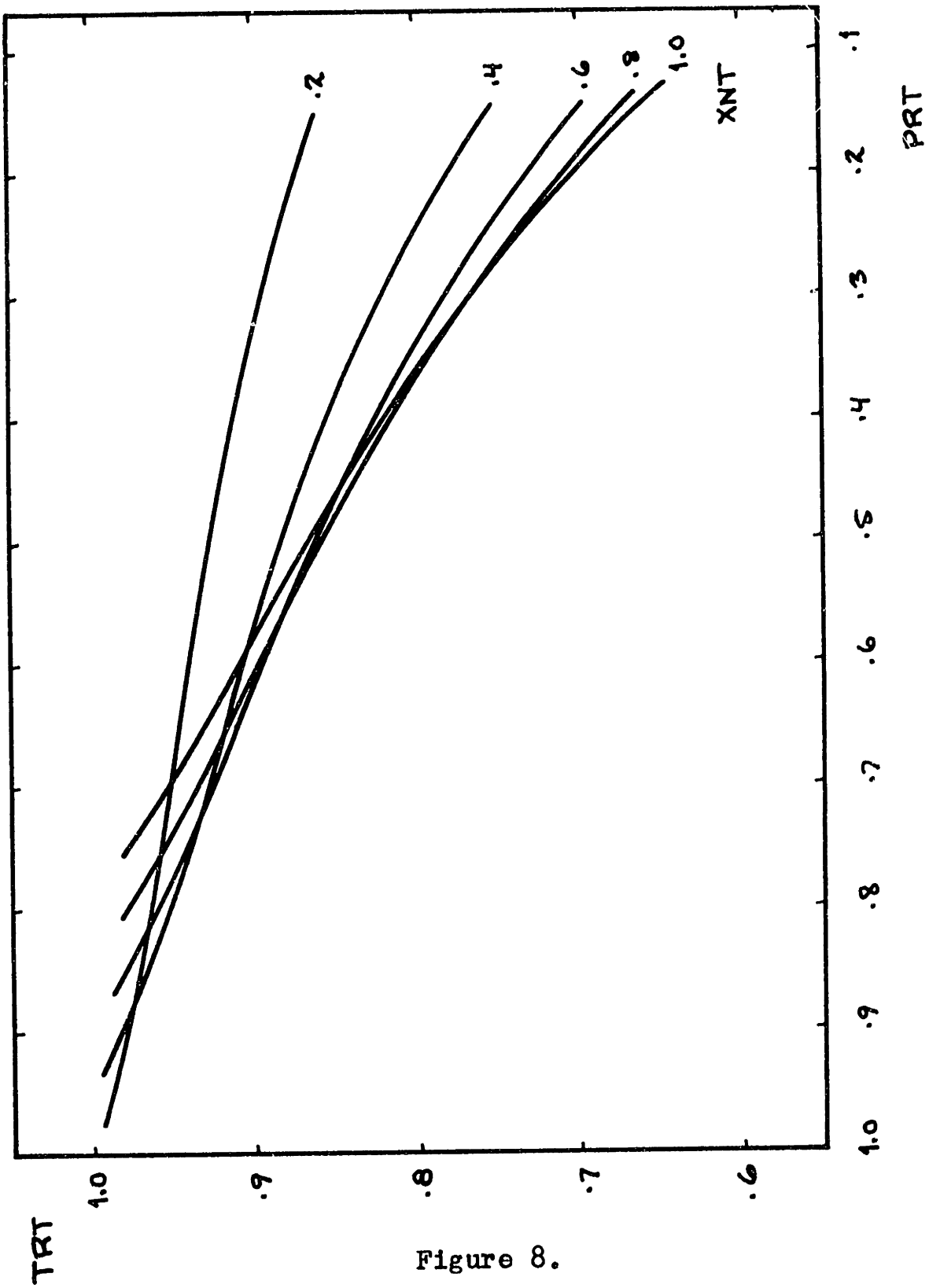

Figure 8.

and 9. The negative slopes of the corrected torque vrs. corrected speed curves for the turbine along with the positive slopes for the compressor exhibit the inherent stability of a single shaft gas turbine.

A turbine is typically much shorter axially than is a matched compressor. Thus, the one element model of the turbine is generally valid for much higher frequencies than is that of the compressor.

d. Linearized Turbomachines

The nonlinear steady state turbomachine characteristics previously presented can be linearized about some operating point. This is accomplished by expanding the functions in Taylor's series about the operating point of interest and considering only the first order difference terms. Nondimensionalizing the resulting equations with respect to the linearization point and using the same causality as before, the linear characteristics can be presented in the following matrix form (2):

$$\begin{bmatrix} \frac{\Delta \dot{m}^{\circ}}{\dot{m}^{\circ})_0} \\ \hline \frac{\Delta T_{02}}{T_{02})_0} \\ \hline \frac{\Delta T}{T)_0} \end{bmatrix} = \left[\begin{array}{c|c|c|c} 1-\phi_1 & \phi_1 & -\frac{1}{2}(1+\phi_2) & \phi_2 \\ \hline -\psi_1 & \psi_1 & 1-\frac{1}{2}\psi_2 & \psi_2 \\ \hline 1-\mu_1 & \mu_1 & -\frac{1}{2}\mu_2 & \mu_2 \end{array}\right] \cdot \begin{bmatrix} \frac{\Delta p_{01}}{p_{01})_0} \\ \hline \frac{\Delta p_{02}}{p_{02})_0} \\ \hline \frac{\Delta T_{01}}{T_{01})_0} \\ \hline \frac{\Delta N}{N)_0} \end{bmatrix} \qquad (19)$$

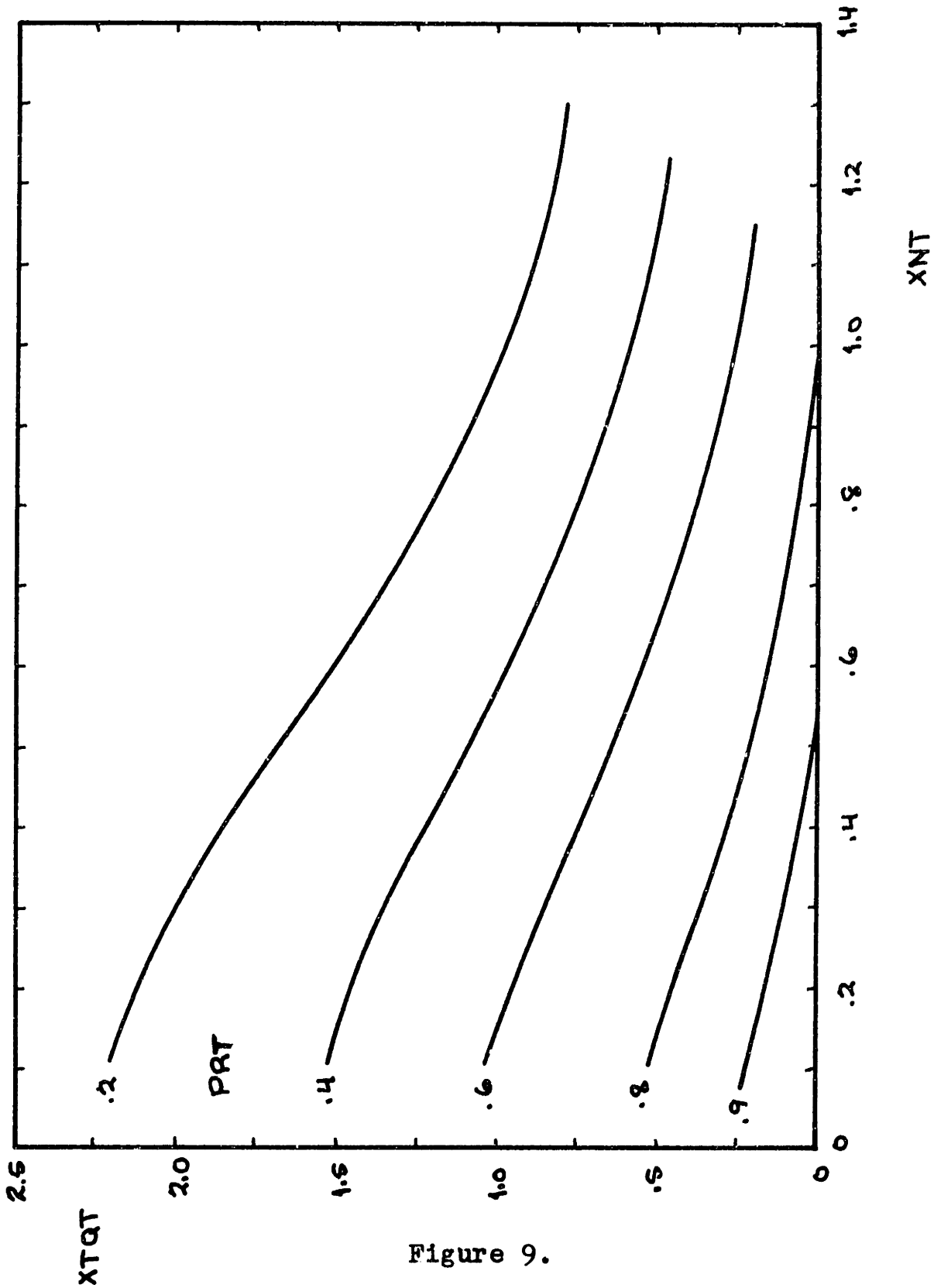

Figure 9.

where,

$$\phi_1 = \left[\frac{\partial\left(\frac{\dot{m}\sqrt{T_{01}}}{p_{01}}\right)}{\partial\left(\frac{p_{02}}{p_{01}}\right)} \cdot \frac{\left(\frac{p_{02}}{p_{01}}\right)}{\left(\frac{\dot{m}\sqrt{T_{01}}}{p_{01}}\right)} \right]_0 \qquad 20)$$

$$\phi_2 = \left[\frac{\partial\left(\frac{\dot{m}\sqrt{T_{01}}}{p_{01}}\right)}{\partial\left(\frac{N}{\sqrt{T_{01}}}\right)} \cdot \frac{\left(\frac{N}{\sqrt{T_{01}}}\right)}{\left(\frac{\dot{m}\sqrt{T_{01}}}{p_{01}}\right)} \right]_0 \qquad 21)$$

$$\psi_1 = \left[\frac{\partial\left(\frac{T_{02}}{T_{01}}\right)}{\partial\left(\frac{p_{02}}{p_{01}}\right)} \cdot \frac{\left(\frac{p_{02}}{p_{01}}\right)}{\left(\frac{T_{02}}{T_{01}}\right)} \right]_0 \qquad 22)$$

$$\psi_2 = \left[\frac{\partial\left(\frac{T_{02}}{T_{01}}\right)}{\partial\left(\frac{N}{\sqrt{T_{01}}}\right)} \cdot \frac{\left(\frac{N}{\sqrt{T_{01}}}\right)}{\left(\frac{T_{02}}{T_{01}}\right)} \right]_0 \qquad 23)$$

$$\mu_1 = \left[\frac{\partial\left(\frac{\tau}{p_{01}}\right)}{\partial\left(\frac{p_{02}}{p_{01}}\right)} \cdot \frac{\left(\frac{p_{02}}{p_{01}}\right)}{\left(\frac{\tau}{p_{01}}\right)} \right]_0 \qquad 24)$$

$$\mu_2 = \left[\frac{\partial\left(\frac{\tau}{\rho_{01}}\right)}{\partial\left(\frac{N}{\sqrt{T_{01}}}\right)} \cdot \frac{\left(\frac{N}{\sqrt{T_{01}}}\right)}{\left(\frac{\tau}{\rho_{01}}\right)} \right]_0 \qquad 25)$$

The subscript 0 outside the brackets and parentheses denotes evaluation at the operating point about which the characteristics have been linearized.

As a result of First Law considerations only four of the above six coefficients are independent. Again choosing the corrected torque as dependent results in the following:

$$\mu_1 = \phi_1 + \frac{1}{\left(1 - T_{01}/T_{02}\right)} \cdot \Psi_1 \qquad 26)$$

$$\mu_2 = \phi_2 + \frac{1}{\left(1 - T_{01}/T_{02}\right)} \cdot \Psi_2 - 1 \qquad 27)$$

Thus, the small scale, steady state operation of any turbomachine passing a compressible fluid can be completely characterized by specifying the operating conditions at linearization and four independent

turbomachine coefficients evaluated at the linearization point.

2. Fuel Burners

The steady state performance of all fuel burners can be characterized by an enthalpy rise and a pressure drop across the component. Taking a steady state energy balance across the fuel burner results in:

$$\dot{m}_1 \cdot h_{o1} + \dot{m}_f \cdot (h_{of} + \eta_B \cdot h_{LHV}) = \dot{m}_2 \cdot h_{o2} \qquad 28)$$

where,

$\dot{m}$ = mass flow rate of gas in lbm/sec

h_o = total enthalpy of fluid stream in ft-lbf/lbm

η_B = combustion efficiency

h_{LHV} = lower heating value of the fuel in ft-lbf/lbm

Subscript 1 refers to the entering gas stream, subscript 2 refers to the leaving gas stream, and subscript f refers to the fuel flow. Implicit in this expression are the assumptions that transverse heat losses and gravity effects are negligible.

The combustion efficiency of a well designed fuel burner operating in its normal regime of operation is relatively constant and is usually in excess of .95. This allows the use of an effective h_{LHV}. In addition h_{of} is generally negligible with respect to h_{LHV}.

Using the perfect gas approximation results in:

$$\dot{m}_1 \cdot C_p \cdot T_{o1} + \dot{m}_f \cdot h_{LHV} - \dot{m}_2 \cdot C_p \cdot T_{o2} = 0 \qquad 29)$$

This type of treatment ignores all combustion problems and treats the fuel burner as a fluid enthalpy mixer.

A square law relationship would be expected to relate total pressure ratio to the corrected weight flow (17). For well designed fuel burners the total pressure ratio is generally in excess of .95. For such a small loss it is possible to include the pressure drop with either the upstream or downstream turbomachine characteristics.

Using the above approximations allows a very simple description of the steady state operation of a fuel burner. The simplified energy balance equation gives the total temperature rise across the component in terms of the mass flows and the thermal and chemical properties of the gas and the fuel. The bond graph representation of the fuel burner can be given as follows:

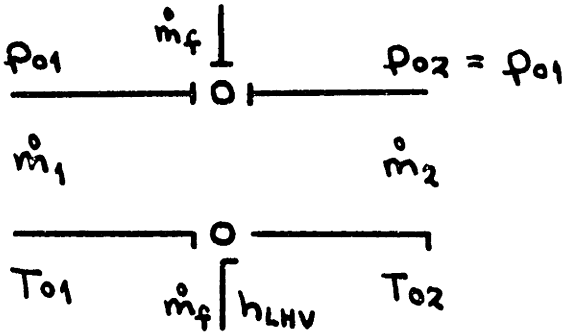

3. Diffusers, Ducts, and Nozzles

The steady state performance of this group of components is extremely simple. Except for very long components transverse heat losses may be neglected. The only other effect of any importance is a total pressure drop across the component. For well designed diffusers, ducts, and smooth nozzles not exhausting to atmosphere or a large chamber the losses will be small and may be lumped with either the upstream or the downstream turbomachine characteristics. For high loss components the familiar square law realtionship should hold.

For those components for which the pressure losses can be lumped elsewhere the steady state behavior is that of an ideal transmission process, i.e., no losses occur. The bond graph representation of such a component is as follows:

$$\frac{p_o}{\dot{m}}$$

$$T_o$$

4. Heat Exchangers

The steady state operation of heat exchangers is

characterized by the pressure drops and enthalpy changes associated with typically two separate fluid streams. Taking an energy balance on the very simple heat exchanger configuration represented below results in:

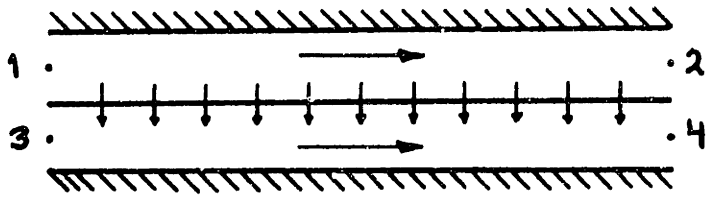

$$\dot{m}_{12} \cdot h_{02} = \dot{m}_{12} \cdot h_{01} - q_b \qquad 30)$$

$$\dot{m}_{34} \cdot h_{04} = \dot{m}_{34} \cdot h_{03} + q_b \qquad 31)$$

where q_b is the total heat flow in ft-lbf/sec. A very simple expression for q_b can be written (1):

$$q_b = \text{const.} \cdot f(\dot{m}_{12}, \dot{m}_{34}) \cdot (T_2 - T_4) \qquad 32)$$

This result is expressed in terms of static temperatures. For most heat exchangers the difference between total and static temperatures is negligible or the effect can be included in the function of the mass flows. Thus, the expression for q_b can be written as the following (neglecting differences in total and

static fluid properties):

$$q = \text{const.} \cdot f(\dot{m}_{12}, \dot{m}_{34}) \cdot (T_{02} - T_{04}) \qquad 33)$$

The function of mass flows serves to express the effect of mass flow rates upon the film coefficients and other parameters.

Again, the pressure losses can, for most cases, be accounted for elsewhere in the system, typically with the turbomachines present.

The extremely simplified discussion above merely serves to illustrate the general structure of heat exchanger operation. More detailed treatments are found in the literature on the subject (1, 18, 19, 20). The bond graph representation of the heat exchanger pictured above is:

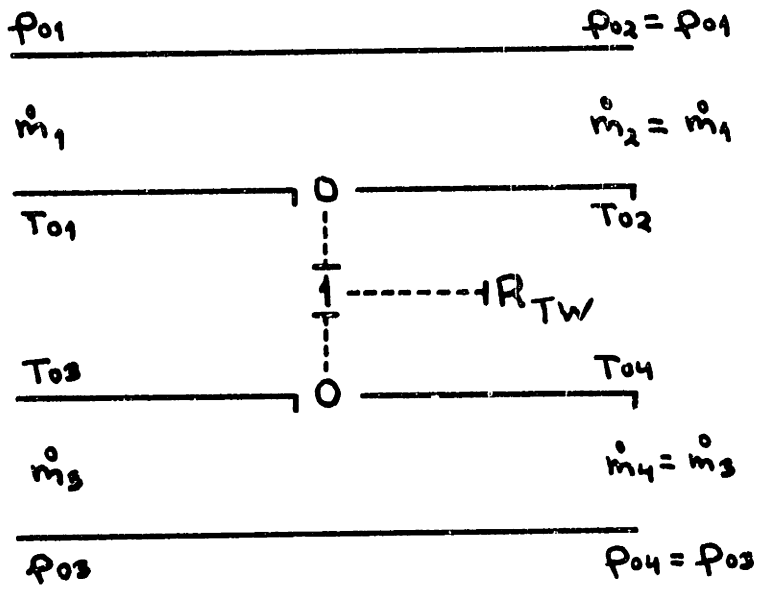

where the R represents the total thermal resistance separating the two fluid streams in °R-sec/ft-lbf, where the resistance is, in general, not constant.

C. Dynamic Elements

1. Mechanical

For gas turbines operating in their normal regime of operation all rotors can be assumed to be rigid bodies. Torsional vibrations are not significant in the overall dynamic behavior. The resulting lumped parameter dynamic element is the familiar rotary inertia from solid body mechanics.

$$\frac{d}{dt}(N) = \left(\frac{30}{\pi I_R}\right)\left(\Sigma \tau_{in}\right) \qquad 34)$$

where,

N = speed of rotation in rpm's

I_R = rotary inertia of rotor in ft-lbf-sec^2

τ_{in} = torque input in ft-lbf

The bond graph representation of this element is:

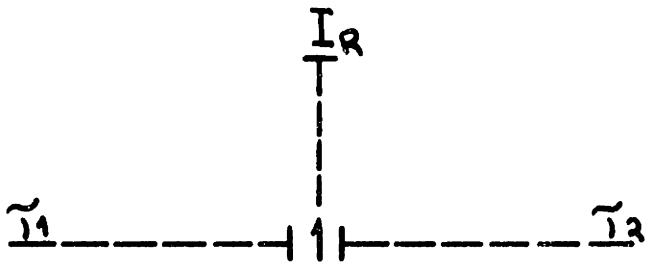

where only two torque inputs are shown.

2. Thermal

The pure thermal lumped parameter dynamic elements are the lumped metal parts in contact with one or more of the fluid streams. Negligible internal temperature gradients are assumed in this approach.

$$\frac{d}{dt}(T) = \frac{1}{C_T} \cdot (\Sigma q_{in}) \qquad 35)$$

where,

T = temperature of lumped element in °R

C_T = thermal capacitance in ft-lbf/°R

q_{in} = heat flow into the element in ft-lbf/sec

The bond graph representation of this element is:

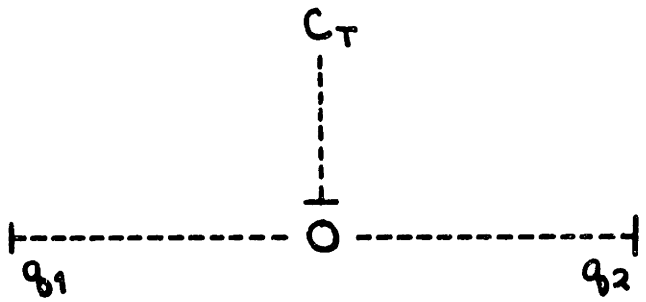

where only two inputs are shown.

3. Fluid

It turns out that the only real interesting dynamics in the gas turbine are the fluid dynamics. Any attempt to analyze the dynamics of the fluid subsystem

must consider the three basic conservation equations and the extremely complex boundary conditions present. These equations are in general coupled and very few exact solutions exist to steady state problems, yet alone transient problems. The fluid dynamics are treated here in an extremely simplified manner. All fluid dynamics are assumed to be those of a duct with the equivalent area and length of the actual component passage. The one dimensional assumption is carried throughout.

a. Lumped Parameter Elements

The mass conservation equation of a one-dimensional fluid stream may be written as:

$$\frac{\partial \rho}{\partial t} + \frac{\partial}{\partial x}(\rho V_x) = 0 \qquad 36)$$

where,

ρ = density of fluid in lbm/ft^3

x = axial distance along the duct in ft

V_x = mean axial velocity of the fluid in ft/sec

Integrating over the area assuming that the fluid properties are constant with area and assuming that the area is constant with time results in:

$$\frac{\partial}{\partial t}(\rho A) + \frac{\partial}{\partial x}(\rho A V_x) = \rho V_x \frac{\partial A}{\partial x} \qquad 37)$$

However,

$$\frac{\partial A}{\partial x} = 0 \qquad 38)$$

is the one-dimensional approximation. Thus,

$$\frac{\partial}{\partial t}(\rho A) + \frac{\partial}{\partial x}(\rho A V_x) = 0 \qquad 39)$$

Integrating over a given length of the duct with the length constant with time results in:

$$\frac{\partial}{\partial t} \cdot \int_L \rho A \cdot dx + \int_L \frac{\partial}{\partial x}(\rho A V_x) dx = 0 \qquad 40)$$

$$\int_L \rho A \cdot dx = \text{mass of fluid in segment} = \bar{\rho} \cdot \text{Vol.} \qquad 41)$$

$$\rho A V_x = \dot{m} \qquad 42)$$

The bar notation represents average values. Thus,

$$\frac{d}{dt}(\bar{\rho}) = \left(\frac{1}{\text{Vol.}}\right) \cdot (\dot{m}_1 - \dot{m}_2) \qquad 43)$$

Neglecting shear stresses and body forces, the one-dimensional momentum conservation equation is:

$$\frac{\partial}{\partial t}\left(\frac{\rho V_x}{g_c}\right) + \frac{\partial}{\partial x}\left(\frac{\rho V_x^2}{g_c} + p\right) = 0 \qquad 44)$$

Carrying through the lumped parameter development results in:

$$\frac{d}{dt}\left(\overline{m^o}\right) = \left(\frac{g_c A}{L}\right)\cdot\left[\, p + \frac{\rho v_x^2}{g_c} \,\right]_2^1 \qquad 45)$$

Introducing the Mach number and the perfect gas approximation:

$$\frac{d}{dt}\left(\overline{m^o}\right) = \left(\frac{g_c A}{L}\right)\cdot\left[\, p\left(1+\gamma M^2\right)\right]_2^1 \qquad 46)$$

where,

γ = ratio of specific heats = c_p/c_v 47)

c_p = specific heat at constant pressure

c_v = specific heat at constant volume

M = Mach number = v_x / a 48)

a = local sonic velocity = $\sqrt{g_c \gamma R T}$ 49)

$$p_o = p\cdot\left(1 + \frac{\gamma-1}{2}\cdot M^2\right)^{\frac{\gamma}{\gamma-1}} \qquad 50)$$

Substituting this into the expression:

$$\frac{d}{dt}\left(\overline{m^o}\right) = \left(\frac{g_c A}{L}\right)\left[\frac{p_o\left(1+\gamma M^2\right)}{\left(1+\frac{\gamma-1}{2}\cdot M^2\right)^{\frac{\gamma}{\gamma-1}}}\right]_2^1 \qquad 51)$$

For M = .5 and γ = 1.4:

$$\frac{d}{dt}\left(\bar{\dot{m}}\right) = \left(\frac{g_c A}{L}\right)\cdot\left[1.14\left(p_{o1} - p_{o2}\right)\right] \qquad 52)$$

For many cases M is less than .5 and the following simplified result can be used:

$$\frac{d}{dt}\left(\bar{\dot{m}}\right) = \left(\frac{g_c A}{L}\right)\left(p_{o1} - p_{o2}\right) \qquad 53)$$

Neglecting viscous work, external work, and heat addition the one-dimensional energy conservation equation may be written as:

$$\frac{\partial}{\partial t}\left[\rho\left(u + \frac{v_x^2}{2g_c}\right)\right] + \frac{\partial}{\partial x}\left[\rho v_x\left(h + \frac{v_x^2}{2g_c}\right)\right] = 0 \qquad 54)$$

where,

u = internal energy of the fluid in ft-lbf/lbm

h = enthalpy of the fluid in ft-lbf/lbm

Carrying through the lumped parameter development:

$$\frac{d}{dt}\left[\overline{\rho\left(u + \frac{v_x^2}{2g_c}\right)}\right] = \frac{1}{Vol.}\left[\dot{m}\left(h + \frac{v_x^2}{2g_c}\right]_2^1\right. \qquad 55)$$

$$h + \frac{v_x^2}{2g_c} = h_o \qquad 56)$$

Again introducing the Mach number and perfect gas

approximation:

$$h_o = c_p \cdot T_o = \text{total enthalpy in ft-lbf/lbm} \qquad 57)$$

$$u + \frac{v_x^2}{2g_c} = c_v \cdot T \left(1 + \frac{\gamma(\gamma-1)}{2} M^2\right) \qquad 58)$$

$$T_o = T \cdot \left(1 + \frac{\gamma-1}{2} \cdot M^2\right) \qquad 59)$$

Substituting this into the expression for the energy conservation:

$$\frac{d}{dt}\left[\overline{\rho c_v T_o}\ \frac{1 + \frac{\gamma(\gamma-1)}{2} M^2}{1 + \frac{\gamma-1}{2} \cdot M^2}\right] = \left[\dot{m}^o c_p T_o\right]_2^1 \cdot \frac{1}{Vol.} \qquad 60)$$

For M = .5 and γ = 1.4:

$$\frac{d}{dt}\left(1.019 \cdot \overline{\rho c_v T_o}\right) = \frac{1}{Vol.}\left(\dot{m}_1 c_p T_{o1} - \dot{m}_2 c_p T_{o2}\right) \qquad 61)$$

For many cases M will be less than .5 and the result may be simplified to:

$$\frac{d}{dt}\left(\overline{\rho T_o}\right) = \left(\frac{\gamma}{Vol.}\right)\left(\dot{m}_1 T_{o1} - \dot{m}_2 \cdot \overline{T}_o\right) \qquad 62)$$

where the exit temperature is generally taken to be the average temperature of the element.

The equation of state may be written as:

$$p_o = \rho R T_o \cdot \left(1 + \frac{\gamma-1}{2} \cdot M^2\right)^{\frac{1}{\gamma-1}} \qquad 63)$$

For $M = .5$ and $\gamma = 1.4$:

$$p_o = 1.13 \cdot \rho R T_o \qquad 64)$$

For low Mach numbers the result may be simplified to:

$$p_o = \rho R T_o \qquad 65)$$

Since the fluid power transfer has been expressed as a function of p_o, $\dot{m}$, and T_o it might prove useful to express the simplified fluid dynamic elements in terms of the same three variables. This can be accomplished by introducing the concept of a polytropic process.

$$(T_o)^{\frac{n}{n-1}} = \text{const.} \cdot p_o \qquad 66)$$

where,

n = the polytropic constant

Introducing the approximate equation of state given above results in:

$$p_o = \text{const.} \cdot \rho^n \qquad 67)$$

$$T_o = \text{const.} \cdot \rho^{n-1} \qquad 68)$$

Differentiating the above with respect to time results in:

$$\frac{d}{dt}(\rho) = \left(\frac{1}{nRT_o}\right) \cdot \frac{d}{dt}(p_o) \qquad 69)$$

$$\frac{d}{dt}(\rho T_o) = \left(\frac{n}{n-1}\right)\left(\frac{p_o}{RT_o}\right) \cdot \frac{d}{dt}(T_o) \qquad 70)$$

By substituting this into the previous simplified dynamic element equations an even more simplified form results.

$$\frac{d}{dt}(p_o) = \left(\frac{nRT_o}{Vol.}\right) \cdot (\dot{m}_1^o - \dot{m}_2^o) \qquad 71)$$

$$\frac{d}{dt}(\dot{m}^o) = \left(\frac{g_c A}{L}\right)(p_{o1} - p_{o2}) \qquad 72)$$

$$\frac{d}{dt}(T_o) = \left(\frac{n-1}{n}\right)\left(\frac{C_p R T_o}{C_v \cdot p_o \cdot Vol.}\right)(\dot{m}_1^o T_{o1} - \dot{m}_2^o T_o) \qquad 73)$$

The polytropic constant, n, equals 1.0 for an isothermal process and equals γ for an isentropic process. These equations may be represented in bond graph form as follows:

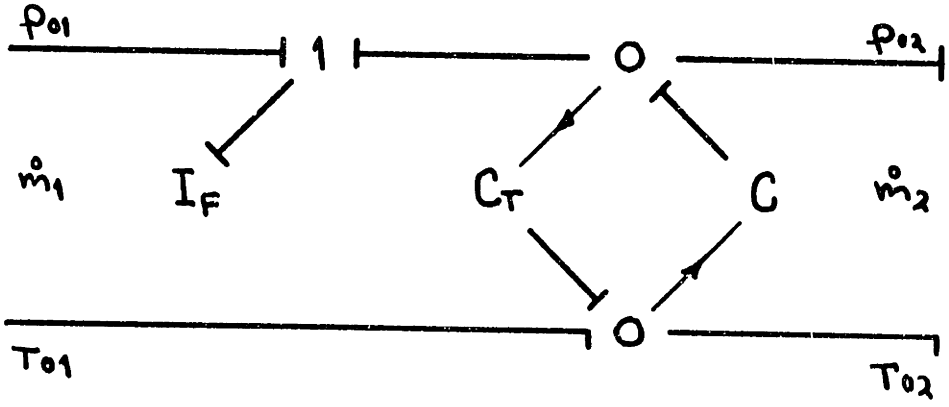

where,

C = fluid mechanical capacitance = $\frac{Vol.}{nRT_o}$ 74)
(in lbm-ft^2/lbf)

I_F = fluid inertance = $\frac{L}{g_c A}$ 75)
(in lbf-sec /lbm-ft)

C_T = fluid thermal capacitance = $\left(\frac{n}{n-1}\right)\left(\frac{\rho_o C_v \cdot Vol.}{RT_o}\right)$ 76)
(in ft-lbf/ R)

The arrows on the bond graph represent coupling between the fluid mechanical and the fluid thermal effects. Any coupling effects associated with the fluid inertance have been lost in the simplification process.

It will be shown in the next chapter that for a lumped parameter fluid element with heat addition, such as a fuel flow, the energy conservation equation 62) is better approximated if the (n-1)/n factor is replaced by 1.0 in equation 73). Equations 71) and 72) remain the same. The bond graph of the equations

remains the same, except for the change in the fluid thermal capacitance, i.e., the dropping of the factor $n/(n-1)$.

The approximations given above can produce significant errors if introduced in the general case. However, the analysis here is concerned with simplified dynamic elements. These elements become perfect transmission elements as all dynamic effects die away. All steady state effects are taken care of elsewhere. The only errors introduced by the above approximations occur in the dynamic characteristics, which are approximations at best to begin with.

b. Polytropic Acoustic Line

The acoustic line treated here will be one with leakage flows to some side storage. This situation will exist for the flow through a turbomachine due to the necessary clearances between stators and rotors. The side or wall storage is assumed to be connected to the main gas stream by linear resistances. The wall storages are assumed to be isolated from one another so that no net axial flow may take place. This line may be represented schematically as follows:

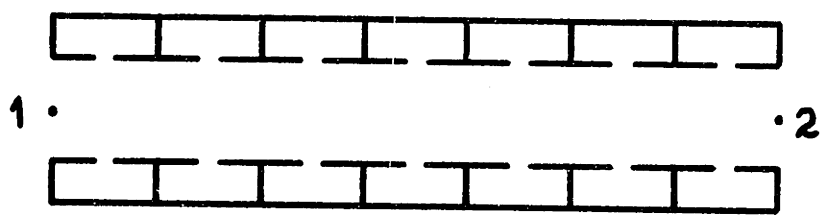

Assuming a polytropic process and the assumptions of the previous section, the differential equations of such a line may be written as:

$$\frac{A}{nRT_o} \cdot \frac{\partial p_o}{\partial t} = - \frac{\partial \dot{m}}{\partial x} - \frac{1}{R'_w} \left(p_o - p_{ow} \right) \qquad 77)$$

$$\frac{1}{g_c A} \cdot \frac{\partial \dot{m}}{\partial t} = - \frac{\partial p_o}{\partial x} \qquad 78)$$

$$\frac{A_w}{nRT_o} \cdot \frac{\partial p_{ow}}{\partial t} = \frac{1}{R'_w} \left(p_o - p_{ow} \right) \qquad 79)$$

where,

p_o = total pressure in the main stream in lbf/ft^2

$\dot{m}$ = mass flow of the main stream in lbm/sec

p_{ow} = total pressure in the wall storage in lbf/ft^2

A = cross sectional area of main stream in ft^2

A_w = wall storage volume per unit length in ft^2

n = polytropic constant

T_o = total temperature of the fluid in °R

R = gas constant in ft-lbf/lbm-°R

R_w = total flow resistance in lbf-sec/lbm-ft^2

$1/R'_w$ = flow conductance per unit length in lbm-ft/lbf-sec

L = length of acoustic line in ft

$$R'_w = L \cdot R_w \qquad 80)$$

Equation 79) may be rewritten as:

$$p_{ow} = \frac{1}{(1 + \tau_2 \cdot S)} \cdot p_o \qquad 81)$$

where,

S = Laplacian operator

$$\tau_2 = \frac{A_w \cdot R'_w}{nRT_o} = \frac{A_w \cdot L \cdot R_w}{nRT_o} \qquad 82)$$

Substituting into equation 77):

$$\frac{\partial \dot{m}}{\partial x} = - \frac{(C + C_w) \cdot S}{L} \cdot \frac{(1 + \tau_1 \cdot S)}{(1 + \tau_2 \cdot S)} \cdot p_o \qquad 83)$$

$$\frac{\partial p_o}{\partial x} = - \frac{I_F}{L} \cdot S \cdot \dot{m} \qquad 84)$$

where,

$$C = \frac{A \cdot L}{nRT_o} \qquad 85)$$

$$C_w = \frac{A_w \cdot L}{nRT_o} \qquad 86)$$

$$\tau_1 = \tau_2 / (1 + C_w/C) \qquad 87)$$

$$I_F = \frac{L}{g_c A} \qquad 88)$$

Differentiating equations 83) and 84) with respect to x and combining results in:

$$\frac{\partial^2 p_o}{\partial x^2} = \left(\frac{Te \cdot S}{L}\right)^2 \cdot p_o \qquad 89)$$

$$\frac{\partial^2 \dot{m}}{\partial x^2} = \left(\frac{Te \cdot S}{L}\right)^2 \cdot \dot{m} \qquad 90)$$

where,

$$Te^2 = I_F \cdot (C + C_w) \frac{(1 + \tau_1 \cdot S)}{(1 + \tau_2 \cdot S)} \qquad 91)$$

Te may be considered as the time required for a pressure disturbance to be propagated from one end of the line to the other. Solutions to equations 89) and 90) imposing appropriate boundary conditions are:

$$p_{o2} = p_{o1} \cdot \cosh(Te \cdot S) - \dot{m}_1 \cdot Z_c \sinh(Te \cdot S) \qquad 92)$$

$$\dot{m}_2 = \dot{m}_1 \cdot \cosh(Te \cdot S) - \frac{p_{o1}}{Z_c} \cdot \sinh(Te \cdot S) \qquad 93)$$

where,

$$Z_c = \frac{I_F}{Te} \qquad 94)$$

These results can be rearranged to suit the desired

causality. The two causalities of interest are:

$$p_{o1} = \frac{Z_c}{\tanh(T_e \cdot s)} \cdot \dot{m}_1 - \frac{Z_c}{\sinh(T_e \cdot s)} \cdot \dot{m}_2 \qquad 95)$$

$$p_{o2} = \frac{Z_c}{\sinh(T_e \cdot s)} \cdot \dot{m}_1 - \frac{Z_c}{\tanh(T_e \cdot s)} \cdot \dot{m}_2 \qquad 96)$$

and,

$$\dot{m}_1 = \frac{1}{Z_c \cdot \tanh(T_e \cdot s)} \cdot p_{o1} - \frac{1}{Z_c \cdot \sinh(T_e \cdot s)} \cdot p_{o2} \qquad 97)$$

$$\dot{m}_2 = \frac{1}{Z_c \cdot \sinh(T_e \cdot s)} \cdot p_{o1} - \frac{1}{Z_c \cdot \tanh(T_e \cdot s)} \cdot p_{o2} \qquad 98)$$

The hyperbolic functions can be expanded im a series for small values of $T_e \cdot s$.

$$\tanh(T_e \cdot s) = T_e \cdot s \left(1 - \tfrac{1}{3}(T_e \cdot s)^2 + \cdots\right) \qquad 99)$$

$$\sinh(T_e \cdot s) = T_e \cdot s \left(1 + \tfrac{1}{6}(T_e \cdot s)^2 + \cdots\right) \qquad 100)$$

For $|T_e \cdot s| \ll 1$

$$\tanh(T_e \cdot s) \cong T_e \cdot s \qquad 101)$$

$$\sinh(T_e \cdot s) \cong T_e \cdot s \qquad 102)$$

Substituting these approximations back into equations 95) through 98) results in the lumped parameter capacitance and inertance. These two processes of necessity have to be spatially separated.

$$p_o = \frac{Z_c}{T_e \cdot s} \cdot \left(\dot{m}_1 - \dot{m}_2 \right) \qquad 103)$$

$$\dot{m} = \frac{1}{Z_c \cdot T_e \cdot s} \cdot \left(p_{o1} - p_{o2} \right) \qquad 104)$$

Introducing the acoustic velocity of the fluid, a, T_e is approximated by:

$$T_e \approx \frac{L}{a} \qquad 105)$$

Considering a sinusoidal input to the line:

$$s = j \cdot \omega \qquad 106)$$

$$|T_e \cdot s| = \frac{\omega \cdot L}{a} \qquad 107)$$

Thus, the criteria for the applicability of the lumped parameter approximation is:

$$\frac{\omega \cdot L}{a} << 1 \qquad 108)$$

where ω is the highest frequency component in the input. It can be seen that as the frequency content of the input increases, the length of the appropriate lumped parameter element decreases.

Equations 103) and 104) are given by the following:

$$p_o = \frac{1}{(C+C_w)\cdot s}\cdot\left[\frac{(1+\tau_2\cdot s)}{(1+\tau_1\cdot s)}\right]\cdot\left(\dot{m}_1^o - \dot{m}_2^o\right) \qquad 109)$$

$$\dot{m}^o = \frac{1}{I_F\cdot s}\left(p_{o1} - p_{o2}\right) \qquad 110)$$

These results agree exactly with the previous lumped parameter elements as the wall storage disappears.

The number of these lumped elements needed to model an acoustic line will depend on the frequency content of the input. The simplest model will contain one element. The bond graph representation of this element is:

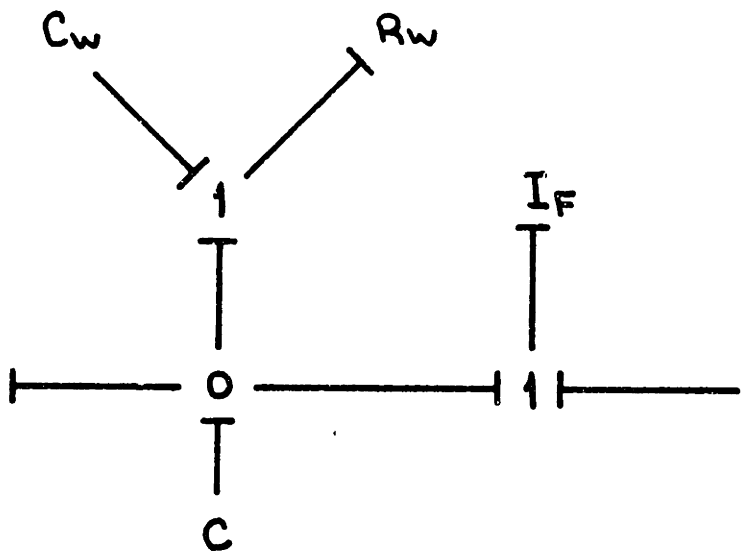

The order of the fluid inertance and fluid capacitance elements in the preceeding model makes no difference and can be altered to suit the input causality of the particular situation. The polytropic constant, n, can be varied from 1.0 for isothermal cases to γ for isentropic cases.

c. Polytropic Thermal Duct

The case considered here will be that of a polytropic, convective duct flow with thermal energy storage in the duct walls and no heat losses to the surroundings.

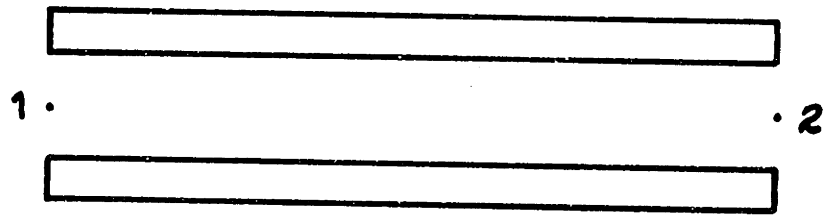

Using the assumptions given previously concerning total properties, and assuming a polytropic process, and assuming a constant mass flow throughout, the differential equations may be written as:

$$\left(\frac{n}{n-1}\right)\rho \cdot C_v \cdot A \frac{\partial T_o}{\partial t} + C_p \cdot \dot{m} \frac{\partial T_o}{\partial x} + h \cdot A_s (T_o - T_w) = 0 \qquad 111)$$

$$\rho_w C_w A_w \frac{\partial T_w}{\partial t} + h A_s (T_w - T_o) = 0 \qquad 112)$$

where,

T_o = total temperature of fluid in °R

ρ = density of fluid in lbm/ft^3

A = cross sectional area of duct in ft^2

C_v = heat capacity at constant volume of fluid in ft-lbf/lbm-°R

C_p = heat capacity at constant pressure of fluid in ft-lbf/lbm-°R

T_w = temperature of wall in °R

ρ_w = density of wall material in lbm/ft^3

A_w = volume of wall per unit length in ft^2

C_w = heat capacity of wall material in ft-lbf/lbm-°R

h = overall heat transfer coefficient in ft-lbf/ft^2-sec-°R or lbf/ft-sec-°R

A_s = effective heat transfer area per unit length in ft

Equation 112) may be written as:

$$T_w = \frac{1}{(1 + \tau_2 \cdot S)} \cdot T_o \qquad 113)$$

where,

$$\tau_2 = \frac{\rho_w A_w C_w}{h A_s} \qquad 114)$$

S = Laplacian operator

Substituting into equation 111):

$$\frac{\partial T_o}{\partial X} = -\left[\frac{C_T}{C_p \cdot \dot{m} \cdot L} \cdot S + \frac{\frac{C_{TW}}{C_p \cdot \dot{m} \cdot L} \cdot S}{(1 + \tau_2 \cdot S)}\right] \cdot T_o \qquad 115)$$

where,

$$C_T = \left(\frac{n}{n-1}\right) \cdot \rho C_v A L \qquad 116)$$

$$C_{TW} = \rho_w C_w A_w L \qquad 117)$$

L = length of duct in ft

A solution to this equation with appropriate boundary conditions is given by:

$$T_{o2} = \exp\left[-\frac{C_T}{C_p \dot{m}} \cdot S - \frac{\frac{C_{TW}}{C_p \dot{m}} \cdot S}{(1 + \tau_2 \cdot S)}\right] \cdot T_{o1} \qquad 118)$$

For small terms inside the brackets the exponential may be simplified by the following approximation:

$$T_{o2} = \frac{(1 + \tau_2 \cdot S) \cdot T_{o1}}{1 + \left(\frac{C_T}{C_p \dot{m}} + \frac{C_{TW}}{C_p \dot{m}} + \tau_2\right) \cdot S + \left(\frac{C_T \cdot \tau_2}{C_p \dot{m}}\right) \cdot S^2} \qquad 119)$$

or equivalently,

$$T_{o2} = \frac{1}{(C_T + C_{Tw}) \cdot s} \left(\frac{1 + \tau_2 \cdot s}{1 + \tau_1 \cdot s} \right) \left(C_p \dot{m} T_{o1} - C_p \dot{m} T_{o2} \right) \qquad 120)$$

where,

$$\tau_1 = \frac{\tau_2}{(1 + C_{Tw}/C_T)} \qquad 121)$$

For this to be approximately valid the following must be true:

$$\left| \frac{C_T}{C_p \dot{m}} \cdot s \right| \ll 1 \qquad 122)$$

and,

$$\left| \frac{C_{Tw}}{C_p \dot{m}} \cdot s \right| \ll 1 \qquad 123)$$

However,

$$\frac{C_T}{C_p \dot{m}} \approx \frac{L}{N_x} \qquad 124)$$

approximates the time it takes for a temperature disturbance to be convected down the duct. Considering sinusoidal inputs to the duct, the above conditions reduce to:

$$\frac{\omega L}{N_x} \ll 1 \qquad 125)$$

and,

$$\sigma \cdot \frac{\omega L}{N_X} << 1 \qquad 126)$$

where,

$$\sigma = \frac{C_{TW}}{C_T} \qquad 127)$$

and ω is the highest frequency component of the input. In general, one of the above terms will be dominant in determining the appropriate lumped parameter duct length.

The exponential can be approximated in a different approach by splitting the terms in the brackets.

$$T_{o2} = \left[\frac{1}{1+\frac{C_T}{C_p \dot{m}} \cdot s}\right] \cdot \left[\frac{1+\tau_2 \cdot s}{1+\left(\sigma \cdot \frac{C_T}{C_p \dot{m}} + \tau_2\right) \cdot s}\right] \cdot T_{o1} \qquad 128)$$

Typical values of the parameters are:

$$\frac{C_T}{C_p \dot{m}} \approx .01 \text{ second}$$

$$\tau_2 \approx 10. \text{ seconds}$$

$$\sigma \approx 1.0$$

Under these conditions further simplification can be

made.

$$T_{o2} = \left(\frac{1}{1 + \frac{C_T}{c_p \dot{m}} \cdot S} \right) \cdot T_{o1} \qquad 129)$$

This expression totally neglects the effect of thermal wall storage.

The bond graph representation of the lumped parameter model including wall storage is:

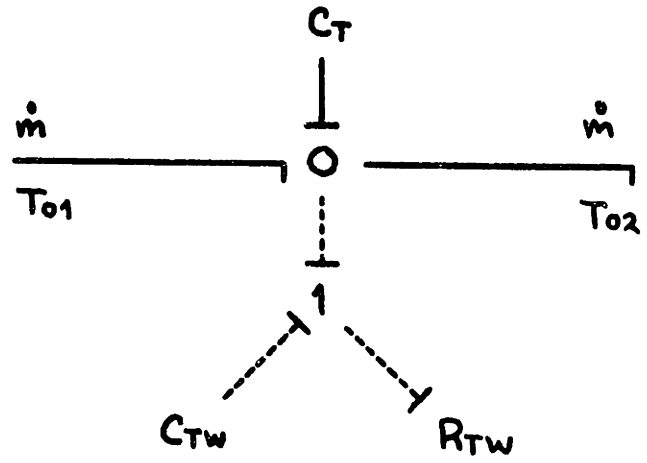

where,

$$R_{TW} = \frac{1}{\lambda A_s L} \qquad 130)$$

The polytropic constant equals γ for an isentropic process and can approach 1.0 as the process approaches isothermal. However, a more usual assumption to make about the nature of the process is that of constant

density. This corresponds to the limit as the polytropic constant approaches infinity.

d. Generalized Fluid Element

A generalized fluid dynamic lumped parameter element in which all of the preceeding dynamic effects are significant can be represented as:

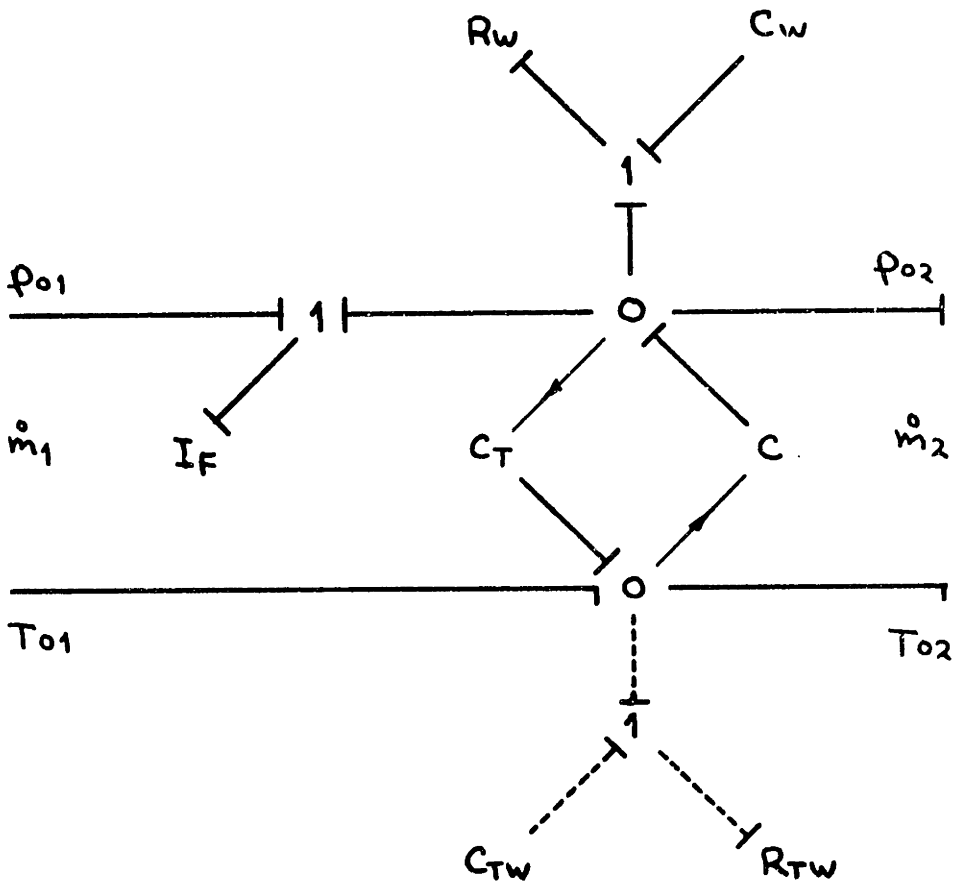

The criteria given before concerning the applicability of the lumped parameter approach can be applied to the general case. The lumped parameter approach will be valid for:

$$\frac{\omega L}{a} << 1 \qquad 131)$$

$$\frac{\omega L}{\nu_x} << 1 \qquad 132)$$

$$\sigma \cdot \frac{\omega L}{\nu_x} << 1 \qquad 133)$$

The degree of accuracy desired will govern the granularity of the length of the particular lumped parameter model used.

D. Component Models

The models of the various basic components can vary widely depending on the engine being modeled, the frequency range of interest, and the desired degree of accuracy. The component models shown here will be the simplest models possible to include dynamic effects, i.e., one element models. The extension to many elements is straightforward.

1. Turbomachines

The general turbomachine element in which fluid mechanical and thermal wall storage effects are considered can be represented by the bond graph shown on the following page. The causality shown is that used in this treatment, but different causalities are surely possible.

Such a model represents a six state variable

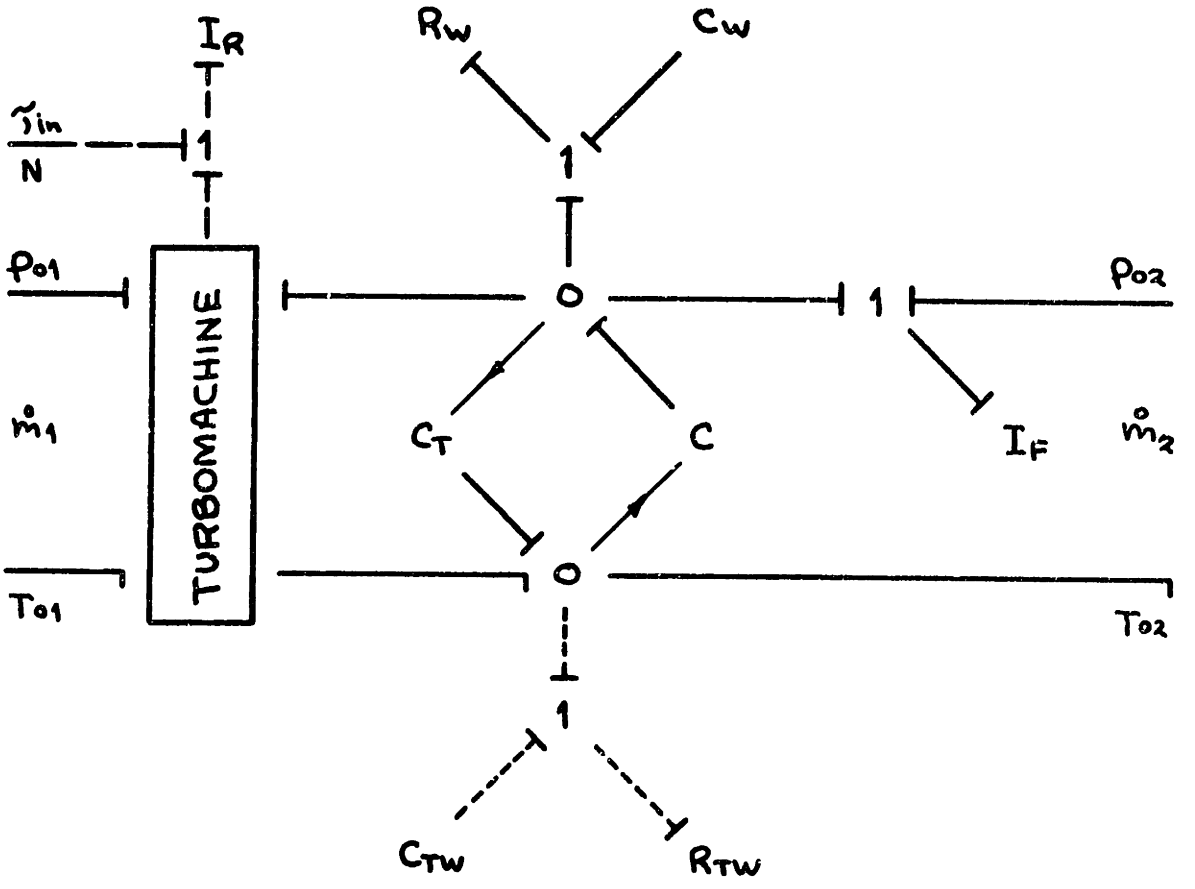

subsystem model and may be of higher order than is practical for a complete engine simulation. Some of the dynamic effects have to be neglected. Inspection of the expressions for the fluid mechanical capacitance and the fluid inertance reveals that conditions that make for a large capacitance make for a small inertance, and vice versa. The nature of the gas turbine dictates that fluid capacitance effects are more important than fluid inertance effects. In addition, both thermal and fluid mechanical wall storage may be considered as secondary effects and can be neglected. With these

simplications the turbomachine element takes on a much more simplified form.

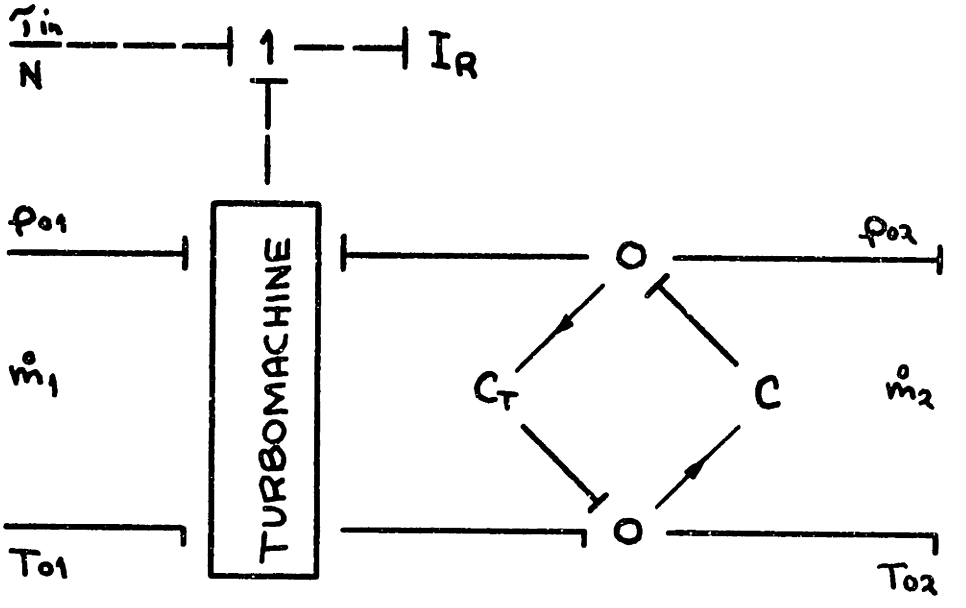

2. Fuel Burners

The steady state and dynamic behavior of fuel burners can be combined into one. The steady state behavior of a fuel burner is simply the steady state solution to the lumped parameter energy conservation equation considering fuel addition. The bond graph representation of the fuel burner element considering all the dynamic effects discussed previously is shown on the following page.

The magnitude of the fuel flow is very small compared with the gas flow and can be neglected in fluid mechanical capacitance effects. In addition,

3. Diffusers, Ducts, and Nozzles

The elemental model of this group of components is identical with that of tho fuel burners except for the lack of any fuel addition. The steady state performance of diffusers, ducts and nozzles in the simplified form discussed previously is quite simply that of an ideal transmission element. The bond graph representation of this group of components is very similar to that of the fuel burners for both the complete and simplified models, and need not be shown here.

4. Heat Exchangers

The component model for a simple heat exchanger is similar to that of the last group. The differences are that the simple heat exchanger has two fluid streams in contact with a common wall and there is a steady state enthalpy difference between exit and entrance for both of the fluid streams.

The bond graph representation of a simple heat exchanger considering all of the dynamic effects discussed is shown on the following page. R_{TW} represents the total thermal resistance of the heat transfer interface and does not necessarily have to be a constant. If fluid inertance and thermal wall storage effects are neglected the bond graph representation is

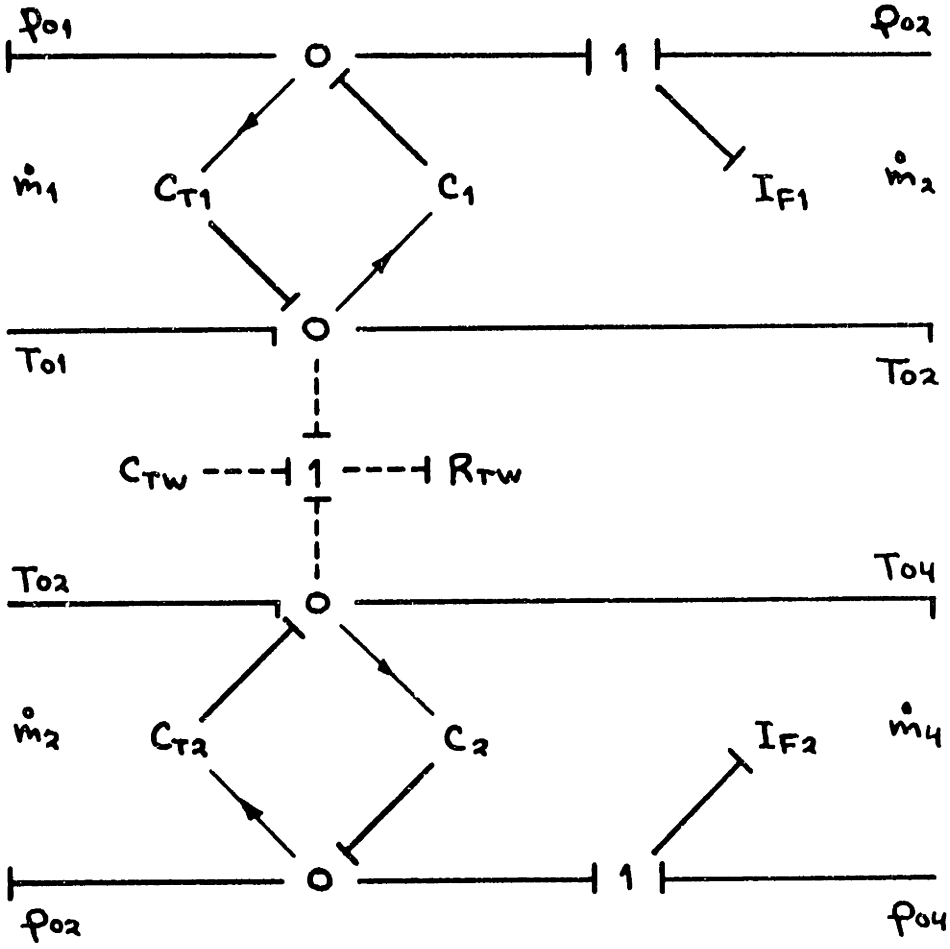

simplified somewhat. The wall thermal capacitance, C_{TW}, and the two fluid inertances, I_{F1} and I_{F2}, will be eliminated. The simplified form is easily seen from the bond graph above and a simplified version need not be shown.

5. Frequency Range of Interest

The component or elemental models given above can be applied to the modeling of any gas turbine in a completely straightforward manner. However, it is easy to get carried away and end up with a model that

is far too complex. Even when limited to one element per component the resulting overall model can be too complex. For example, a simple cycle, single shaft gas turbine model with one element per component would have fourteen state variables if some simplifications weren't made.

There are basically three dynamic regimes of operation for the gas turbine:

i) low frequency

ii) medium frequency

iii) high frequency

In the low frequency regime the rotary inertias and wall thermal capacitances dominate. All other dynamics are assumed to be instantaneous. Representative frequencies in this regime are on the order of .01 cycles per second.

In the medium frequency regime the rotary inertias and fluid capacitances dominate. The wall thermal dynamics are so slow that they may be assumed to be constant. The fluid inertia effects are assumed to be instantaneous. Typical frequencies in this regime are on the order of 1 cycle per second.

In the high frequency regime the fluid dynamics dominate. All other dynamics are assumed to be constant. Typical frequencies in this regime are on

the order of 100 cycles per second.

The three regimes given are somewhat vague and overlapping, and only serve as a very rough guideline. For the purposes of this analysis the medium frequency range will be the one of interest. The only dynamic elements considered will be the rotary inertia and the two fluid capacitances.

E. Case Study

1. Design Information

The gas turbine chosen for analysis in this study is a simple cycle, single shaft engine such as that shown in figure 1. Due to the difficulty in obtaining manufacturer's data, this engine was more or less fabricated from a variety of sources (16, 21, 22, 23, 24). The engine specifications at the design point are:

Pressure Ratio = 5.0

Compressor Isentropic Efficiency = 84%

Turbine Inlet Temperature = 1280 °F

Turbine Isentropic Efficiency = 88%

Compressor Discharge Mass Flow = 100 lbm/sec

Inlet Pressure = 14.175 psia

Inlet Temperature = 80 °F

Roter Speed = 7200 rpm

Power Output = 6948 hp

The compressor and turbine performance maps are those shown in figures 4 through 9. Even though this set of design and performance data is fabricated it is felt to be fairly realistic.

2. Mathematical Model

For the purposes of modeling the above mentioned gas turbine the effects of the inlet and exhaust are neglected. In addition, the remaining three basic components are modeled with only one element per component. All fluid inertia effects and wall storage effects, both fluid and thermal, are neglected. By judiciously grouping the component models, the overall engine model may be represented by the bond graph shown in figure 10. The two capacitances shown represent the total lumped capacitances of the entire engine. The mechanical inertia represents the rotary inertias of the rotor and the load. The load applied is an assumed propeller law type of load, i.e., the torque varies as the square of the speed. All inlet conditions are assumed to be constant.

a. Nonlinear Model

The nonlinear equations describing the gas turbine consist of the differential equations for the three state variables and the compressor and turbine performance maps. The polytropic approximation is

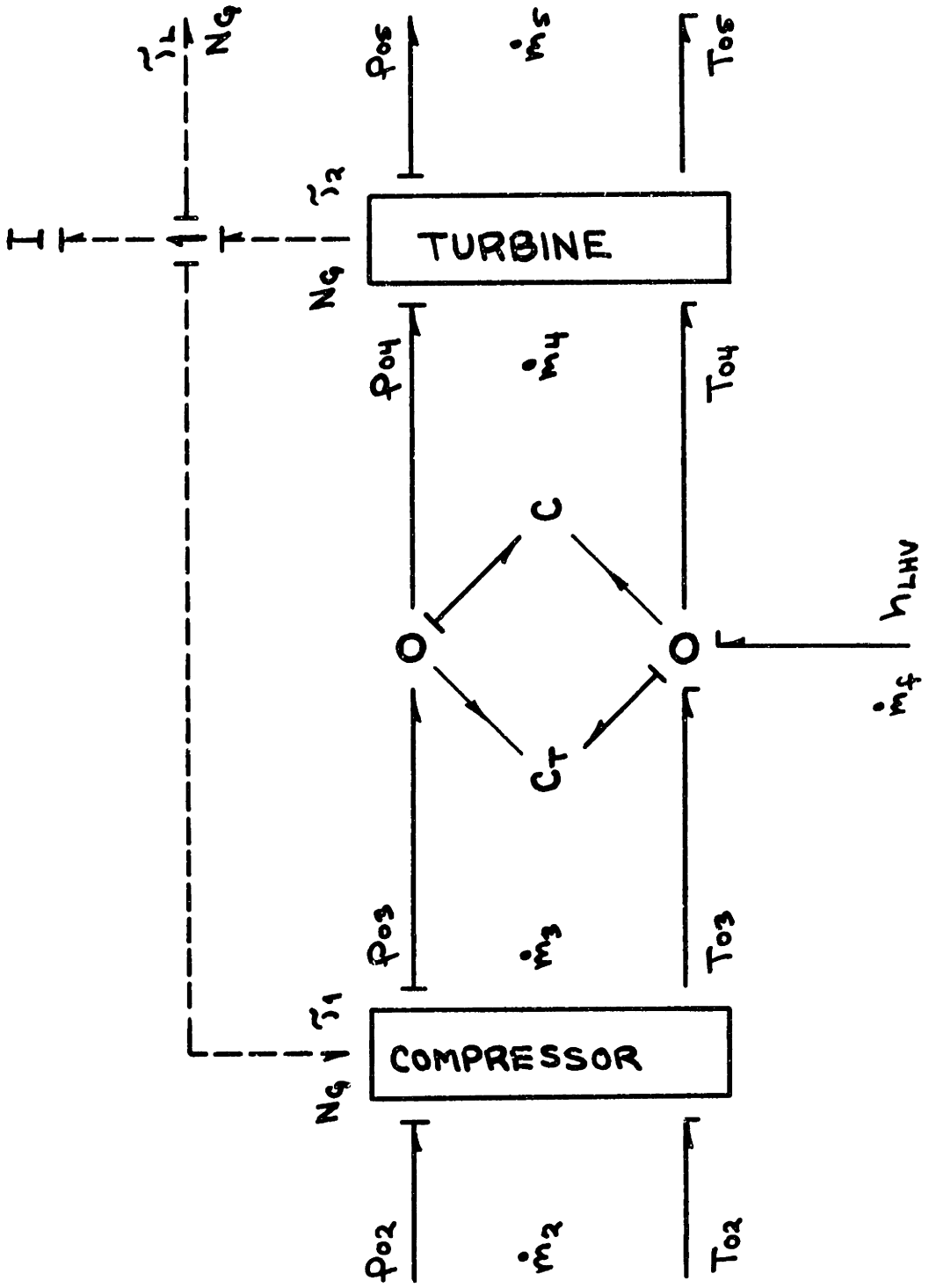
TURBINE
COMPRESSOR
C
O
O
C_T
τ_1
N_G
τ_2
N_G
τ_1
N_G
P_{05}
$\dot{m}_5$
T_{05}
P_{04}
$\dot{m}_4$
T_{04}
P_{03}
$\dot{m}_3$
T_{03}
P_{02}
$\dot{m}_2$
T_{02}
h_{LHV}
$\dot{m}_f$

Figure 10.

used to express the lumped parameter mass conservation equation in terms of the total pressure. In the lumped parameter energy conservation equation the effects of the density are neglected, i.e., the density is assumed to be constant. The system differential equations are:

$$\frac{d}{dt}(p_{o3}) = \left(\frac{nRT_{o4}}{Vol.}\right)\cdot\left[\dot{m}_3 - \dot{m}_4\right] \qquad 134)$$

$$\frac{d}{dt}(T_{o4}) = \left(\frac{\gamma RT_{o4}}{p_{o3}\cdot Vol.}\right)\cdot\left[\dot{m}_3\cdot T_{o3} + \dot{m}_f\left(\frac{h_{LHV}}{c_p}\right) - \dot{m}_4 T_{o4}\right] \qquad 135)$$

$$\frac{d}{dt}(N_g) = \left(\frac{30}{\pi I}\right)\cdot\left[\tau_2 - \tau_1 - \tau_3\right] \qquad 136)$$

where,

p_{o3} = compressor discharge total pressure in lbf/ft^2

T_{o3} = compressor discharge total temperature in °R

$\dot{m}_3$ = compressor discharge mass flow in lbm/sec

τ_1 = compressor torque in ft-lbf

T_{o4} = turbine inlet total temperature in °R

$\dot{m}_4$ = turbine inlet mass flow in lbm/sec

τ_2 = turbine torque in ft-lbf

N_g = rotational speed of rotor in rpm's

$\dot{m}_f$ = fuel flow in lbm/sec

τ_3 = load torque in ft-lbf

The independent turbomachine characteristics can be

expressed as:

$$\frac{\dot{m}_3\sqrt{T_{02}}}{p_{02}} = f_1\left(\frac{p_{03}}{p_{02}}, \frac{N_G}{\sqrt{T_{02}}}\right) \qquad 137)$$

$$\frac{T_{03}}{T_{02}} = f_2\left(\frac{p_{03}}{p_{02}}, \frac{N_G}{\sqrt{T_{02}}}\right) \qquad 138)$$

$$\frac{\dot{m}_4\sqrt{T_{04}}}{p_{03}} = f_3\left(\frac{p_{05}}{p_{03}}, \frac{N_G}{\sqrt{T_{04}}}\right) \qquad 139)$$

$$\frac{T_{05}}{T_{04}} = f_4\left(\frac{p_{05}}{p_{03}}, \frac{N_G}{\sqrt{T_{04}}}\right) \qquad 140)$$

An algebraic model of these characteristics has been formulated and is given in Appendix I.

The compressor and turbine torques can be determined from a steady state energy balance.

$$\tilde{\tau}_1 = \left(\frac{30\,C_p}{\pi}\right).\frac{\dot{m}_3\,(T_{03}-T_{02})}{N_G} \qquad 141)$$

$$\tilde{\tau}_2 = \left(\frac{30\,C_p}{\pi}\right).\frac{\dot{m}_4\,(T_{04}-T_{05})}{N_G} \qquad 142)$$

b. Linear or Incremental Model

The preceeding equations can be linearized about some operating point, where this operating point is not necessarily a steady state point. The results can be written in the following matrix form:

$$\frac{d}{dt}\begin{bmatrix} \rho_{03} \\ T_{04} \\ N_4 \end{bmatrix} = \begin{bmatrix} F_{11} & F_{12} & F_{13} \\ F_{21} & F_{22} & F_{23} \\ F_{31} & F_{32} & F_{33} \end{bmatrix} \cdot \begin{bmatrix} \rho_{03} \\ T_{04} \\ N_4 \end{bmatrix} + \begin{bmatrix} 0 & 0 & G_{13} \\ G_{21} & 0 & G_{23} \\ 0 & G_{32} & G_{33} \end{bmatrix} \begin{bmatrix} \dot{m}_f \\ \zeta_3 \\ 1 \end{bmatrix} \quad 143)$$

By assuming that the quantities inside the parentheses on the right hand side of equations 134) and 135) represent some average, constant values, the matrix formulation above reduces to twelve state dependent coefficients. G_{21} and G_{32} are constant.

In the above formulation the state variables represent the full values of the engine variables. In general, the matrix of coefficients only holds for some small region of the state space. As a large scale transient is marched out the coefficients have to be changed as needed.

The coefficients can be obtained in a straightforward manner and are given as follows:

$$F_{11} = \left(\frac{nRT_{04}}{Vol.}\right) \cdot \left[\phi_{11} \cdot \frac{\dot{m}_3}{\rho_{03}} - (1-\phi_{12}) \cdot \frac{\dot{m}_4}{\rho_{03}}\right]_0 \quad 144)$$

$$F_{12} = \left(\frac{nRT_{04}}{Vol.}\right) \cdot \left[\frac{1}{2}(1+\phi_{22}) \cdot \frac{\dot{m}_4}{T_{04}}\right]_0 \quad 145)$$

$$F_{13} = \left(\frac{nRT_{04}}{Vol.}\right) \cdot \left[\phi_{21} \cdot \frac{\dot{m}_3}{N_G} - \phi_{22} \cdot \frac{\dot{m}_4}{N_G}\right]_0 \quad 146)$$

$$F_{21} = \left(\frac{\gamma RT_{04}}{\rho_{03} \cdot Vol.}\right)\left[(\phi_{11}+\psi_{11})\frac{\dot{m}_3 T_{03}}{\rho_{03}} - (1-\phi_{12})\frac{\dot{m}_4 T_{04}}{\rho_{03}}\right]_0 \quad 147)$$

$$F_{22} = \left(\frac{\gamma RT_{04}}{\rho_{03}\, Vol.}\right) \cdot \left[\frac{1}{2}(1+\phi_{22})\, \frac{\dot{m}_4}{T_{04}}\right]_0 \quad 148)$$

$$F_{23} = \left(\frac{\gamma RT_{04}}{\rho_{03} \cdot Vol.}\right)\left[(\phi_{21}+\psi_{21})\frac{\dot{m}_3 T_{03}}{N_G} - \phi_{22}\frac{\dot{m}_4 T_{04}}{N_G}\right]_0 \quad 149)$$

$$F_{31} = \left(\frac{30}{\pi I}\right) \cdot \left[(1-\mu_{12})\frac{\tau_2}{\rho_{03}} - \mu_{11}\frac{\tau_1}{\rho_{03}}\right]_0 \quad 150)$$

$$F_{32} = \left(\frac{30}{\pi I}\right)\left[-\frac{1}{2}\mu_{22} \cdot \frac{\tau_2}{T_{04}}\right]_0 \quad 151)$$

$$F_{33} = \left(\frac{30}{\pi I}\right)\left[\mu_{22}\cdot\frac{\tau_2}{N_G} - \mu_{21}\cdot\frac{\tau_1}{N_G}\right]_0 \quad 152)$$

$$G_{13} = \left(\frac{nRT_{04}}{Vol.}\right)\cdot\left[\dot{m}_3\left(1-\phi_{11}-\phi_{21}\right)\right.$$

$$\left. - \dot{m}_4\left(\tfrac{1}{2}+\phi_{12}-\tfrac{1}{2}\phi_{22}\right)\right]_0 \quad 153)$$

$$G_{21} = \left(\frac{\gamma RT_{04}}{p_{03}\cdot Vol.}\right)\cdot\left(\frac{h_{LHV}}{C_p}\right) \quad 154)$$

$$G_{23} = \left(\frac{\gamma RT_{04}}{p_{03}\cdot Vol.}\right)\cdot\left[\dot{m}_3 T_{03}\left(1-\phi_{11}-\phi_{21}-\psi_{11}-\psi_{21}\right)\right.$$

$$\left. - \dot{m}_4 T_{04}\left(\phi_{12}-\tfrac{1}{2}-\tfrac{1}{2}\phi_{22}\right)\right]_0 \quad 155)$$

$$G_{32} = \left(\frac{30}{\pi I}\right) \quad 156)$$

$$G_{33} = \left(\frac{30}{\pi I}\right)\cdot\left[\tau_2\left(\mu_{12}-\tfrac{1}{2}\mu_{22}\right) - \tau_1\left(1-\mu_{11}-\mu_{21}\right)\right]_0$$

157)

The turbomachinery coefficients are those given in

equations 20 through 27. The second subscript om the turbomachinery coefficients designates which turbomachine the coefficient is describing, i.e., 1 designates the compressor and 2 designates the turbine. The first subscript is as used before. All the terms not inside brackets are assumed to be some constant average value. The subscript 0 outside the brackets denotes evaluation at the linearization point.

CHAPTER III. COMPUTER SIMULATION

A. Choice of Computer Representation

The question as to which type of computer simulation to use is in many cases answered by the type of computer available. However, if a choice is possible some very simple criteria should govern the selection. Foremost among these criteria are the following:

i) cost per solution

ii) speed

iii) accuracy

iv) repeatability

v) adaptability

In terms of the previously given set of nonlinear system equations (134 through 142) a digital simulation would probably be the simplest and most straightforward to implement. The digital simulation has the advantages of high accuracy and excellent repeatability, and is fairly adaptable prior to run time. However, due to the high cost per solution, the non-real time nature of the solution, and the little or no hands on capability during run time the digital simulation is not used as the primary method.

It becomes obvious very quickly that the limiting factor in the analog simulation of any gas turbine is

the difficulty in accurately representing the full scale turbomachinery characteristics. Reference to works on the subject reveal a seemingly inordinate amount of analog equipment used in the turbomachinery representation (9, 10, 25). Even though an analog simulation would rate high on the criteria listed previously, it is not used as the primary simulation method due to the lack of analog equipment available.

Since a hybrid simulation by definition uses both analog and digital computers, it should ideally contain the best characteristics of both. In reality this is not the case due to interfacing and other considerations that will become evident shortly. The fundamental question that must be answered for the hybrid simulation is what should be the level of information transfer between the two computers? This should be as low as possible, with the majority of the computation being done on the analog computer and a minumum of computation and information transfer being done by the digital computer. However, a very real problem exists in trying to find the best compromise governed by analog equipment limitations and digital computation costs. The fewer nonlinear and function generation capabilities the analog computer has, the more computation and information transfer has to be

done by the digital computer.

In spite of the fact that a hybrid simulation introduces some additional problems to be considered, it is used as the primary simulation method in hopes of obtaining a simulation that contains many, if not all, of the attributes of both analog and digital simulations.

B. Analog Simulation

Due to equipment limitations the Mechanical Engineering EAI 680 analog computer is only suitable for simulation of linear models of gas turbines. The two possible linear models are the small scale or perturbation model and the large scale linear model. An analog computer simulation of the perturbation model can be used to provide extremely valuable dynamic information regarding stability and control systems design problems. A perturbation simulation of the gas turbine described in the previous chapter is used in the next chapter for the design of an appropriate fuel control for the engine. The large scale linear model is of necessity limited to the same range as is the perturbation model and is not generally used in dynamic analysis. This is due to the loss of information determined by the ratio of allowable perturbations to the steady state operating point

about which the system has been linearized. However, an analog simulation of the large scale linear model of a gas turbine can prove useful in checking out fuel control simulations in which the limiting of particular full scale variables is important. In addition, the large scale linear simulation can be used as a basis for a very simple hybrid simulation technique.

The differential equations of the open loop perturbation model of the gas turbine are given in the following matrix form:

$$\frac{d}{dt}\begin{bmatrix}\Delta p_{03}\\ \Delta T_{04}\\ \Delta N_G\end{bmatrix} = \begin{bmatrix}F_{11} & F_{12} & F_{13}\\ F_{21} & F_{22} & F_{23}\\ F_{31} & F_{32} & F_{33}\end{bmatrix}\cdot\begin{bmatrix}\Delta p_{03}\\ \Delta T_{04}\\ \Delta N_G\end{bmatrix} + \begin{bmatrix}0 & 0\\ G_{21} & 0\\ 0 & G_{32}\end{bmatrix}\cdot\begin{bmatrix}\Delta \dot{m}_f\\ \Delta T_L\end{bmatrix} \qquad 158)$$

where the Δ's refer to perturbations about some steady state operating point. The coefficients are as given in equations 144) through 157). The analog computer block diagram of this set of equations is shown in figure 11. The responses of this simulation to step increases in fuel flow and load torque of 3% of maximum are shown in figures 12 and 13 respectively.

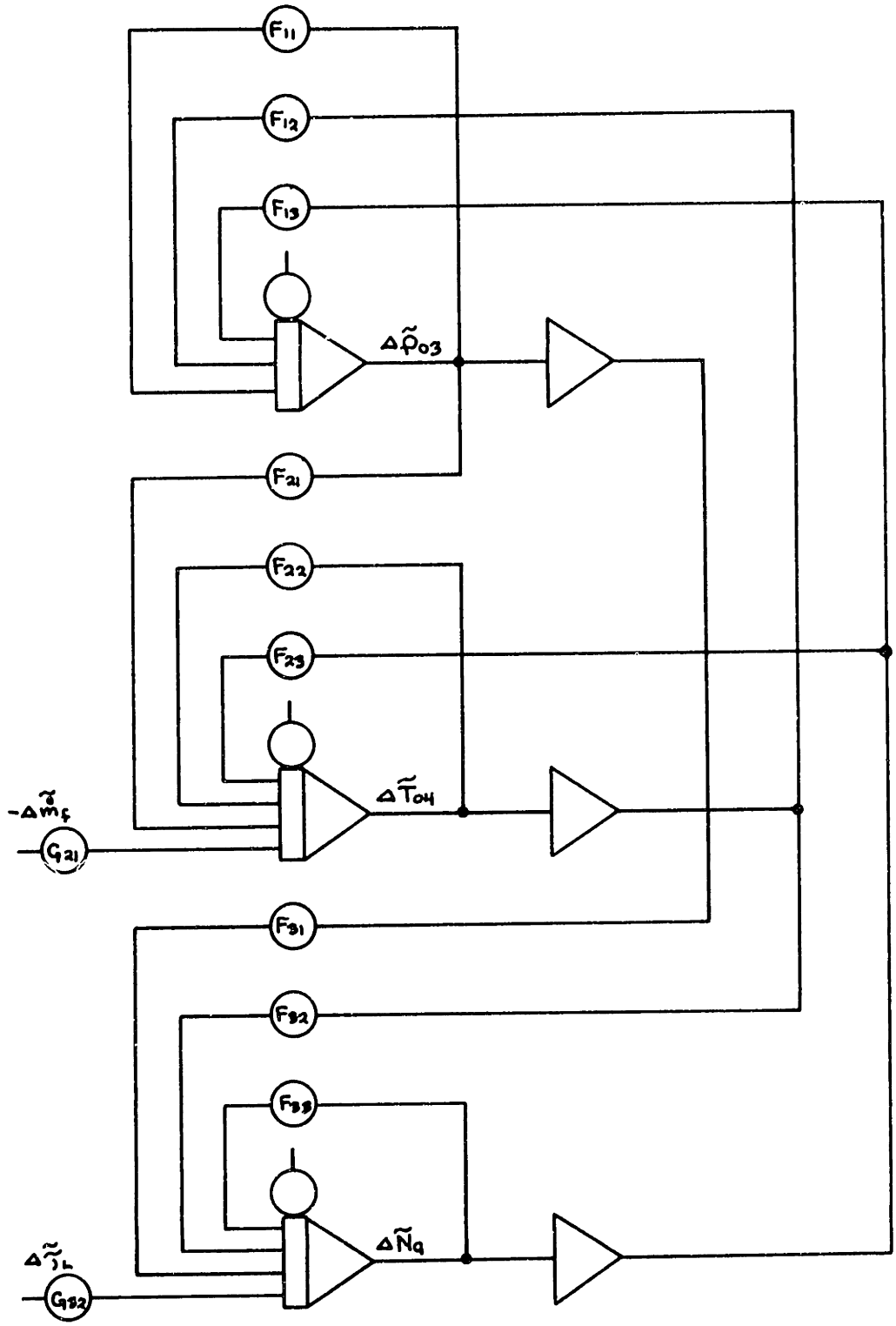
F11
F12
F13
$\Delta\tilde{\rho}_{03}$
F21
F22
F23
$\Delta\tilde{T}_{04}$
$-\Delta\tilde{m}_f$
G21
F31
F32
F33
$\Delta\tilde{N}_q$
$\Delta\tilde{\gamma}_L$
G32

Figure 11.

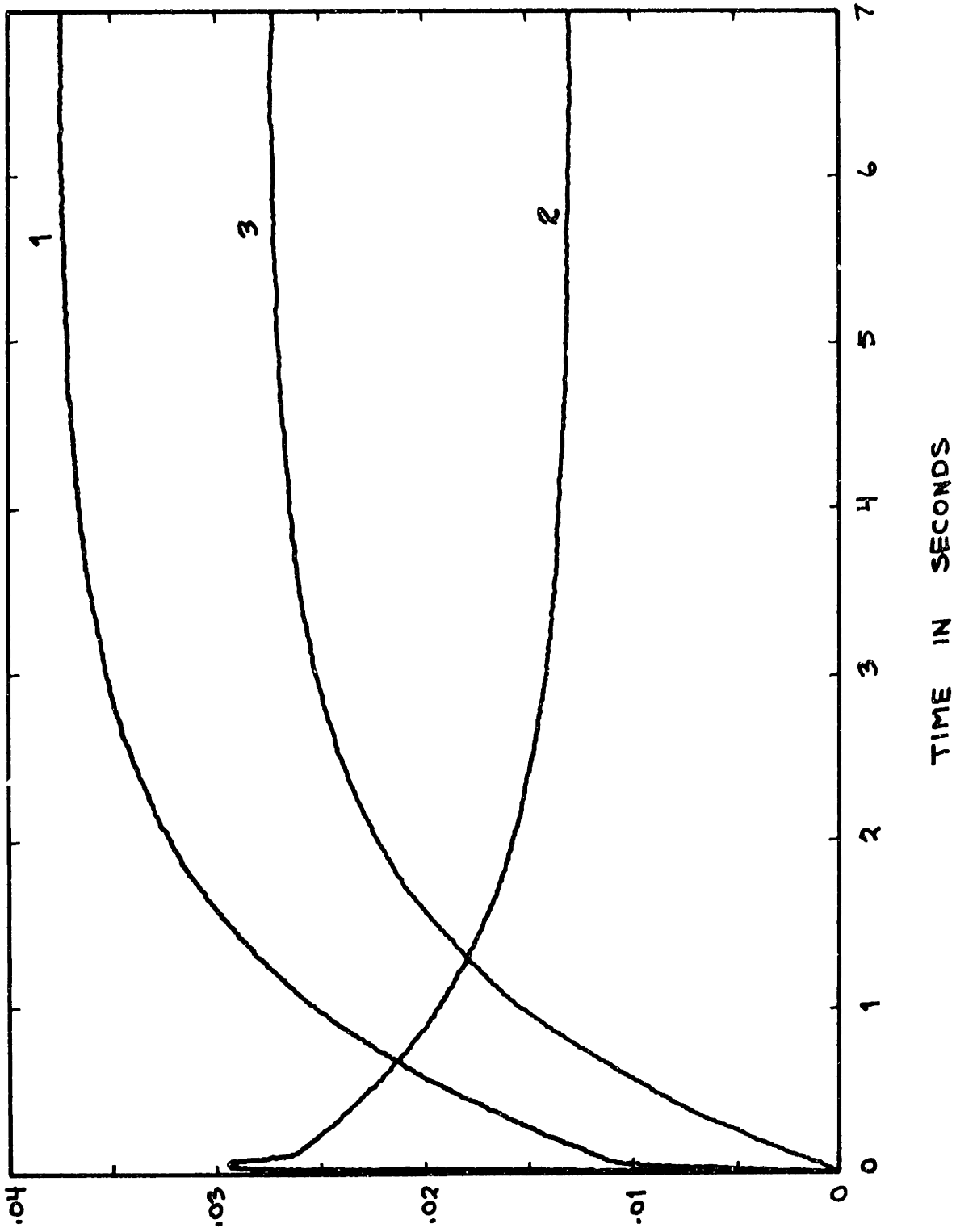

Figure 12.

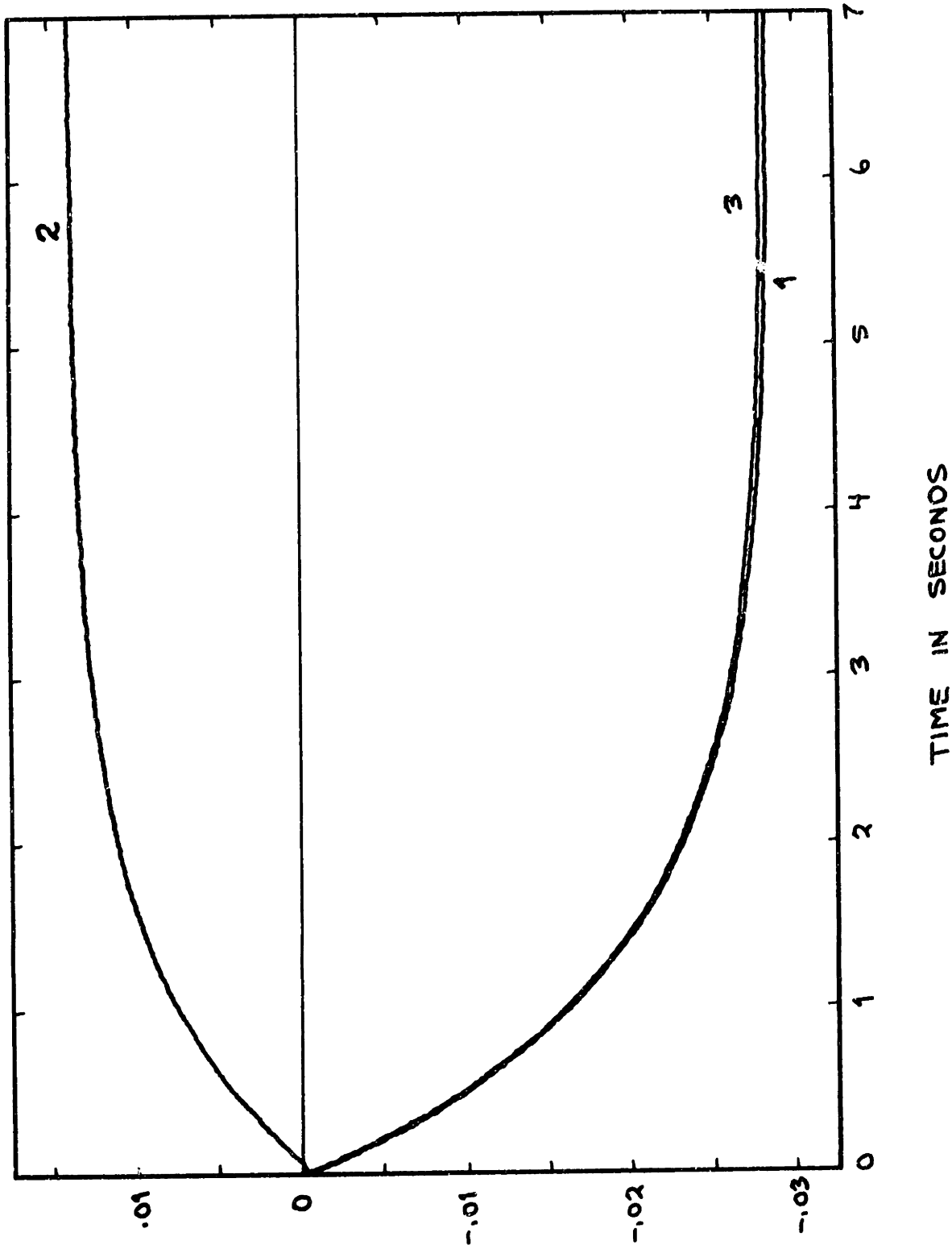

Figure 13.

In both of these responses the load torque is taken to be proportional to shaft speed squared. The change in load torque is accomplished by a change in the constant of proportionality. Curves 1, 2, and 3 of these responses represent $\Delta\tilde{P}_{03}$, $\Delta\tilde{T}_{04}$, and $\Delta\tilde{N}_G$ respectively. The tilda notation indicates that the variables have been scaled with respect to their maximum values.

From figures 12 and 13 it is possible to extract some general information regarding the dynamic characteristics of the single shaft gas turbine modeled. First of all, the single shaft gas turbine is inherently stable, which is to be expected. In addition to this, the gas turbine dynamics are essentially the rotor dynamics for all but the smallest elapsed times following an input disturbance. The variables $\Delta\tilde{P}_{03}$ and $\Delta\tilde{T}_{04}$ have some very fast initial transients following a fuel flow disturbance and then more or less follow the rotor speed, $\Delta\tilde{N}_G$, in a quasi-steady state fashion. For a load torque disturbance, $\Delta\tilde{P}_{03}$ and $\Delta\tilde{T}_{04}$ follow $\Delta\tilde{N}_G$ in a quasi-steady fashion for all times.

C. Hybrid Simulation

The simplest hybrid simulation conceptually is based on the large scale linear model previously

described. This model has fourteen coefficients in all, twelve state dependent and two assumed constant. The hybrid simulation uses DAM's (digital-to-analog multipliers) to implement the twelve variable coefficients. The values of the state and auxiliary variables are obtained digitally through the use of ADC's (analog-to-digital converters). The block diagram of the analog portion of the hybrid simulation, minus the timing circuitry, is shown in figure 14. The solid lines represent analog signals and the dashed lines represent digital signals. The pots are included downstream of the DAM's to allow for scaling of the DAM settings relative to their maximum values. This allows for DAM settings closer to 1.0 resulting in a more efficient use of the DAM bits available. The analog block diagram of the timing circuitry is shown in figure 15. This circuitry uses the analog clock and a BCD (binary coded decimal) counter to keep an accurate account of the elapsed time during a simulation run.

1. Description of Operation

The fundamental operation of this hybrid simulation is as follows:

i) The digital computer puts the analog computer into IC (initial condition) mode and then into

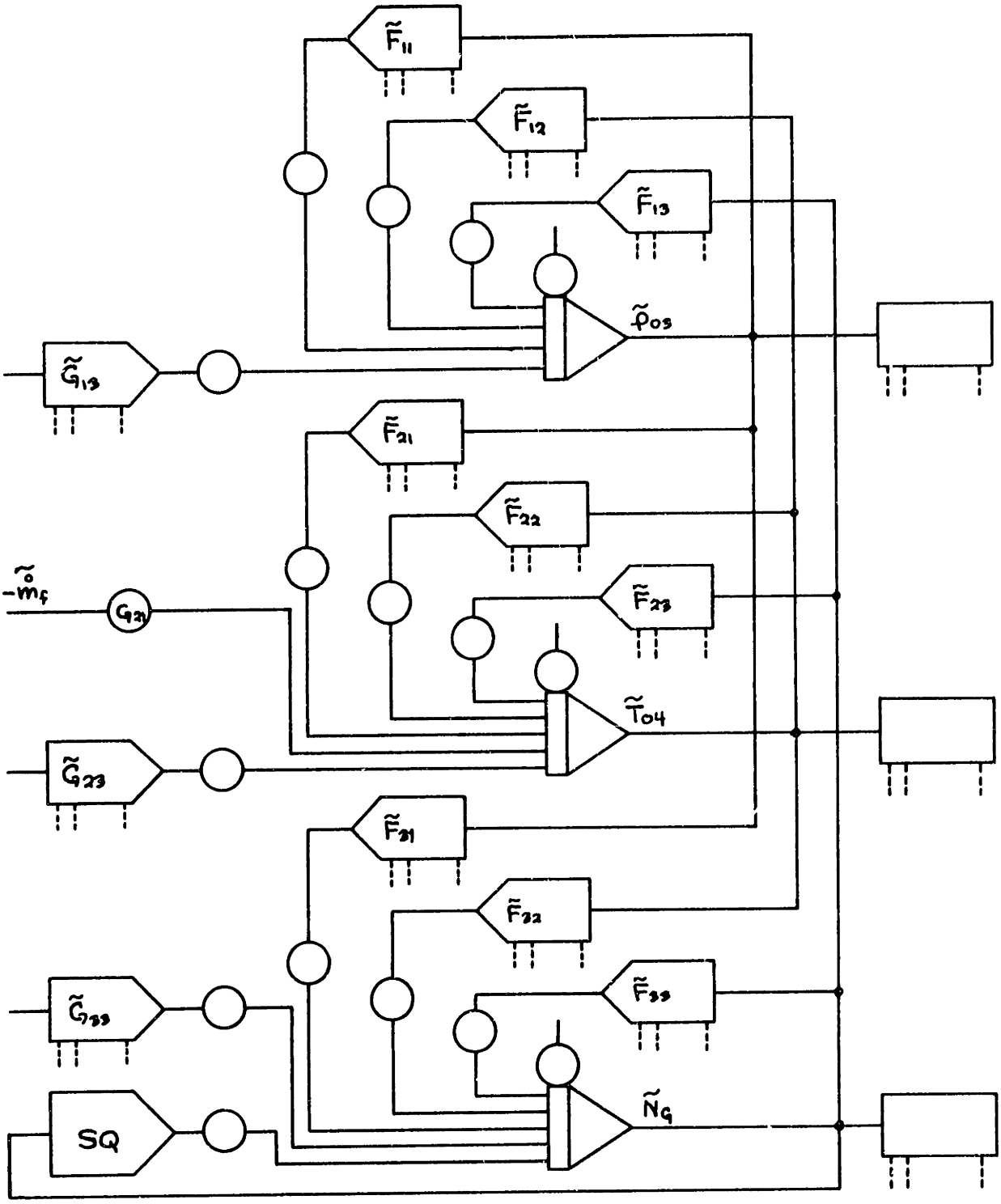
$\tilde{F}_{11}$
$\tilde{F}_{12}$
$\tilde{F}_{13}$
$\tilde{\rho}_{03}$
$\tilde{G}_{13}$
$\tilde{F}_{21}$
$\tilde{F}_{22}$
$-\tilde{\dot{m}}_f$
G_{23}
$\tilde{F}_{23}$
$\tilde{T}_{04}$
$\tilde{G}_{23}$
$\tilde{F}_{31}$
$\tilde{F}_{32}$
$\tilde{G}_{33}$
$\tilde{F}_{33}$
SQ
$\tilde{N}_4$

Figure 14.

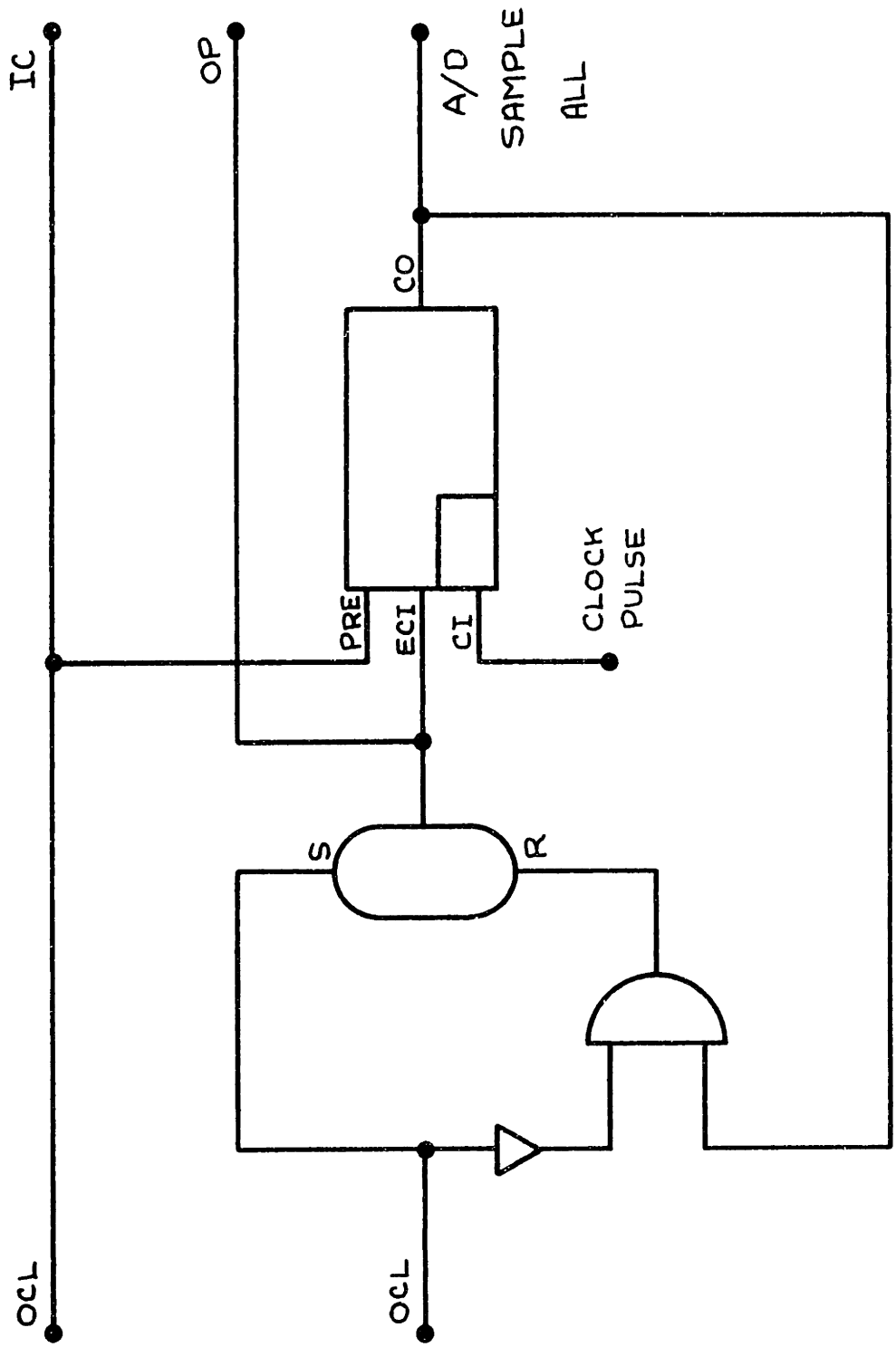

Figure 15.

HOLD mode.

ii) The digital computer reads the initial values of the state and auxiliary variables through the ADC's and stores them for output purposes.

iii) The digital computer calculates the values of the coefficients in terms of the values of the state variables just read.

iv) The digital computer sets the coefficients on the DAM's.

v) The digital computer puts the analog computer in OP (operate) mode.

vi) The analog computer integrates the linear system differential equations.

vii) When a pulse from the counter is sensed the analog computer puts itself into HOLD and the digital computer simultaneously reads the present values of the state and auxiliary variables through the ADC's and stores them.

viii) The digital computer checks to see if the state variables are outside some prescribed linear range corresponding to the present values of the coefficients. If the state variables are outside this range operation is transferred to step iii). If the state variables are within this range

operation is transferred to step v).

This sequence of steps proceeds from initial conditions until some prescribed final time is reached. The output of the simulation is a plot of the digitally stored state and auxiliary variables. A printout of the results is possible if desired. The computer listing of the digital part of the hybrid simulation is given in Appendix II.

The analog variables are scaled with respect to their maximum values. Again, the tilda notation denotes these scaled variables. The time is scaled down to one-tenth of real time to avoid loss of analog signals during the required HOLD periods. The hybrid technique used here can require HOLD periods up to one second in duration. With the fast integrating times associated with $\tilde{P}_{03}$ and $\tilde{T}_{04}$ these relatively long HOLD periods can allow for considerable drift if the time is not scaled down.

2. Results and Discussion

Figure 16 is the simulated open loop response of the gas turbine described in the last chapter to a step drop in fuel flow at the design point with standard load torque.

Step drop in $\tilde{\dot{m}}_f$: .4723 to .1959

Initial conditions : $\tilde{P}_{03} = .625$

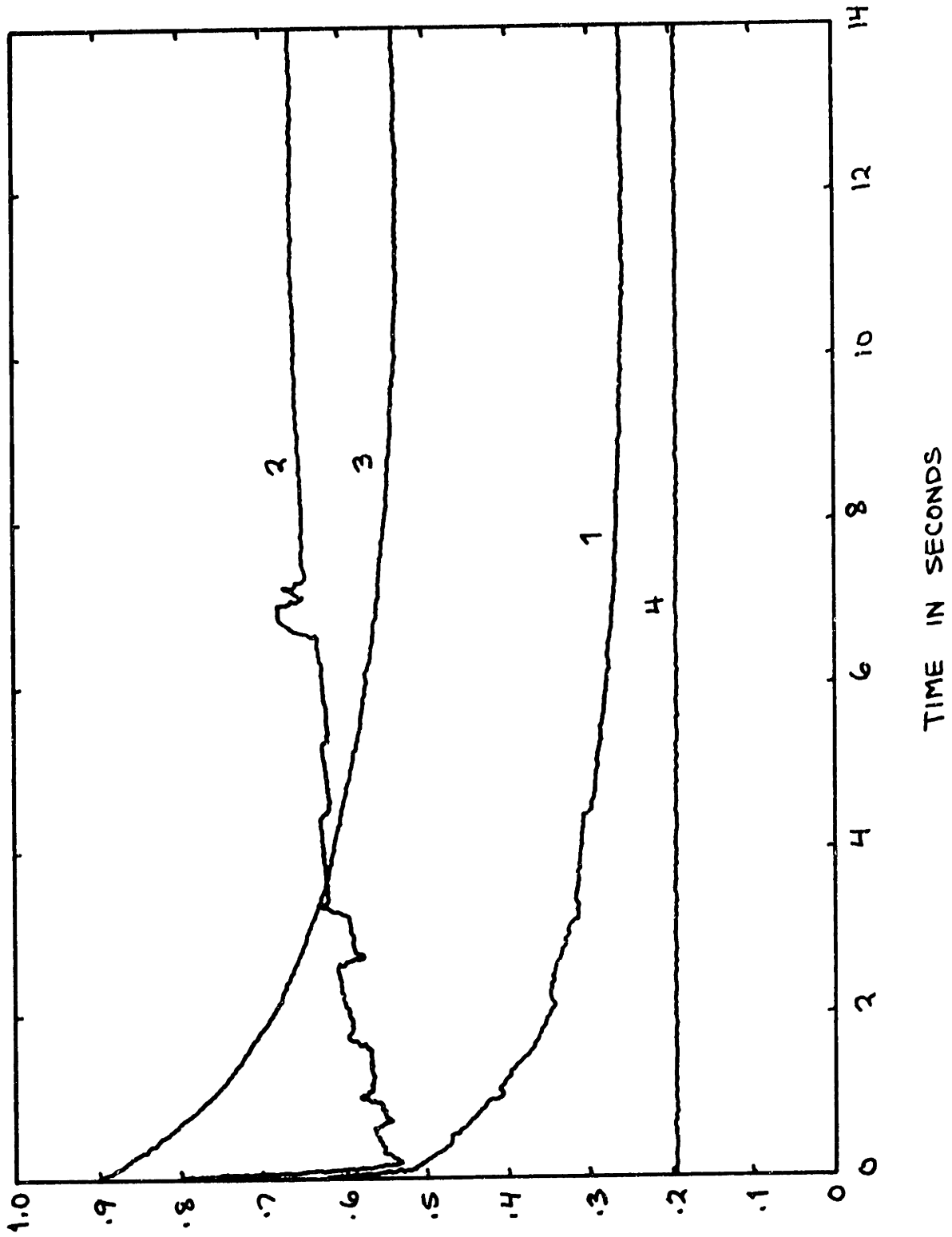

Figure 16.

Initial conditions : $\tilde{T}_{04} = .8056$

(continued) $\tilde{N}_G = .900$

Figure 17 is the simulated open loop response of the engine to a step drop in load torque with constant fuel flow.

Step drop in $\tilde{\tau}_L$: .06335 to 0.0

Fuel flow : $\tilde{\dot{m}}_f = .1959$

Initial conditions : $\tilde{P}_{03} = .234$

$\tilde{T}_{04} = .7285$

$\tilde{N}_G = .495$

In both of these responses, curves 1, 2, 3, and 4 refer to $\tilde{P}_{03}$, $\tilde{T}_{04}$, $\tilde{N}_G$, and $\tilde{\dot{m}}_f$ respectively.

An inspection of figures 16 and 17 will reveal some rather noisy responses corresponding to $\tilde{P}_{03}$ and especially $\tilde{T}_{04}$. In addition to this, the steady state values of the state variables do not closely agree with those predicted from a steady state analysis. The discrepancies are listed below.

Figure 16	$\tilde{P}_{03}$	$\tilde{T}_{04}$	$\tilde{N}_G$
hybrid simulation:	.26	.67	.53
steady state analysis:	.234	.730	.495
Figure 17			
hybrid simulation:	.60	.55	.97
steady state analysis:	.611	.561	.986

The errors associated with this simulation can be

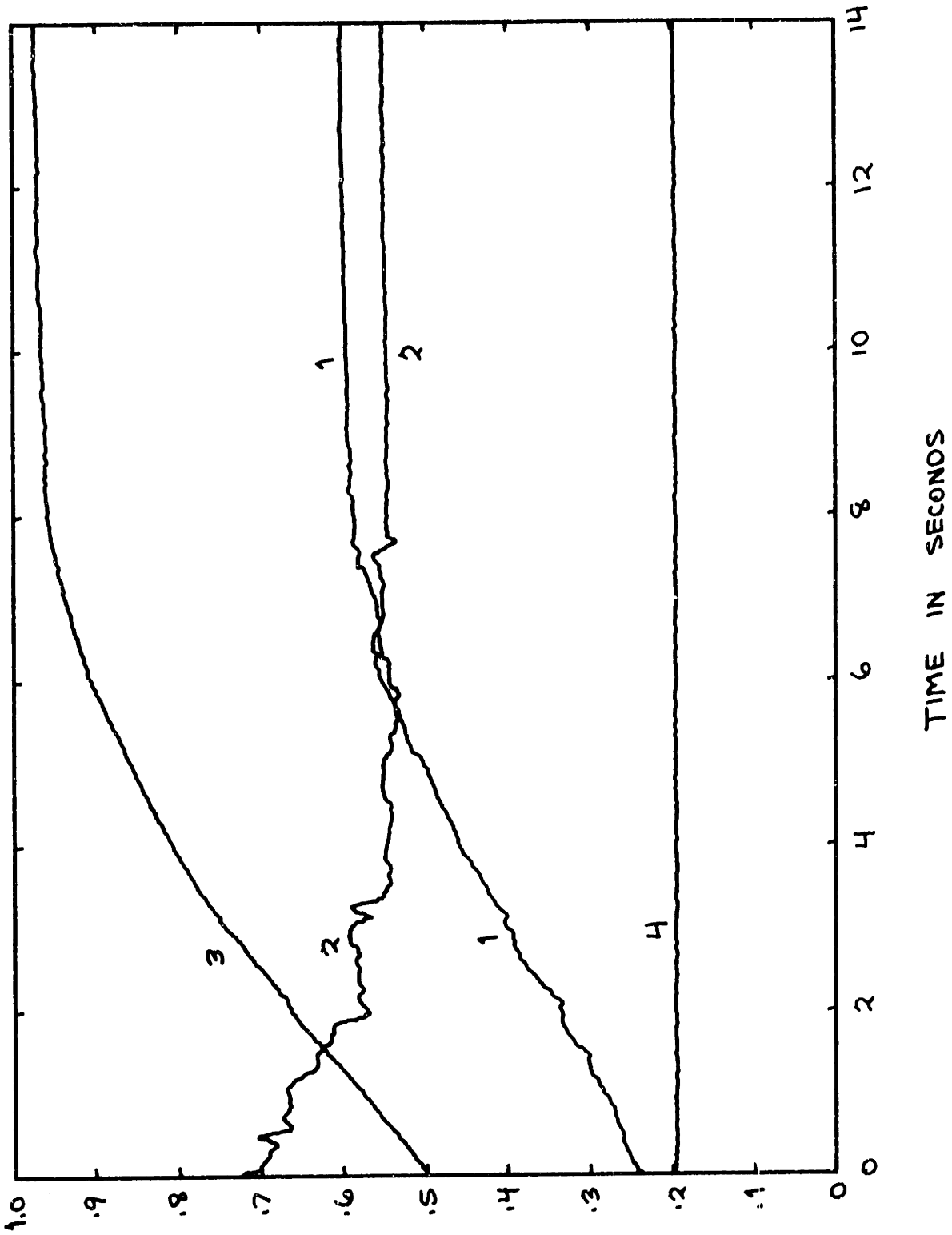

Figure 17.

grouped into two distinct groups. In the first group are the errors associated with the piecewise linear approximation to the nonlinear system equations. The second group contains the errors associated with the conversion processes and the conversion hardware. The noisy response curves have to be attributable to the second group only, while the steady state error is probably caused by both types of errors.

For all responses of this hybrid simulation the piecewise linear range of the state variables is taken to be 2% of maximum value. Although a detailed error analysis is not performed it is felt that the errors associated with the piecewise linear approximation contribute a minor percentage of the total steady state error. A detailed error analysis is beyond the scope of this thesis.

The hybrid operations of setting a DAM and reading an ADC have some errors associated with them. The fundamental, inescapable error is due simply to the maximum possible resolution associated with the conversion hardware, usually expressed in bits. For the Mechanical Engineering 1130-680 hybrid facility this is 10 bits for the DAM's (.001 machine units) and 9 bits for the ADC's (.002 machine units). This resolution is about the same magnitude as the noise

level on the EAI 680 analog computer and should not in itself cause any appreciable errors. Any other errors associated with the conversion processes are probably due to ncise and other spurious inputs.

Inspection of several successive responses revealed that the noise error appears to be random in character, while the steady state error is more or less repeatable. A monitoring of requested DAM settings and actual DAM settings as read from ADC's indicates that the combined processes have a resolution on the order of 7 bits (.01 machine units). The errors of this combined process appear to be random in nature, accounting for the noisy response curves. The very fact that steady state errors are more or less repeatable tends to indicate a basic error in the system equations in terms of a misevaluated constant or that the error is due to the piecewise linear approximation. An inspection of the system equations failed to uncover an error in constant evaluation.

The fact that the $\tilde{N}_G$ responses are smooth and that the $\tilde{\rho}_{03}$ and $\tilde{T}_{04}$ curves are noisy can be explained by the relative magnitudes of the gains associated with these three state variables. $\tilde{T}_{04}$ has the highest gains of the three with $\tilde{\rho}_{03}$ second. The gains associated with $\tilde{T}_{04}$ and $\tilde{\rho}_{03}$ are the same order of magnitude

and are almost two orders of magnitude larger than those associated with $\tilde{N}_q$. Thus, the $\tilde{N}_q$ circuitry has time constants such that the random errors associated with the setting of DAM's are effectively filtered out. On the other hand, the time constants of the $\tilde{\rho}_{03}$ and $\tilde{T}_{04}$ circuitry are the same order of magnitude as the shortest possible elapsed time between setting of DAM's. This allows $\tilde{\rho}_{03}$ and $\tilde{T}_{04}$ to effectively track the random DAM setting errors with appropriate gains and lags.

This type of tracking error can be reduced by two separate techniques. The first is to somehow make sure that the errors associated with the conversion processes are small enough so that the system outputs are essentially noise free. This technique may also help to reduce the steady state errors. However, this method of error reduction is directly coupled to the conversion hardware, which is for most cases out of the user's control. The second technique is to make the longest elapsed time between changes of DAM settings small compared with the smallest time constant of the system being simulated. This can be accomplished by time scaling the simulation to slow it down or by increasing the effective rate of change of DAM settings.

However, since it can be assumed that the hybrid

simulation was well designed to begin with it is not usually possible to increase the sampling rate. The sampling rate is determined by the amount of digital calculation required, which is commensurate with the amount of analog equipment available. Thus, the only possible solution is to slow down the simulation, keeping the sampling rate the same.

From this qualitative type of analysis two methods seem possible for a reduction in simulation errors. The first of these is to make the linear range of the state variables smaller and the second is to slow down the simulation. Since both of these methods will result in longer simulation runs and, thus, rising digital costs neither method was used. The trade-offs are complex to say the least, and a detailed analysis would be required to find the best solution to the problems inherent in this type of simulation.

For the purposes of this thesis the errors are recognized and accepted. From this point on all hybrid responses will be hand smoothed to eliminate the seemingly random noise. This hand smoothing is performed in preference to filtering as considerable information can be lost through the use of filters, either analog or digital. No attempt is made to

correct for the steady state errors. Figures 18 and 19 represent a hand smoothing of figures 16 and 17 respectively.

3. Possible Improved Hybrid Simulation

With reference to the fundamental sequence of operation of the hybrid simulation just described, it is apparent that considerable digital computation is required. If additional analog equipment were available beyond that offered by the Mechanical Engineering EAI 680 analog computer an improved hybrid simulation would be possible. This improved simulation would piecewise linearize the turbomachinery characteristics only. All other nonlinearities in equations 134) through 142) would be handled directly on the analog computer.

The linearized independent turbomachinery characteristics can be expressed as:

$$\frac{\dot{m}\sqrt{T_{01}}}{p_{01}} = C_1 + C_2 \cdot \frac{p_{02}}{p_{01}} + C_3 \cdot \frac{N}{\sqrt{T_{01}}} \qquad 159)$$

$$\frac{T_{02}}{T_{01}} = C_4 + C_5 \cdot \frac{p_{02}}{p_{01}} + C_6 \cdot \frac{N}{\sqrt{T_{01}}} \qquad 160)$$

where,

$$C_1 = \left(\frac{\dot{m}\sqrt{T_{01}}}{p_{01}}\right)_o \cdot \left(1 - \phi_1 - \phi_2\right) \qquad 161)$$

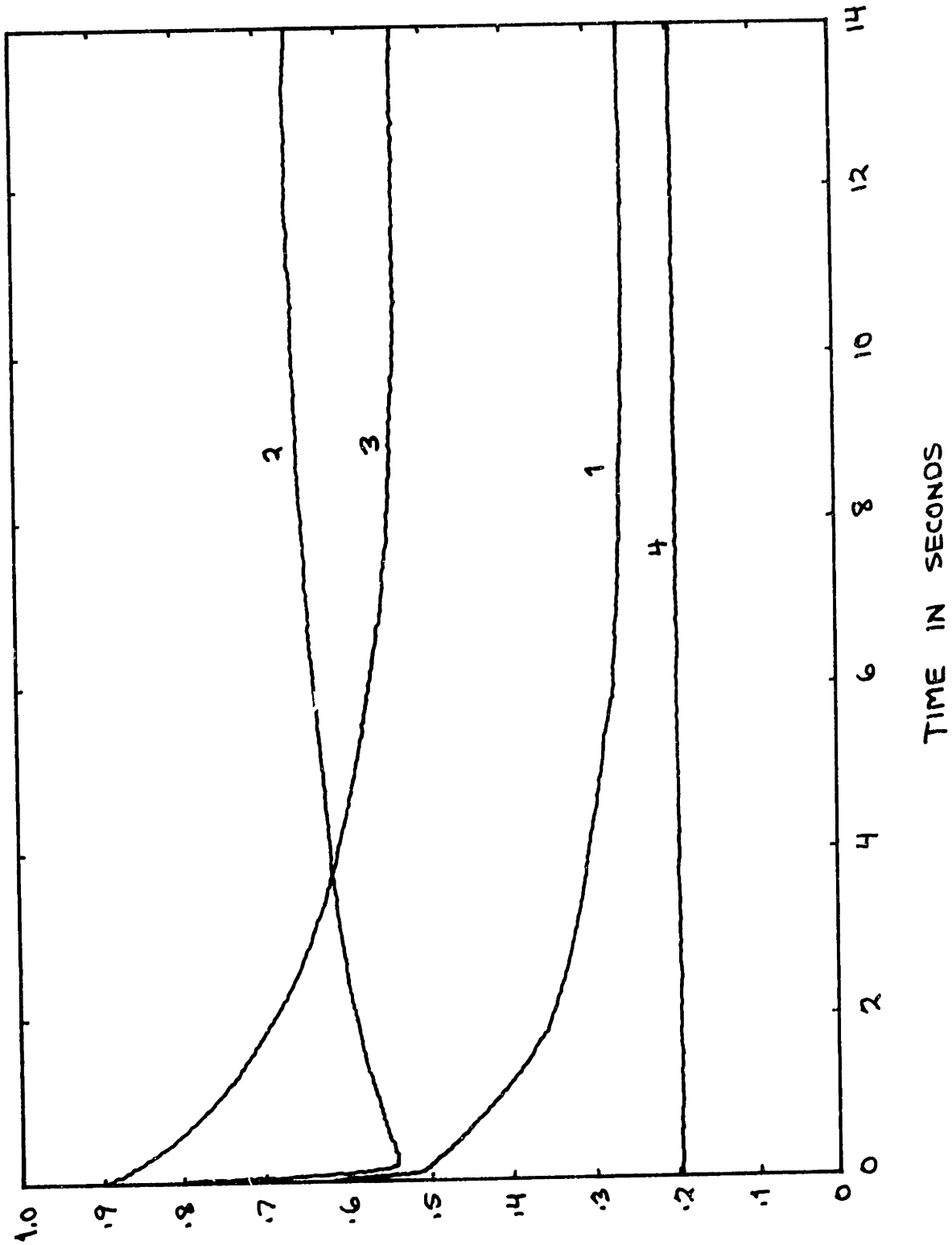

Figure 18.

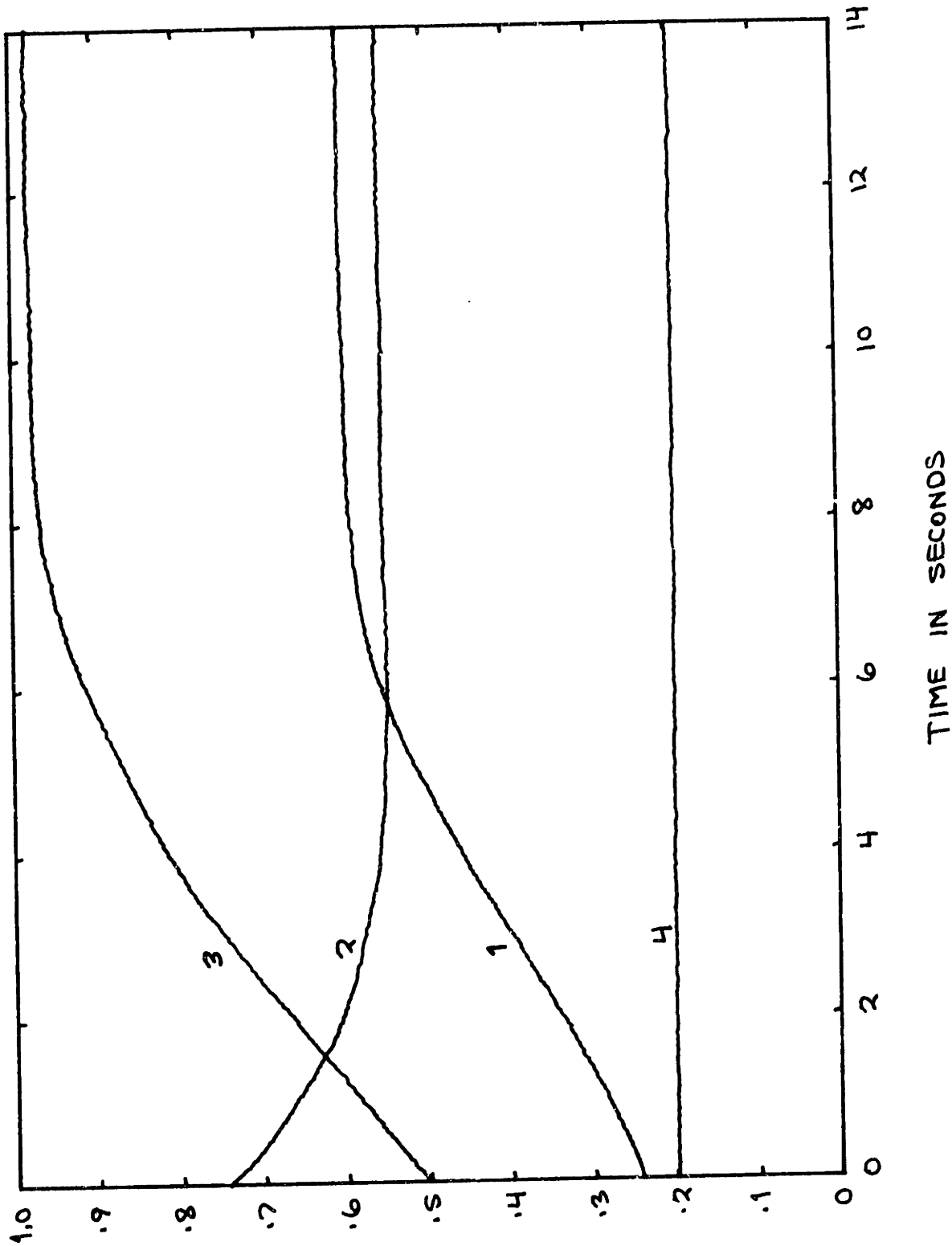

Figure 19.

$$C_2 = \phi_1 \qquad 162)$$

$$C_3 = \phi_2 \qquad 163)$$

$$C_4 = \left(\frac{T_{02}}{T_{01}}\right)_0 \cdot \left(1 - \psi_1 - \psi_2\right) \qquad 164)$$

$$C_5 = \psi_1 \qquad 165)$$

$$C_6 = \psi_2 \qquad 166)$$

The ϕ's and ψ's are those defined in equations 20) through 23), and the subscript 0 outside the parentheses denotes evaluation at the linearization point. Upon rearranging and including the torque:

$$\dot{m} = \frac{p_{01}}{\sqrt{T_{01}}} \cdot \left[C_1 + C_2 \cdot \frac{p_{02}}{p_{01}} + C_3 \frac{N}{\sqrt{T_{01}}} \right] \qquad 167)$$

$$T_{02} = T_{01} \cdot \left[C_4 + C_5 \cdot \frac{p_{02}}{p_{01}} + C_6 \frac{N}{\sqrt{T_{01}}} \right] \qquad 168)$$

$$\tau = \left(\frac{30 C_p}{\pi}\right) \frac{\dot{m}\,(T_{01} - T_{02})}{N} \qquad 169)$$

An inspection of these equations reveals that, in general, each turbomachine thus represented would require three multipliers, four dividers, one square

rooter, three summers, and six DAM's. This represents a considerable investment in analog equipment, but it might prove to be worthwhile.

In terms of the particular gas turbine model used in this thesis, such a hybrid simulation would require six multipliers, five dividers, one square rooter, nine summers, three integrators, twelve DAM's, seven ADC's, about twenty pots, and about ten inverters. This represents quite an increase in analog equipment over that presently available.

The turbomachinery coefficients, the C's, are dependent on the pressure ratio and corrected speed only. The coefficients are constant for some prescribed linear range and would be stored in two-dimensional arrays in the digital computer. The only computation required of the digital computer would be to read the values of the pressure ratios and the corrected speeds, and to determine the array indices by means of some modulo arithmetic calculations, and to set the DAM's to the corresponding coefficient values.

This digital computation represents a bare minimum and would allow for a greatly increased sampling rate. This simulation might even allow for continuous operation without putting the analog computer in HOLD, resulting in a hybrid simulation that would be far

superior to that used here.

D. Digital Simulation

The digital simulation used in this thesis is used only as a means of checking the accuracy with which the hybrid simulation integrates the system differential equations. The validity of this checking procedure depends on the assumption that the digital simulation is capable of producing more accurate results, which is the case in practice. In addition the digital simulation is used to check the validity of the polytropic approximation used in the development of the system differential equations. The digital simulation is used to predict open loop response only. The extension to closed loop response is very straightforward.

Two distinct methods of digital simulation can be used. The first is basically the digital implementation of the hybrid simulation used in this thesis. This type of simulation uses a piecewise linear model of the gas turbine and integrates the equations using matrix exponentiation (2, 26). The second is the numerical integration of the complete nonlinear system equations. Variations in this method can be found and consist primarily of differences in the representation of the turbomachinery characteristics. For cases in

which the characteristics are available in the form of performance maps only, some sort of table look-up is necessary. By far the most efficient method in this case is offered by the piecewise linear approximation to the characteristics presented in the preceeding section. The other method of representing the turbomachinery is functional or algebraic representation, and is typically much more difficult to come by.

The digital simulation used in this thesis uses DYSYS to integrate the nonlinear differential equations, and uses the algebraic representation of the turbomachinery characteristics given in Appendix I. The computer listing of the digital simulation is given in Appendix III.

1. Analysis of Polytropic Approximation

The first area to be investigated with the digital simulation is the validity of the polytropic approximation introduced to obtain equations 71) and 73) from equations 43) and 62). This is done by using the system equations 134) through 142) with three different forms for equations 134) and 135). These three forms are:

a) $$\frac{d}{dt}(\rho_3) = \left(\frac{1}{Vol.}\right)\cdot\left[\dot{m}_3 - \dot{m}_4\right] \qquad 134\text{-a)}$$

$$\frac{d}{dt}(\rho_3 T_{04}) = \left(\frac{\gamma}{Vol.}\right)\cdot\left[\dot{m}_3 T_{03} + \dot{m}_f\left(\frac{h_{LHV}}{c_p}\right) - \dot{m}_4 \cdot T_{04}\right] \qquad 135\text{-a)}$$

$$p_{03} = \rho_3 R T_{04} \qquad 65\text{-a)}$$

This form represents the lumped parameter fluid mass and energy conservation equations with the approximate equation of state giving the total pressure.

b) $$\frac{d}{dt}(p_{03}) = \left(\frac{nRT_{04}}{Vol.}\right)\cdot\left[\dot{m}_3 - \dot{m}_4\right] \qquad 134\text{-b)}$$

$$\frac{d}{dt}(T_{04}) = \left(\frac{n-1}{n}\right)\left(\frac{\gamma R T_{04}}{p_{03}\cdot Vol.}\right)\cdot\left[\dot{m}_3 T_{03} + \dot{m}_f\left(\frac{h_{LHV}}{c_p}\right) - \dot{m}_4 T_{04}\right] \qquad 135\text{-b)}$$

This form represents the polytropic approximation applied to both the mass and energy conservation equations. The terms in the parentheses preceeding the brackets are assumed to take on some constant average value.

c) $$\frac{d}{dt}(p_{03}) = \left(\frac{nRT_{04}}{Vol.}\right)\cdot\left[\dot{m}_3 - \dot{m}_4\right] \qquad 134\text{-c)}$$

$$\frac{d}{dt}(T_{04}) = \left(\frac{\gamma R T_{04}}{p_{03}\cdot Vol.}\right)\cdot\left[\dot{m}_3\cdot T_{03} + \dot{m}_f\left(\frac{h_{LHV}}{c_p}\right) - \dot{m}_4 T_{04}\right] \qquad 135\text{-c)}$$

This is the form finally used. This representation applies the polytropic approximation to relate density

changes to pressure changes in the mass conservation equation, but assumes that the density is constant in the energy conservation equation. Again, the terms in the parentheses preceeding the brackets are assumed to be constant.

Figure 20 represents the response of the system representation described in a) to a step drop in fuel flow at the design point. Figures 21 and 22 represent the responses of the system representations described in b) and c) respectively. From these responses it can be seen that neither approximation b) or c) accurately describe the results of using representation a). However, representation c) is the approximation used in the system equations because after .1 second elapsed time this gives the same result as a).

2. Comparison of Results

The responses of this section use the system representation a) of the preceeding section since the results are identical to c) after .1 second and representation a) is slightly more stable in the integration scheme used, allowing for the use of larger time steps.

Figure 23 represents the response of the digital gas turbine simulation to a step drop in fuel flow at

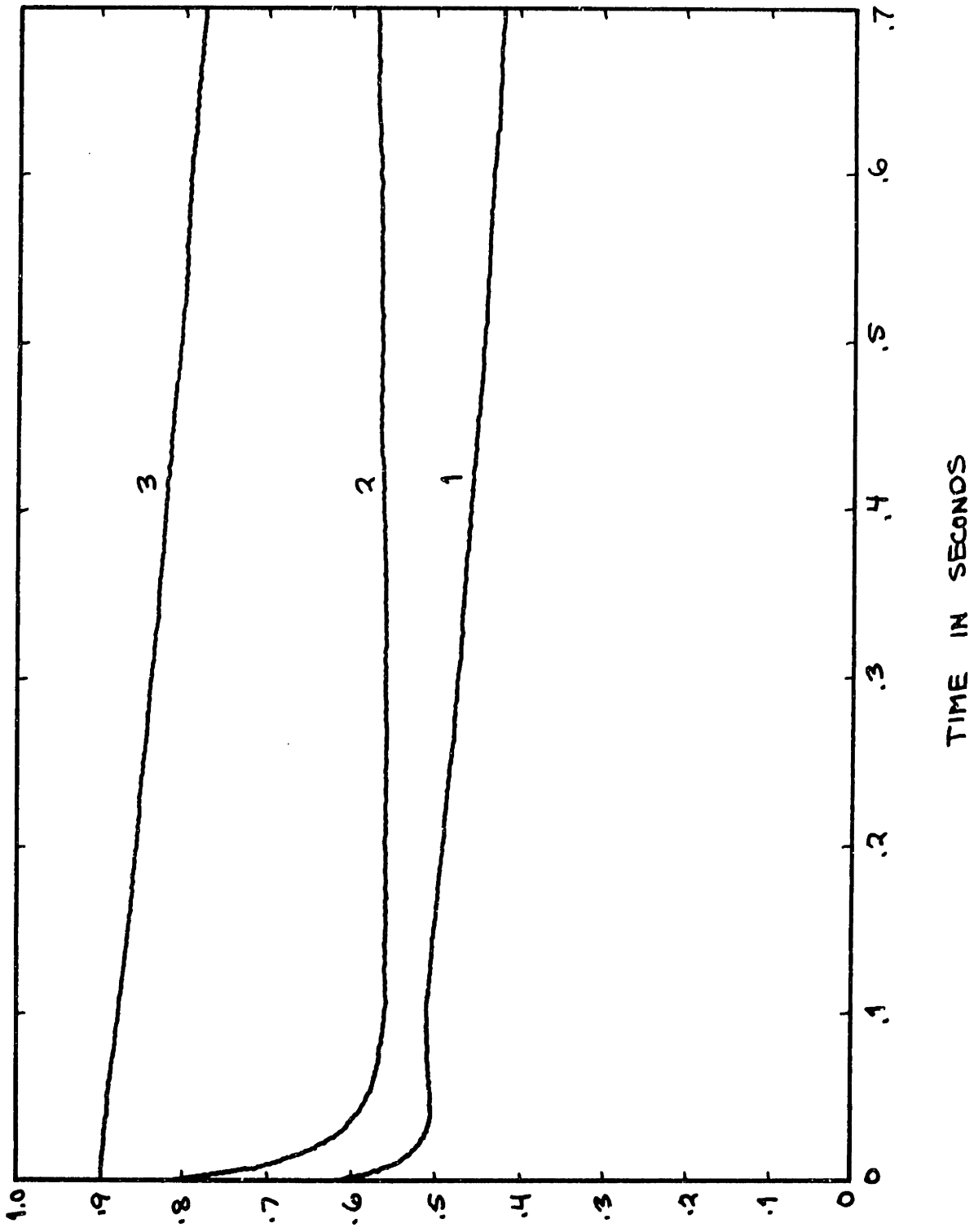

Figure 20.

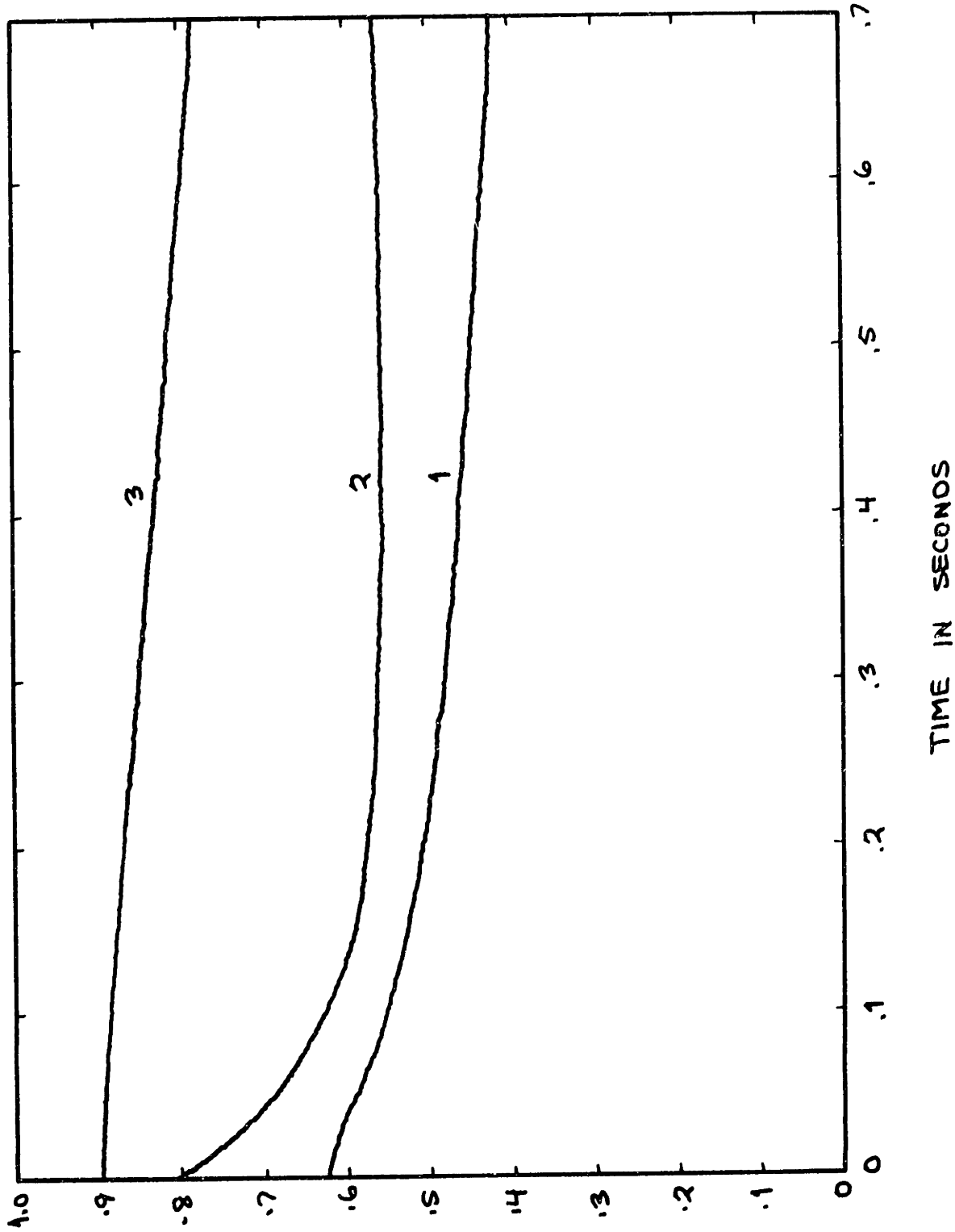

Figure 21.

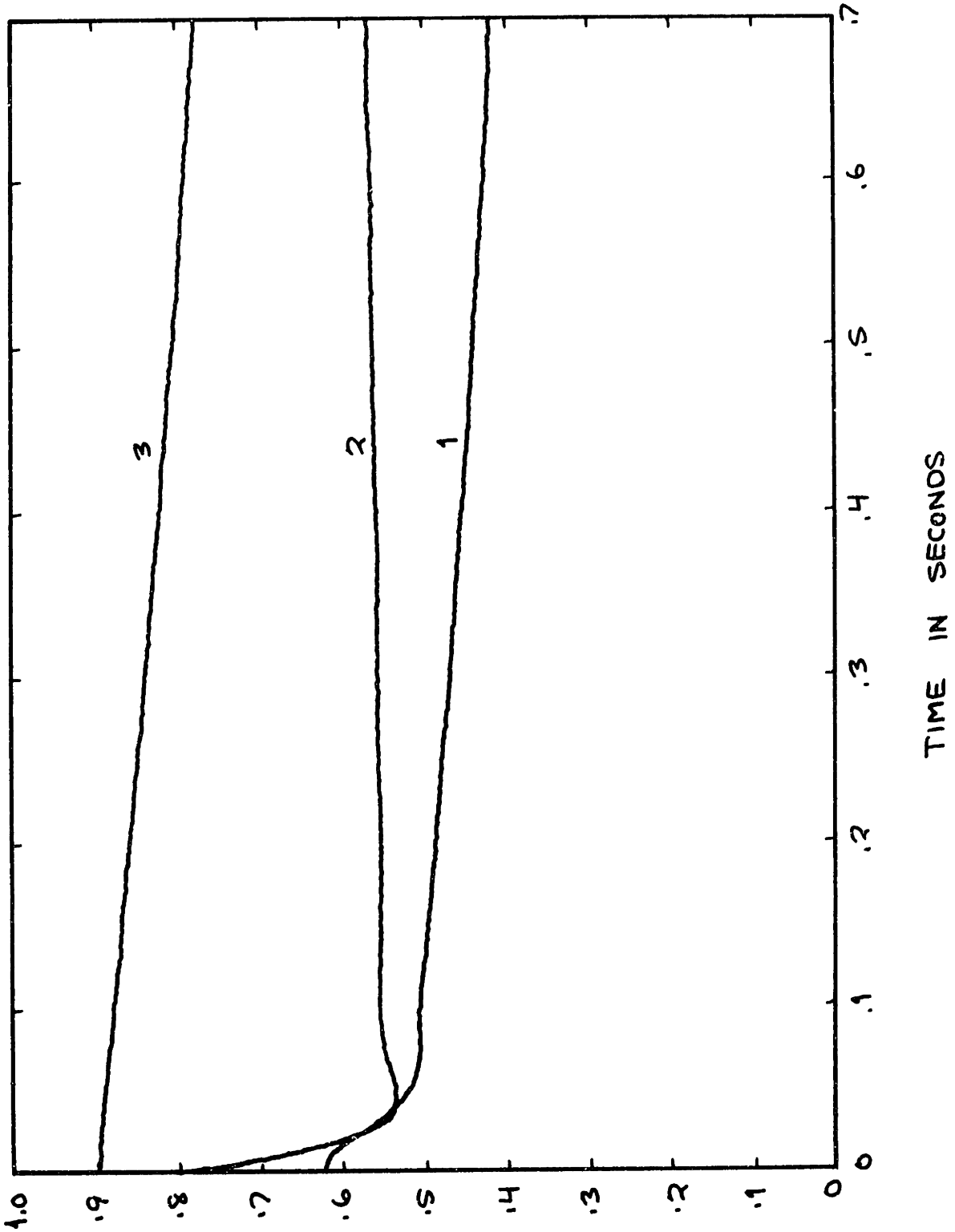

Figure 22.

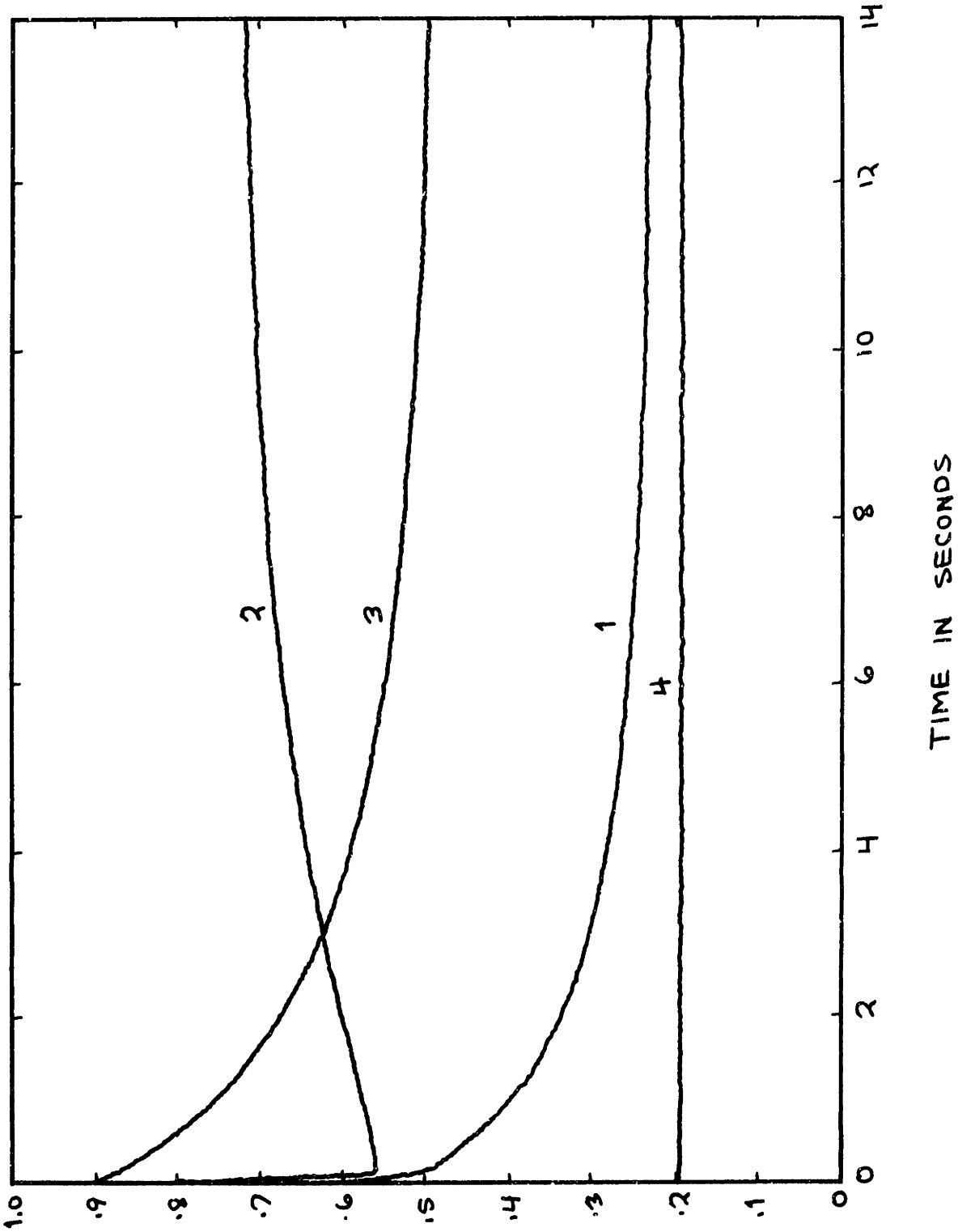

Figure 23.

the design point with standard load torque. This is the digital "analog" of the hybrid response of figure 18.

Step drop in $\tilde{\dot{m}}_f$: .4723 to .1959

Initial conditions: $\tilde{P}_{03} = .625$

$\tilde{T}_{04} = .8056$

$\tilde{N}_G = .900$

Figure 24 is the response of the digital simulation to a step drop in load torque with constant fuel flow. This is the analog of figure 19.

Step drop in $\tilde{\tau}_L$: .06335 to 0.0

Fuel flow: $\tilde{\dot{m}}_f = .1959$

Initial conditions: $\tilde{P}_{03} = .234$

$\tilde{T}_{04} = .7285$

$\tilde{N}_G = .495$

The nomenclature for the response curves is the same as that given previously.

From comparisons of figure 18 with figure 23 and figure 19 with figure 24 it is apparent that the hybrid simulation suffers somewhat from substandard accuracy. The nature of the difference indicates that if the steady state error of the hybrid simulation could be reduced the two simulations might produce more nearly identical results. The breakdown of the steady state errors is given by the following:

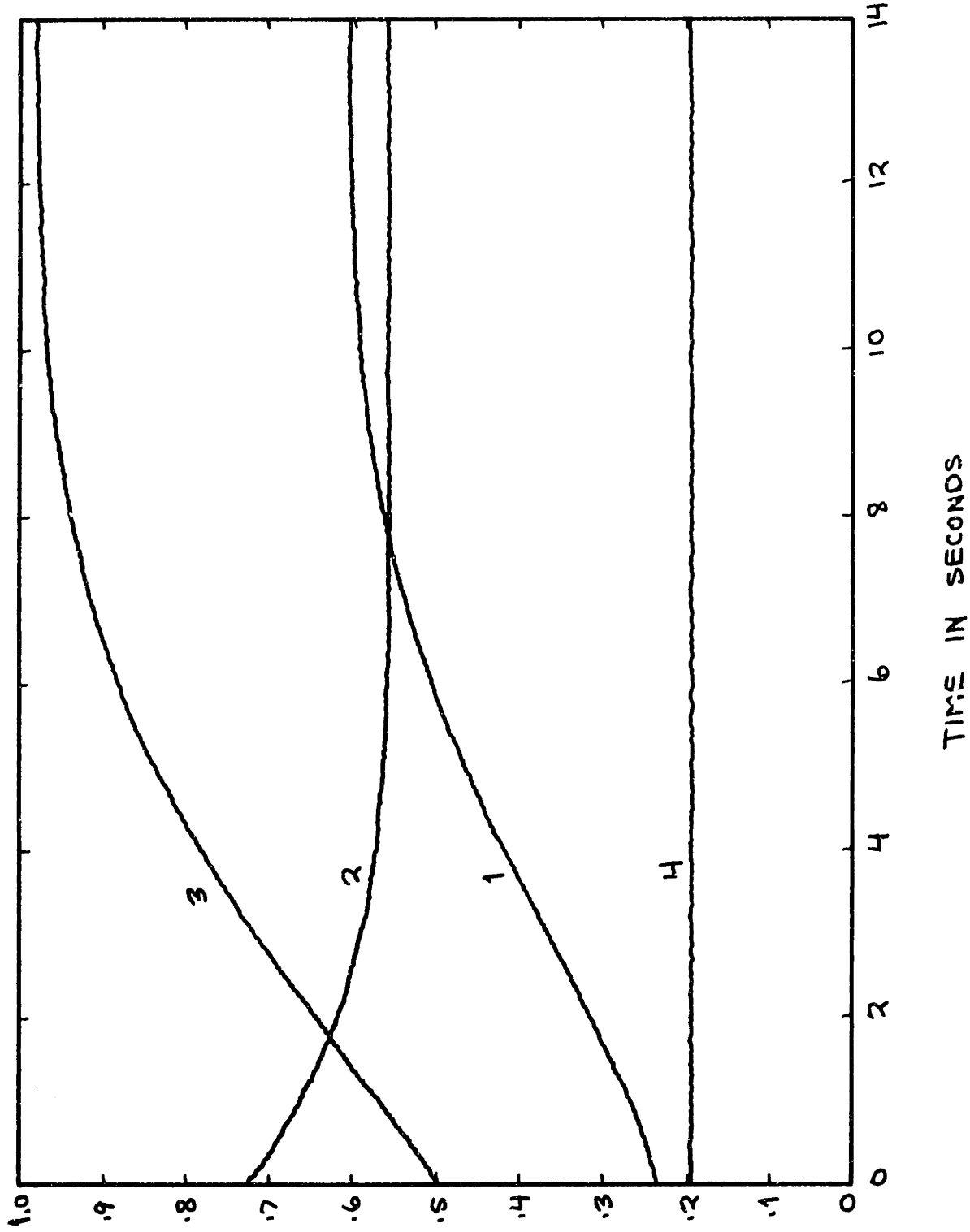

Figure 24.

Step drop in $\tilde{\dot{m}}_f$	$\tilde{P}_{03}$	$\tilde{T}_{04}$	$\tilde{N}_G$
hybrid simulation:	.26	.67	.53
steady state analysis:	.234	.730	.495
digital simulation:	.230	.719	.497
Step drop in $\tilde{\tau}_L$			
hybrid simulation:	.60	.55	.97
steady state analysis:	.611	.561	.986
digital simulation:	.608	.561	.984

This comparison only serves to indicate how accurately the hybrid simulation can integrate the system differential equations and does not give an indication of the accuracy of the model used in describing engine performance.

CHAPTER IV. CONTROL

A. Basic Control Requirements

Modern day gas turbines of necessity have a multitude of control requirements that have to be satisfied for successful engine operation. An attempt to discuss any but the most fundamental of these requirements is beyond the scope of this thesis. The following listing serves to illustrate some of the variety of control requirements that are imposed on gas turbine fuel controls.

i) Maintain a desired speed of rotation.

ii) Limit the rates at which the engine is allowed to accelerate or decelerate.

iii) Limit the rate of change of fuel flow.

iv) Limit the maximum and/or minimum of engine variables such as turbine inlet temperature, compressor discharge pressure, rotational speed, and fuel flow.

v) Provide scheduling of variable geometry and bleed air devices.

vi) Provide scheduling of engine startup and shutdown.

For a further listing and discussion of gas turbine fuel control requirements, the interested reader is referred to works on the subject (27, 28, 29, 30, 31,

32, and 33).

For the purposes of this thesis only a few of the more fundamental fuel control requirements are imposed.

i) Speed regulation

ii) Engine acceleration and deceleration limiting

iii) Transient fuel rate limiting

1. Speed Regulation

For most applications involving gas turbines the ability to set a desired speed and have the fuel control maintain the engine at that speed is a very desirable attribute. Speed is typically directly associated with variables of interest, such as jet engine thrust, power generation frequency, and speed in propulsion applications. The ability to maintain a given engine speed gives the ability to control the output variable of interest.

The design of a speed regulator for a particular gas turbine is a straightforward application of classical control theory, discussed in great detail in any undergraduate text on systems analysis and control theory. The three basic types of regulators that are applicable to this problem are proportional (P), proportional-integral (PI), and proportional-integral-derivative (PID) regulators. Of these three the PI

regulator is chosen because it has the ability to accurately hold a preselected speed and because it is fairly simple to implement and provides for good performance. An attempt to implement a PID regulator failed to produce any significant improvements in system performance over that of the PI regulator.

The PI regulator for the single shaft gas turbine takes the following form:

$$\Delta\tilde{\dot{m}}_f = \left(K_1 + \frac{K_2}{S}\right)\cdot\left(\tilde{N}_{G\,set} - \tilde{N}_G\right) \qquad 170)$$

where,

K_1 = proportional constant

K_2 = integral constant

S = Laplacian operator

$\tilde{N}_{G\,set}$ = desired engine speed (scaled)

$\tilde{N}_G$ = actual engine speed (scaled)

$\Delta\tilde{\dot{m}}_f$ = change in fuel flow (scaled)

The constants K_1 and K_2 have to be determined for each different application, and can be evaluated by a "knob turning" technique on the analog computer.

The value of K_1 is chosen to be 5.0 to provide what seems to be a reasonable proportional gain. If K_1 were chosen to be too large, a small speed disturbance would cause a very large change in the turbine

inlet temperature, which is undesirable. Figure 25 shows a series of controlled engine speed responses to a step increase in speed demand for various values of K_2. The value of K_2 of 6.25 is chosen to provide a response with good rise time, reasonable overshoot, and good settling time. The response of all the variables to a step rise in speed demand of .01 at the design point is shown in figure 26. The response to a step rise in torque of .01 at the design point is shown in figure 27. The nomenclature is the same as previously used for the hybrid simulation, except that the variables represent perturbations.

The PI regulator provides a perfectly satisfactory solution to the speed regulation requirement, and is used as the speed regulation section of the full blown fuel control used to control the hybrid simulated gas turbine case study.

The problem of designing an optimal speed regulator for a gas turbine can be handled quite readily using modern control theory principles. One problem with this approach is that the constants in the perturbation model of the gas turbine are state dependent and, thus, the optimal regulator coefficients are state dependent. This would add more complexity to an already complex fuel control. Another problem is

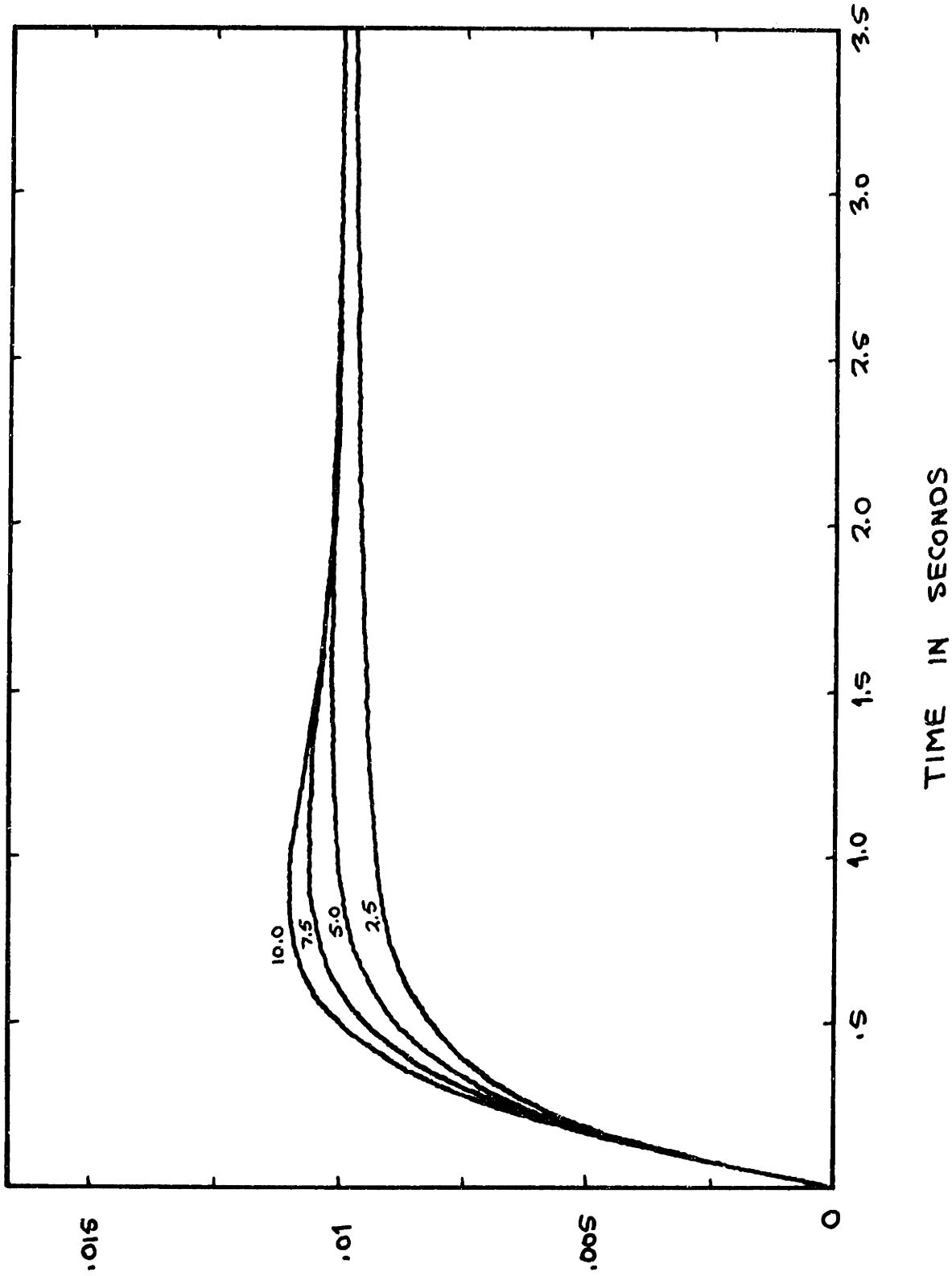

Figure 25.

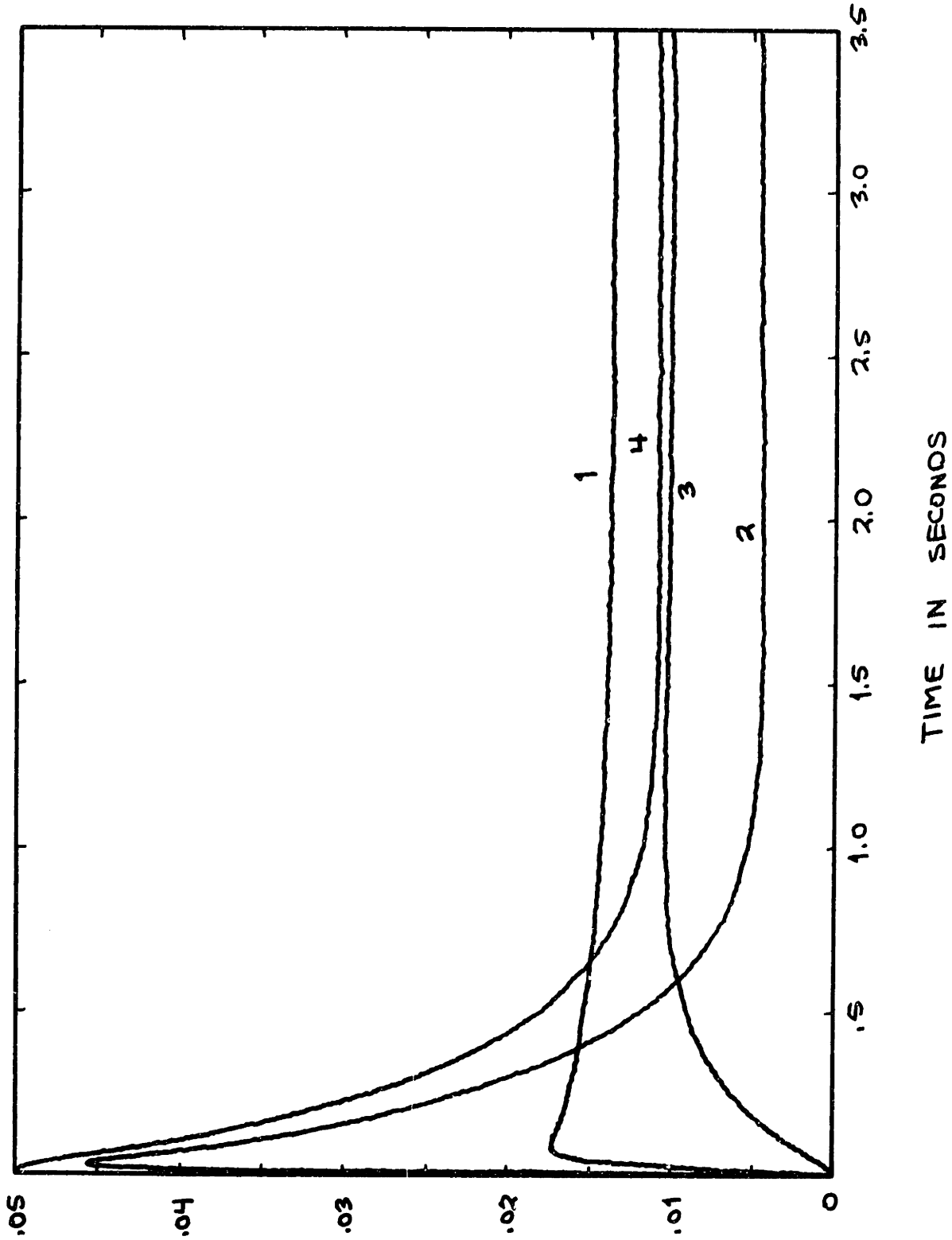

Figure 26.

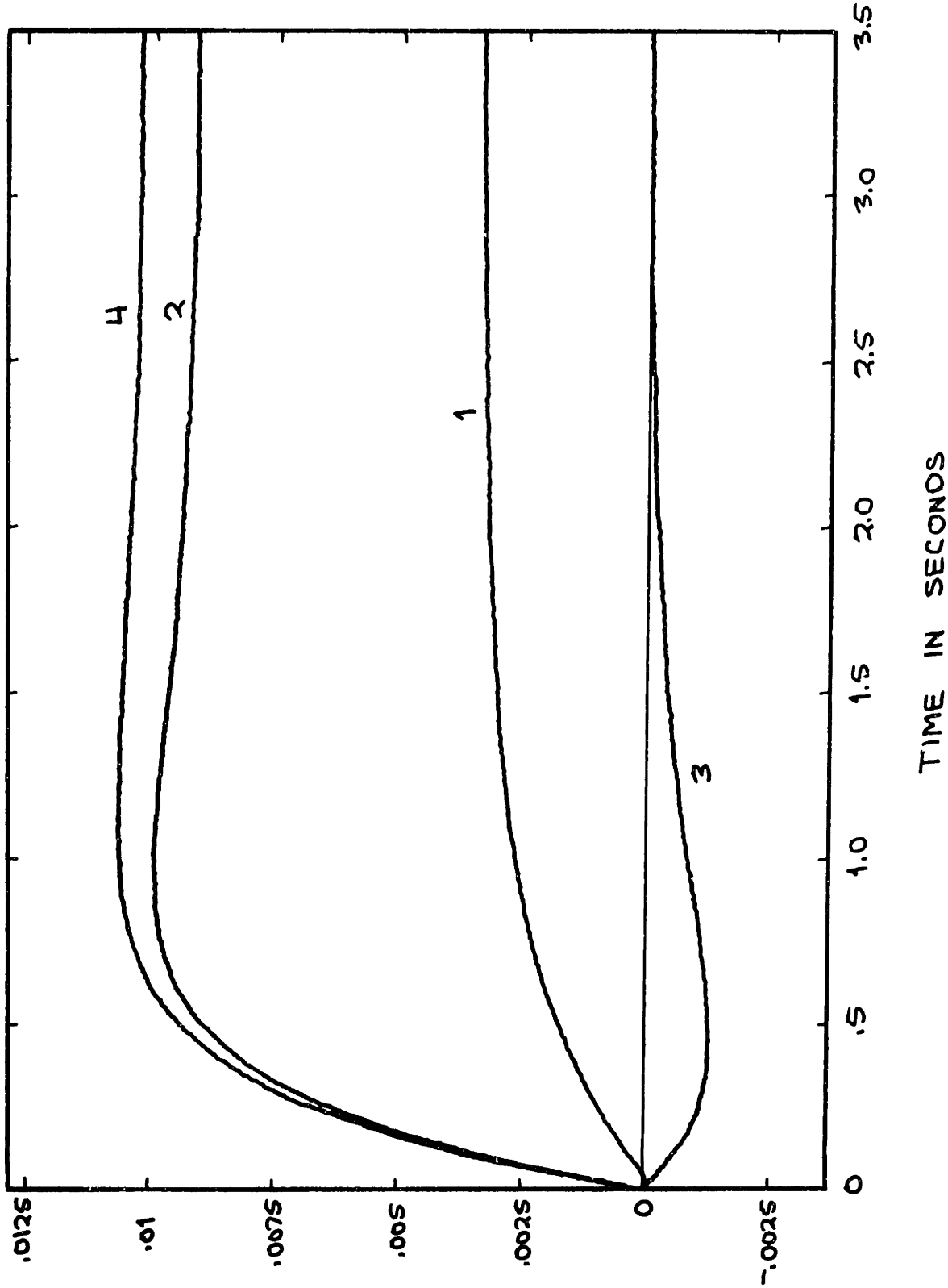
.0125
.01
.0075
.005
.0025
0
-.0025
0
.5
1.0
1.5
2.0
2.5
3.0
3.5
TIME IN SECONDS
1
2
3
4

Figure 27.

that modern control theory regulators have to know beforehand the zero of the state space to function properly. This would require another control loop to determine the zero of the state space given the inputs and demands. Thus, although a modern control theory approach to the speed regulation problem could provide for improved performance, it might also provide for increased complexity and cost outweighing any advantages.

2. Engine Acceleration and Deceleration Limiting

Acceleration and deceleration limiting are actually designed to provide safe operating limits for the gas turbine, while allowing it to accelerate and decelerate in the minimum possible amount of time. Acceleration limiting prevents compressor surge and excessive turbine inlet temperatures by limiting the maximum instantaneous value of fuel flow. Deceleration limiting prevents extinguishing the burner flame by limiting the minimum instantaneous value of fuel flow. Marscher (6) and Zalmanzon and Cherkasov (33) give discussions of some of the possible methods of effecting acceleration and deceleration limiting. All of these methods are basically fuel-air ratio limiters and hope to determine the air mass flow through the engine by sensing a few selected engine

variables and thus schedule an appropriate fuel flow to avoid exceeding any of the limits just described. The variations appear in determining which are the best variables to measure to give the best estimate of air flow with the fewest number of sensors.

The temperature limiting operation of the fuel-air ratio limiter used in this thesis is very straightforward. By taking an energy balance across the fuel burner and assuming that exit mass flow is equal to the compressor discharge mass flow results in a simple expression for the fuel flow.

$$\dot{m}_f = \left(\frac{c_p}{h_{LHV}}\right) \cdot \left[\dot{m}_3\right] \cdot \left[T_{04} - T_{03}\right] \qquad 171)$$

By introducing the maximum allowable turbine inlet temperature the maximum allowable fuel flow can be defined for compressor operation away from surge.

$$\dot{m}_{f\,max} = \left(\frac{c_p}{h_{LHV}}\right) \cdot \left[\dot{m}_3\right] \cdot \left[T_{04\,max} - T_{03}\right] \qquad 172)$$

The compressor flow and temperature characteristics can be written as:

$$\dot{m}_3 = \frac{p_{02}}{\sqrt{T_{02}}} \cdot f_1\left(\frac{p_{03}}{p_{02}}, \frac{N_G}{\sqrt{T_{02}}}\right) \qquad 173)$$

$$T_{03} = T_{02} \cdot f_2\left(\frac{p_{03}}{p_{02}}, \frac{N_G}{\sqrt{T_{02}}}\right) \qquad 174)$$

Thus,

$$\dot{m}_{f\,max} = \left(\frac{C_p}{h_{LHV}}\right) \cdot \left[f_1\right] \cdot \left[T_{04\,max} - f_2\right] \qquad 175)$$

or equivalently,

$$\dot{m}_{f\,max} = f'\left(p_{02}, p_{03}, T_{02}, N_G, C_p, h_{LHV}, T_{04\,max}\right) \qquad 176)$$

$T_{04\,max}$ has to be known beforehand and it is generally assumed that C_p and h_{LHV} are constant. With this, the expression for the instantaneous maximum fuel flow is simplified.

$$\dot{m}_{f\,max} = f\left(p_{02}, p_{03}, T_{02}, N_G\right) \qquad 177)$$

In one particular type of fuel control for an aircraft gas turbine (27), the dependence on p_{02} is neglected. Apparently a good enough indication of compressor discharge mass flow is obtained without sensing p_{02}, since the fuel control is presently being produced. In this thesis p_{02} and T_{02} are assumed to be constant so that the expression for the maximum fuel flow to

avoid exceeding the maximum allowable turbine inlet temperature is simplified further.

$$\dot{m}_{f\,max} = f(p_{03}, N_G) \qquad 178)$$

This expression for $\dot{m}_{f\,max}$ only takes consideration of temperature limiting. The fuel-air ratio limiter takes advantage of the operating characteristics of the gas turbine to provide for surge protection. By simply limiting the fuel flow it is possible to use the torque and flow characteristics of the compressor and turbine to keep the compressor from surging. This amounts to limiting the turbine inlet temperature near the compressor surge region. Thus, there are two temperature limits defined in the acceleration limiting characteristics of the fuel control. The first is that corresponding to the maximum allowable turbine inlet temperature and the second is that corresponding to compressor operation with an appropriate surge margin of safety; it is not advisable to closely follow the compressor surge line for an engine acceleration. Typically, the maximum turbine inlet temperature determines the acceleration fuel flow at high rotor speeds, while the surge limit determines the acceleration fuel flow at low rotor speeds.

The maximum fuel flow consistent with the surge limit is a function of the compressor and turbine characteristics and has to be determined from performance calculations. A typical fuel control (27) schedules the maximum fuel flow consistent with the surge limit as a function of p_{o3}, T_{o2}, and N_g. For the engine used here it has been determined that by limiting the turbine inlet temperature to 1700 °F it is possible to avoid compressor surge for the normal engine operating range. Thus, the maximum fuel flow for an engine acceleration is given by the functional form of equation 178)

Deceleration fuel limiting is necessary to insure that the fuel flow does not fall below the minimum necessary for successful burner operation. The deceleration fuel limit is generally taken as a fixed fraction of the acceleration fuel limit. In this analysis the fraction is taken to be .25.

The acceleration fuel flow is expressed as the following in an attempt to make the functional relation of equation 178) simpler (11):

$$\frac{\dot{m}_{f\,max}}{N_g} = f(p_{o3}) \qquad 179)$$

Such a simplification can make the engine more sluggish

during accelerations and decelerations, but also reduces the fuel control complexity. The functional relation of equation 179) is shown in figure 28, in which the variables have been scaled with respect to maximum values. In many cases it would probably suffice to use a linear relation (11).

The fuel-air ratio limiter provides for very good surge and temperature protection on a fast transient basis. However, due to the assumptions of constant specific heat and effective lower heating value of the fuel, the fuel-air ratio limiter can suffer from low static accuracy. A good turbine inlet temperature limiter might be provided by a combination of a fuel-air ratio limiter for fast transients and some type of direct temperature sensor to provide for good static accuracy.

3. Transient Fuel Rate Limiting

Transient fuel rate limiting is very simply limiting the maximum rate at which the fuel flow is allowed to change. This is done to avoid severe thermal shocks to the fuel burner and the turbine and to avoid extinguishing the burner flame. In order to allow for good speed regulation this transient rate limiting must not be enforced for some speed interval about the desired speed setting. This allows the

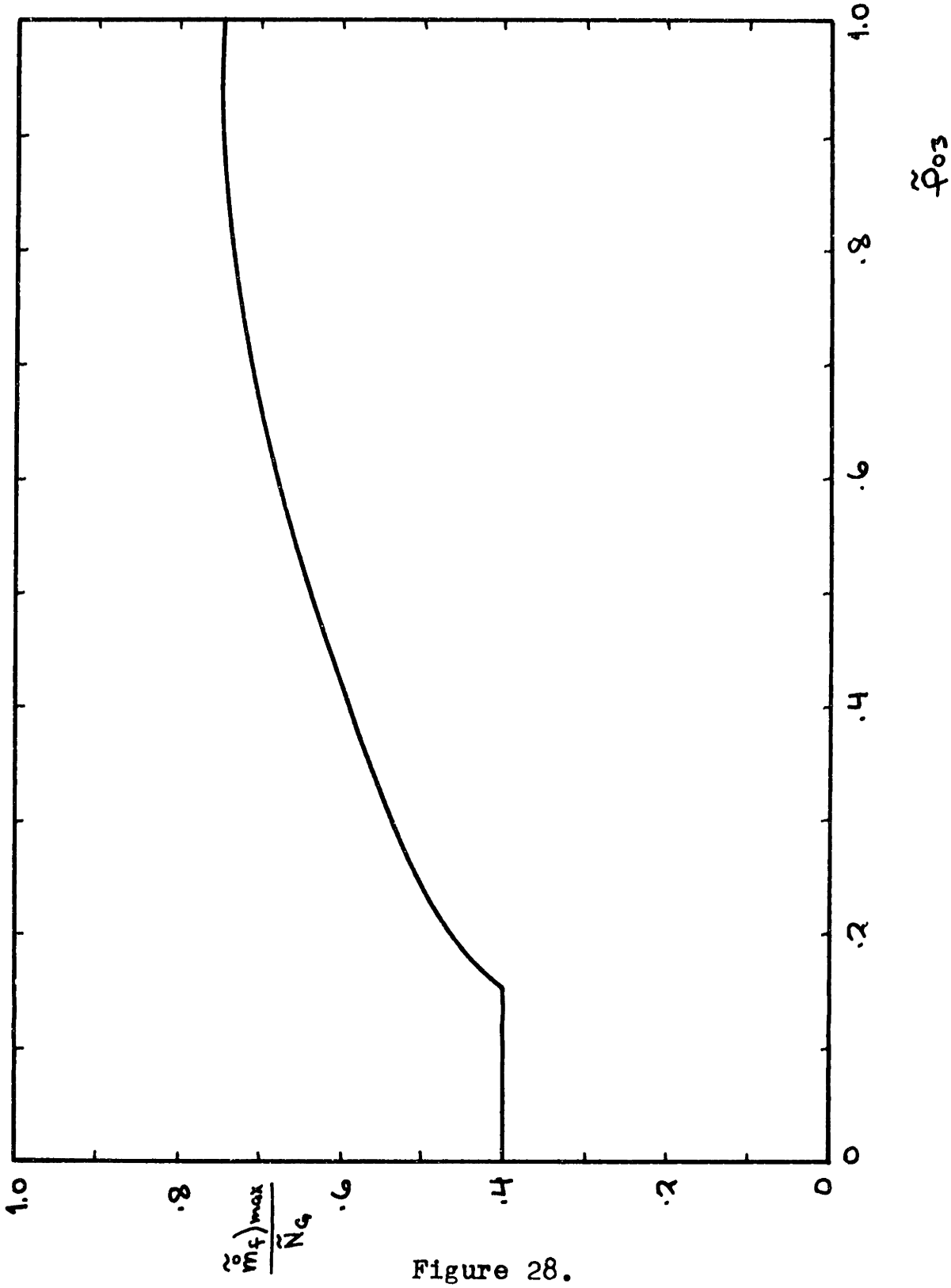

Figure 28.

speed regulator to have free reign to compensate for minor disturbances. This unrestricted range is taken to be 1% of maximum speed on the fuel control used in this analysis.

4. Fuel Control Configuration

The analog block diagram of the fuel control is shown in figure 29. From this diagram it is evident that the fuel control schedules fuel flow as a function of desired engine speed, actual engine speed, and compressor discharge pressure, all in scaled form. The value of the steady state fuel flow prior to the disturbance must also be known. In a real situation the initial value of the fuel flow would be zero prior to engine startup, and the fuel control would schedule the fuel flow from there. The values of the constants indicated in figure 29 are:

$K_1 = 5.0$

$K_2 = 6.25$

$K_3 = 1.0$

$K_4 = .25$

$K_5 = .01$

This set of values has been arrived at by a more or less trial and error method. These values have been chosen as they seem to provide acceptable behavior of the gas turbine used in this analysis.

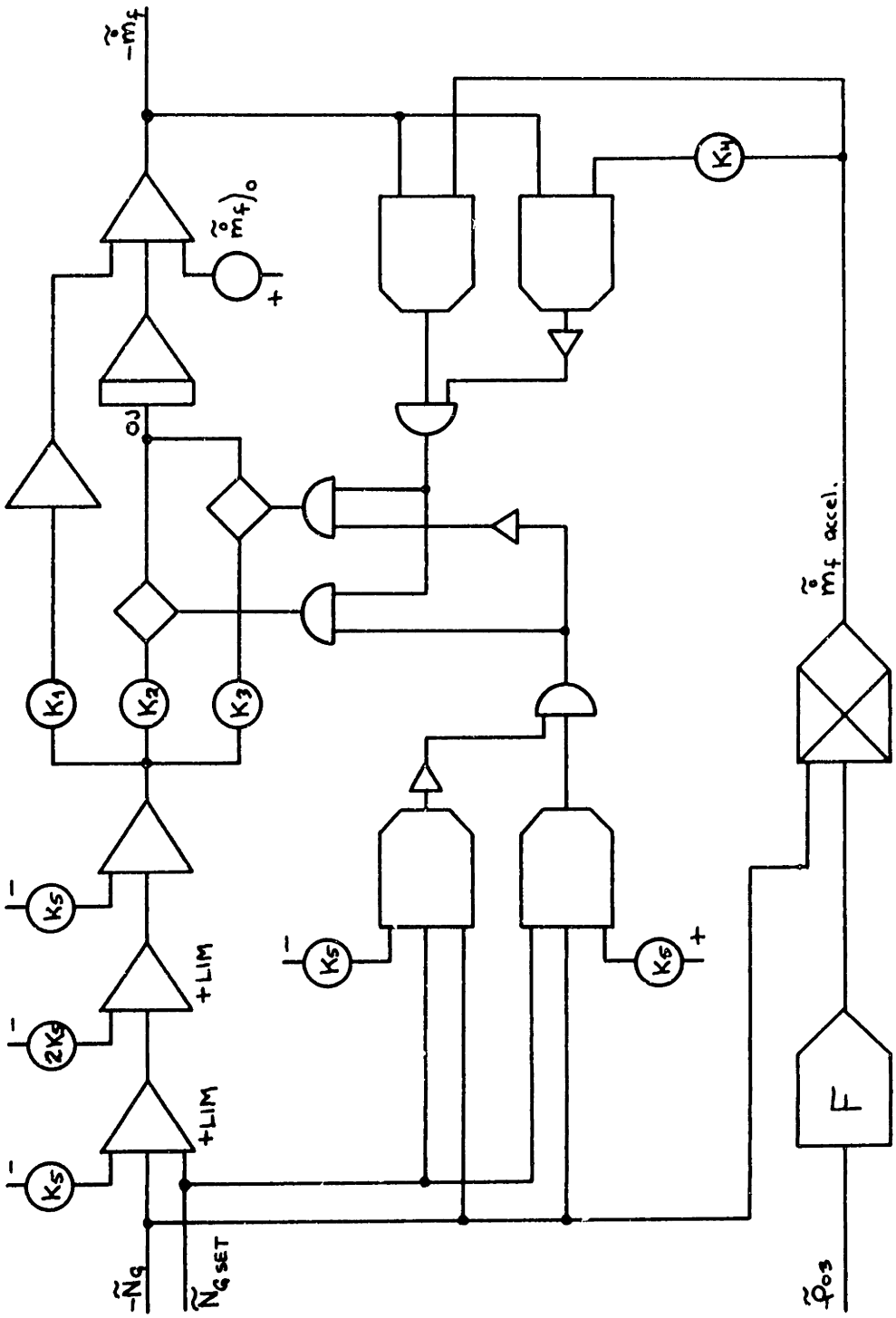
$\tilde{\dot{m}}_f$
$(\tilde{\dot{m}}_f)_o$
+
OJ
K_4
K_1
K_2
K_3
$\tilde{\dot{m}}_f$ accel.
K_5
K_5
K_5
+LIM
+LIM
2Kg
K_5
F
$\tilde{N}_g$
$\tilde{N}_{g\,SET}$
$\tilde{p}_{os}$

Figure 29.

B. Closed Loop Response Characteristics

To investigate the closed loop response characteristics of the gas turbine used in this analysis, the engine is subjected to two different classes of input disturbances:

i) Changes in speed setting

ii) Changes in load torque

Inlet pressure and temperature are maintained constant at all times.

1. Changes in Speed Setting

For responses to changes in speed setting the load torque is not changed from its standard dependence on the square of the rotor speed. Three different speeds are chosen along this standard load torque operating line and all possible combinations of accelerations and decelerations between any two of the speeds are simulated. These three steady state operating points are:

i) Design speed:

$$\tilde{\rho}_{03} = .625$$
$$\tilde{T}_{04} = .8056$$
$$\tilde{N}_G = .900$$
$$\tilde{\dot{m}}_f = .4723$$

ii) Intermediate speed:

$$\tilde{\rho}_{03} = .4075$$

ii) Intermediate speed:

(continued) $\tilde{T}_{04} = .7445$

$\tilde{N}_G = .72$

$\tilde{\dot{m}}_f = .3132$

iii) Half design speed:

$\tilde{P}_{03} = .2115$

$\tilde{T}_{04} = .7378$

$\tilde{N}_G = .45$

$\tilde{\dot{m}}_f = .1807$

The six possible combinations of accelerations and decelerations are shown in figures 30 through 35.

Figure 30: Deceleration; $\tilde{N}_G = .9$ to $.72$

Figure 31: Deceleration; $\tilde{N}_G = .9$ to $.45$

Figure 32: Deceleration; $\tilde{N}_G = .72$ to $.45$

Figure 33: Acceleration; $\tilde{N}_G = .72$ to $.9$

Figure 34: Acceleration; $\tilde{N}_G = .45$ to $.72$

Figure 35: Acceleration; $\tilde{N}_G = .45$ to $.9$

The steady state values of the state variables and the fuel flow as predicted from the hybrid simulation are listed below. Of necessity, $\tilde{N}_G$ agrees almost exactly with the selected value of the engine speed due to PI speed regulator.

Figure 30	$\tilde{P}_{03}$	$\tilde{T}_{04}$	$\tilde{N}_G$	$\tilde{\dot{m}}_f$
hybrid simulation:	.41	.715	.72	.31
steady state analysis:	.4075	.7445	.72	.3132

Figure 31	$\tilde{P}_{03}$	$\tilde{T}_{04}$	$\tilde{N}_G$	$\tilde{\dot{m}}_f$
hybrid simulation:	.215	.71	.45	.175
steady state analysis:	.2115	.7378	.45	.1807
Figure 32				
hybrid simulation:	.21	.72	.45	.18
steady state analysis:	.2115	.7378	.45	.1807
Figure 33				
hybrid simulation:	.625	.77	.90	.435
steady state analysis:	.625	.8056	.90	.4723
Figure 34				
hybrid simulation:	.415	.735	.72	.30
steady state analysis:	.4075	.7445	.72	.3132
Figure 35				
hybrid simulation:	.62	.79	.90	.46
steady state analysis:	.625	.8056	.90	.4723

From a look at these results it is apparent that the closed loop hybrid simulation still suffers from static inaccuracies, although not as great as the inaccuracies of the open loop simulation.

Figure 32 serves to illustrate the three basic regions of the fuel control operation. From time 0 to about 2.2 seconds elapsed time the fuel flow response is governed by the transient rate limiter. This response is linear with time. From 2.2 to 4.6 seconds elapsed time the fuel flow is being limited by the

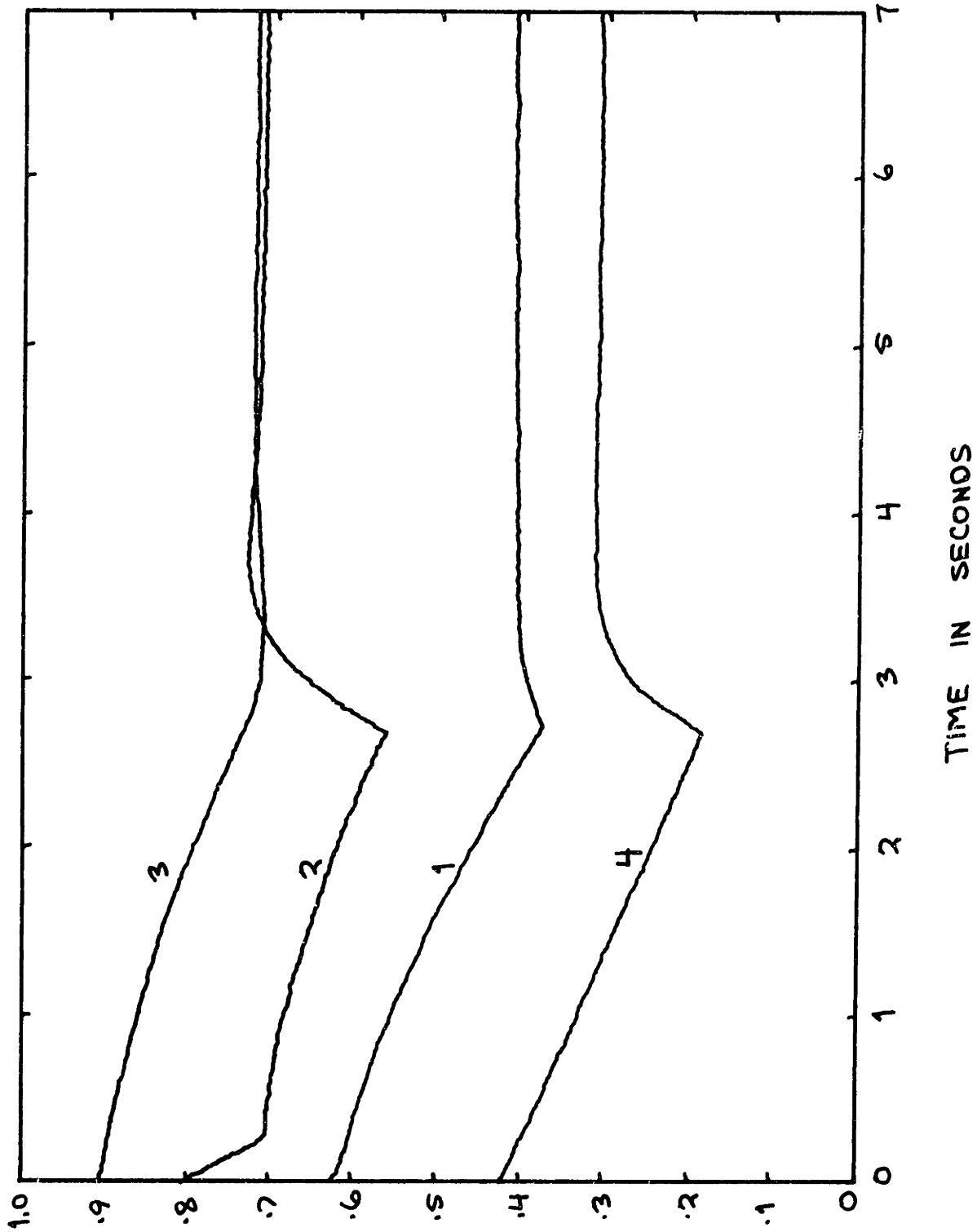

Figure 30.

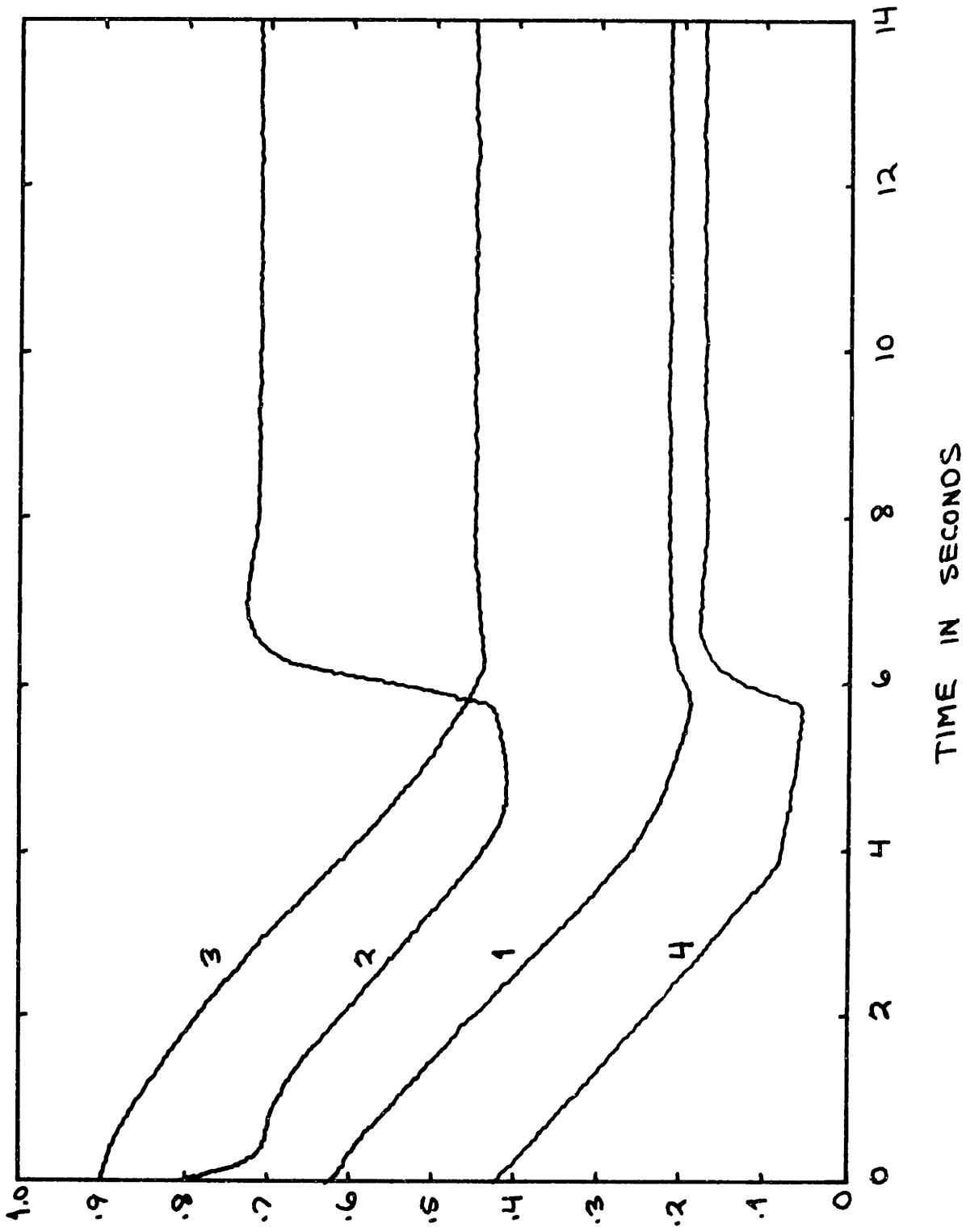

Figure 31.

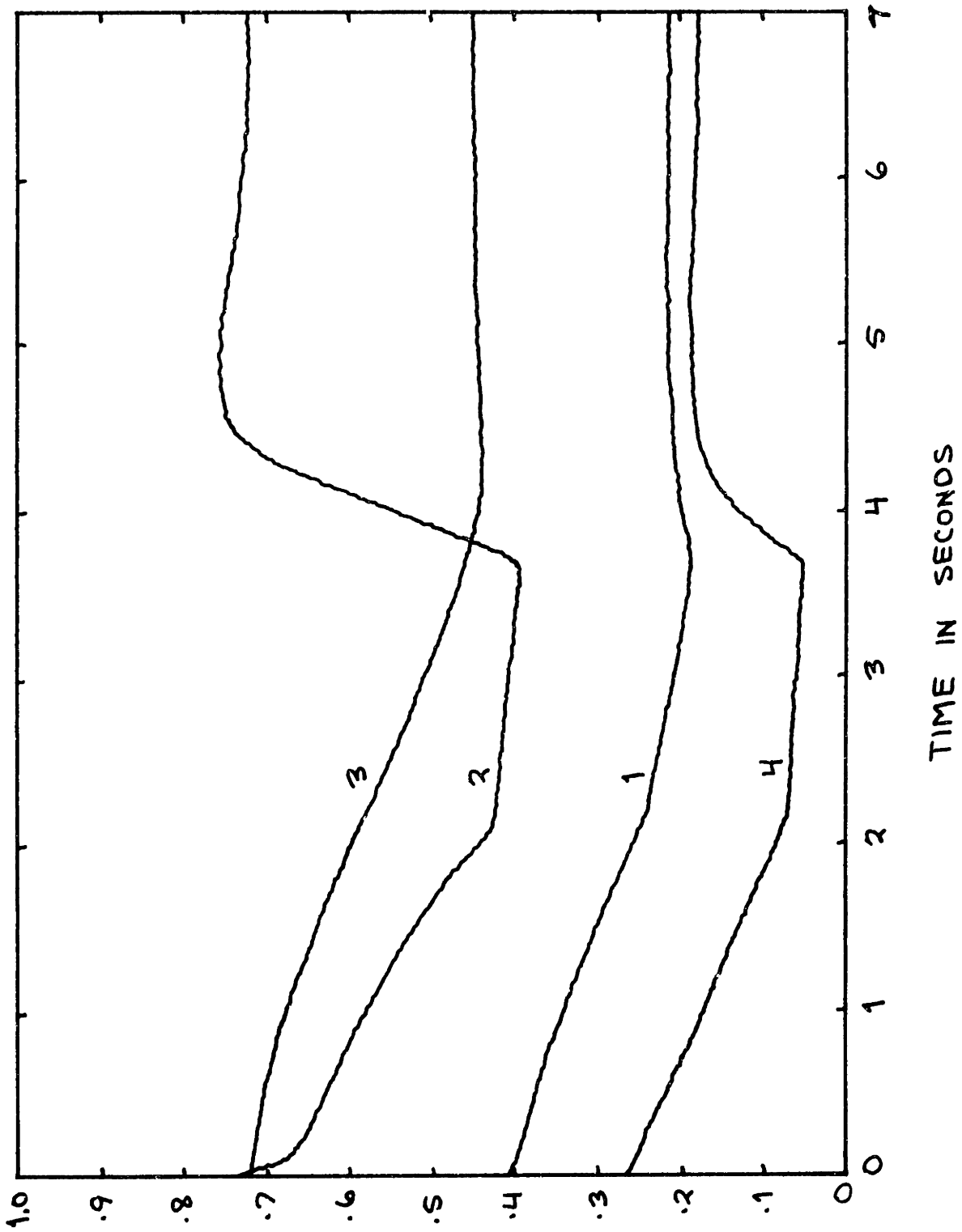

Figure 32.

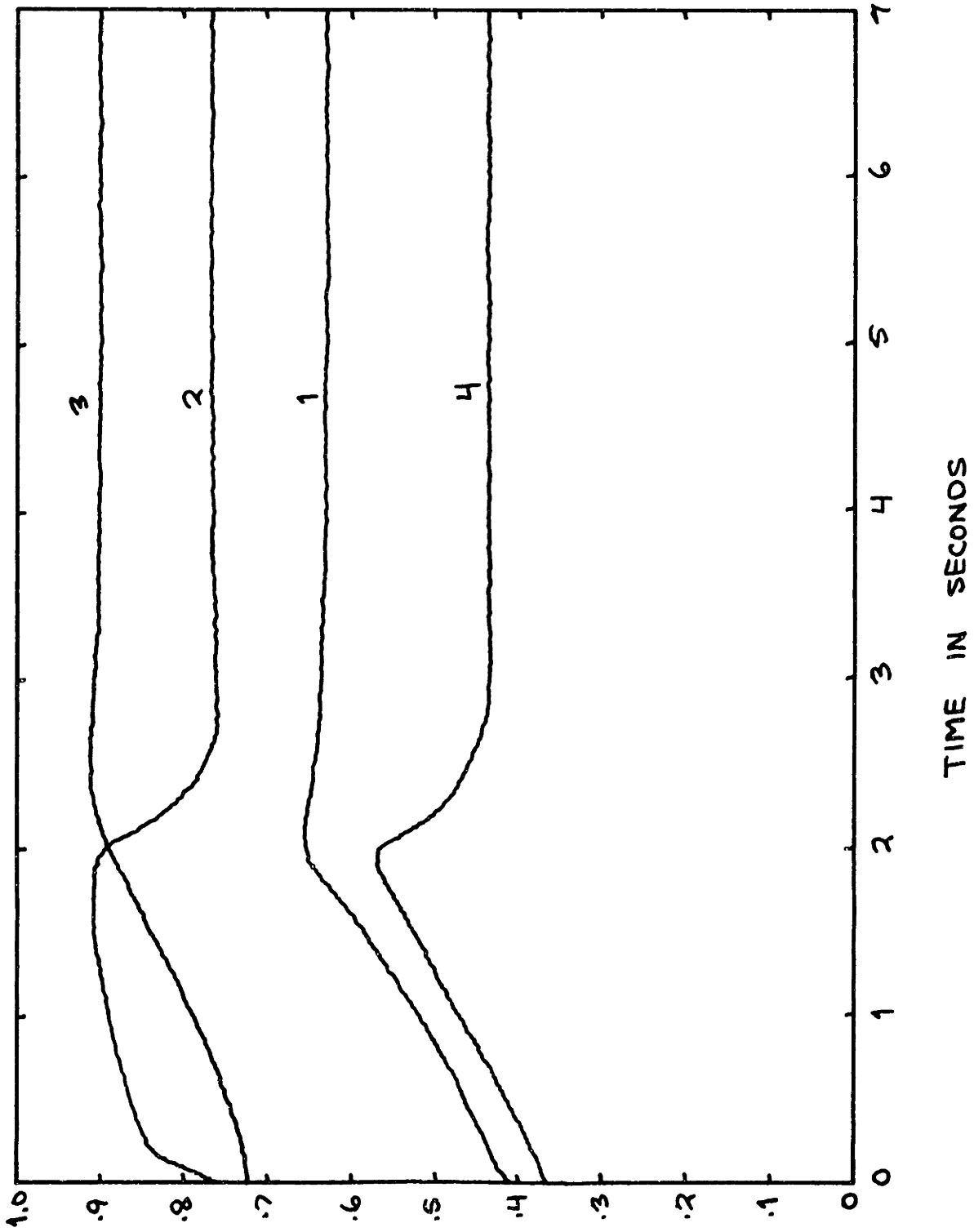

Figure 33.

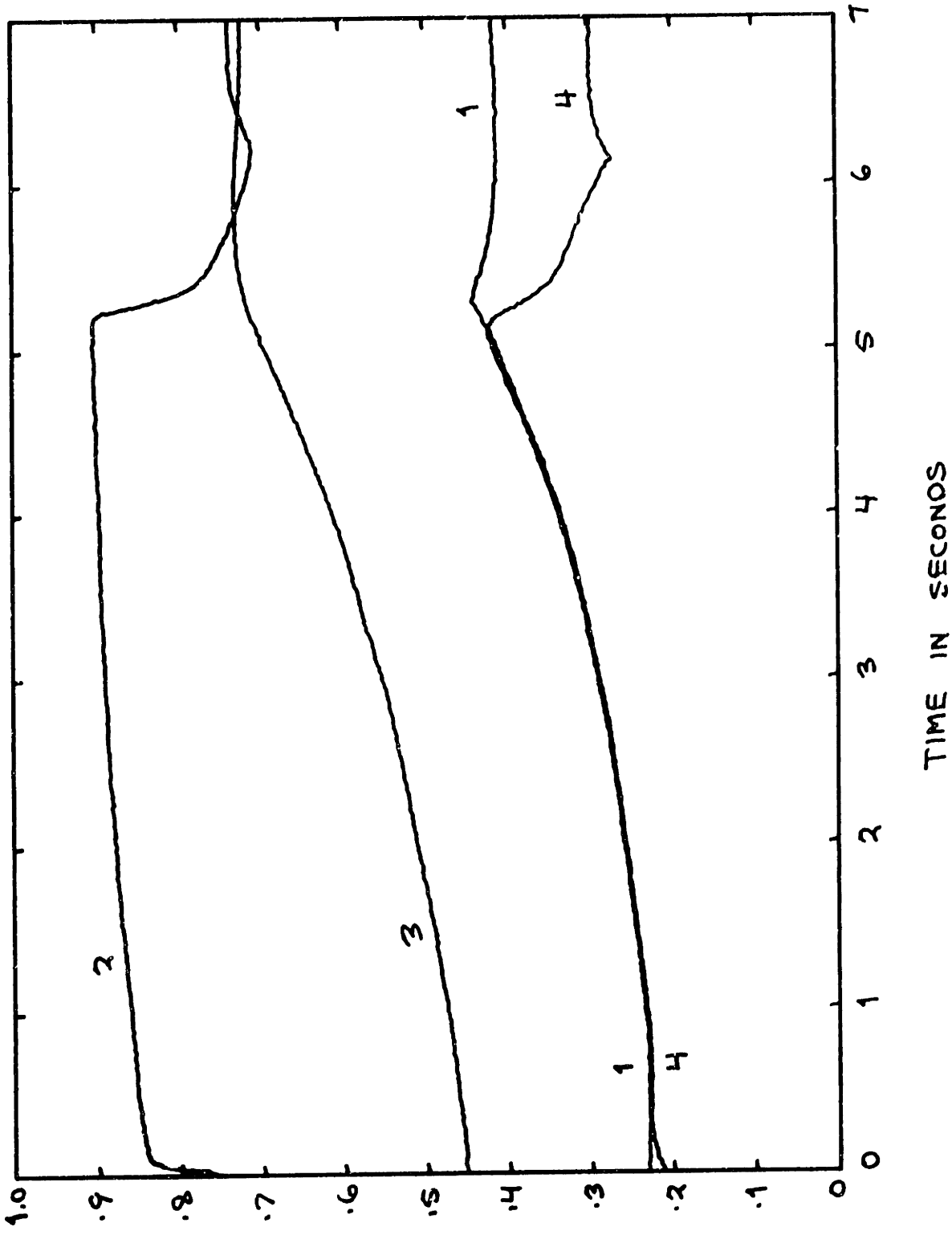

Figure 34.

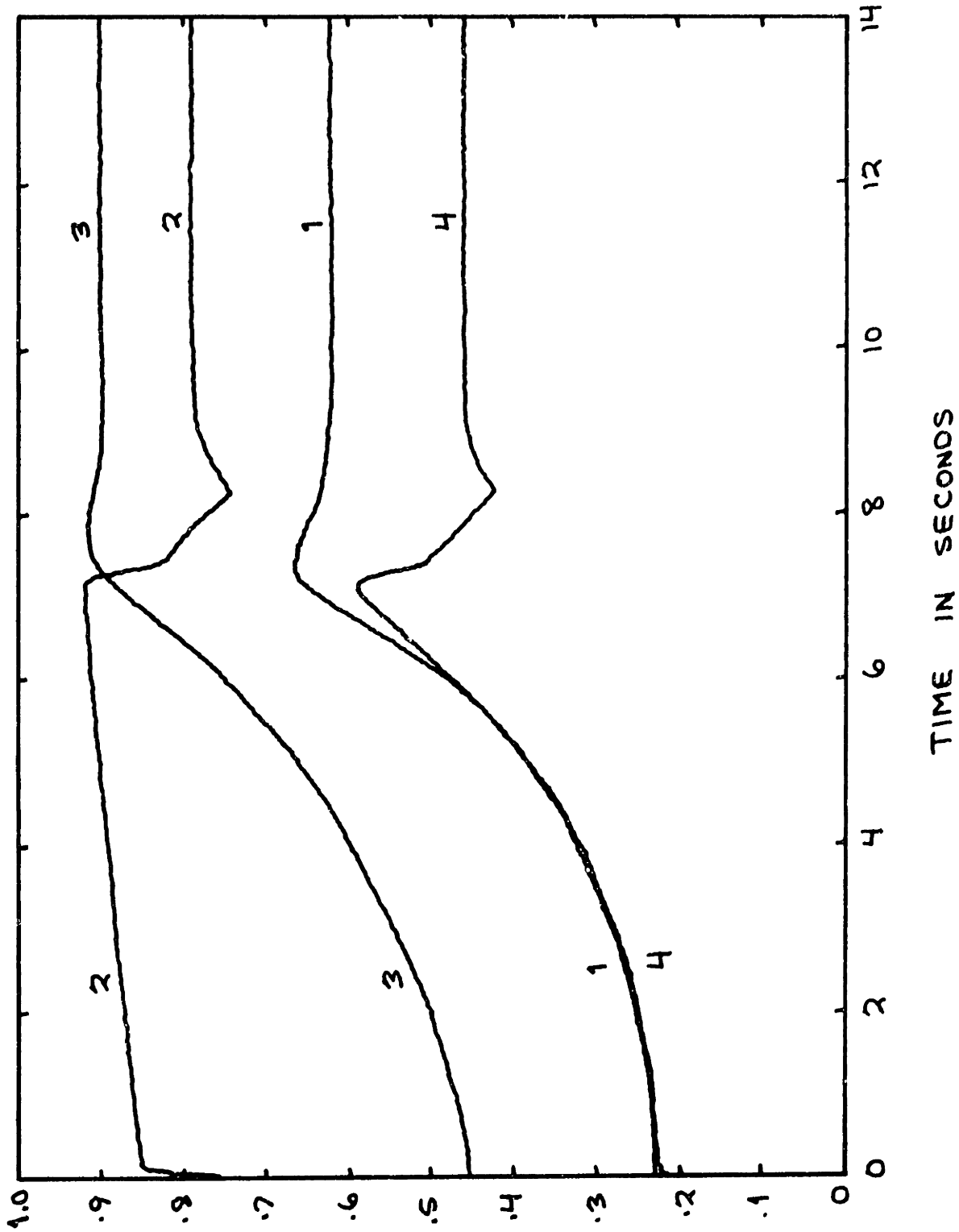

Figure 35.

deceleration limit. At about 4.6 seconds elapsed time the speed comes within 1% of the speed setting and the speed regulator takes over. This is evident in the typical PI response of the fuel flow to the final steady state value. Figure 35 gives a very graphic depiction of the operation of the acceleration fuel limiting characteristics of the fuel control. At the standard load torque steady state operating point of half design speed the fuel flow is very close to the acceleration fuel schedule. Thus, the fuel flow very quickly reaches the acceleration limit and follows the schedule as the speed increases. Due to the scaling of the variables the fuel flow is almost exactly superimposed upon the compressor discharge pressure. At about 7.3 seconds elapsed time the speed regulator takes over. However, due to inertia the speed passes right through the regulator range and the transient rate limiting is evident from about 7.7 to 8.3 seconds elapsed time. At 8.3 seconds the speed regulator takes over to bring the speed to the desired value. This passing right through the speed regulator range might indicate that the range ought to be increased.

2. Changes in Load Torque

A steady state analysis was not carried out to

determine the effect of varying the load torque. The steady state analysis used in the calculations for speed variations is based on a steepest descent optimization routine and has somewhat high operating costs. Figures 36 through 38 represent changes in load torque at the design point.

Figure 36: 50% rise in $\tilde{\gamma}_L$

Figure 37: 50% drop in $\tilde{\gamma}_L$

Figure 38: 100% drop in $\tilde{\gamma}_L$

Since a comparison with accurate steady state results is not available it is not known how accurately the hybrid simulation integrates the system equations subject to a load torque disturbance. It seems reasonable to expect accuracies on the same order as those associated with the changes of demand speed.

Figure 37 best illustrates the engine response to a change in load torque. Due to the high rotary inertia associated with the gas turbine the speed does not change by more than about 5%. The three regions of fuel control operation are again evident.

Figure 36 indicates that the steady state fuel flow prior to the load disturbance is fairly close to the acceleration limit. For this reason the engine cannot generate enough excess torque to bring the engine speed back into regulation quickly; the speed has not

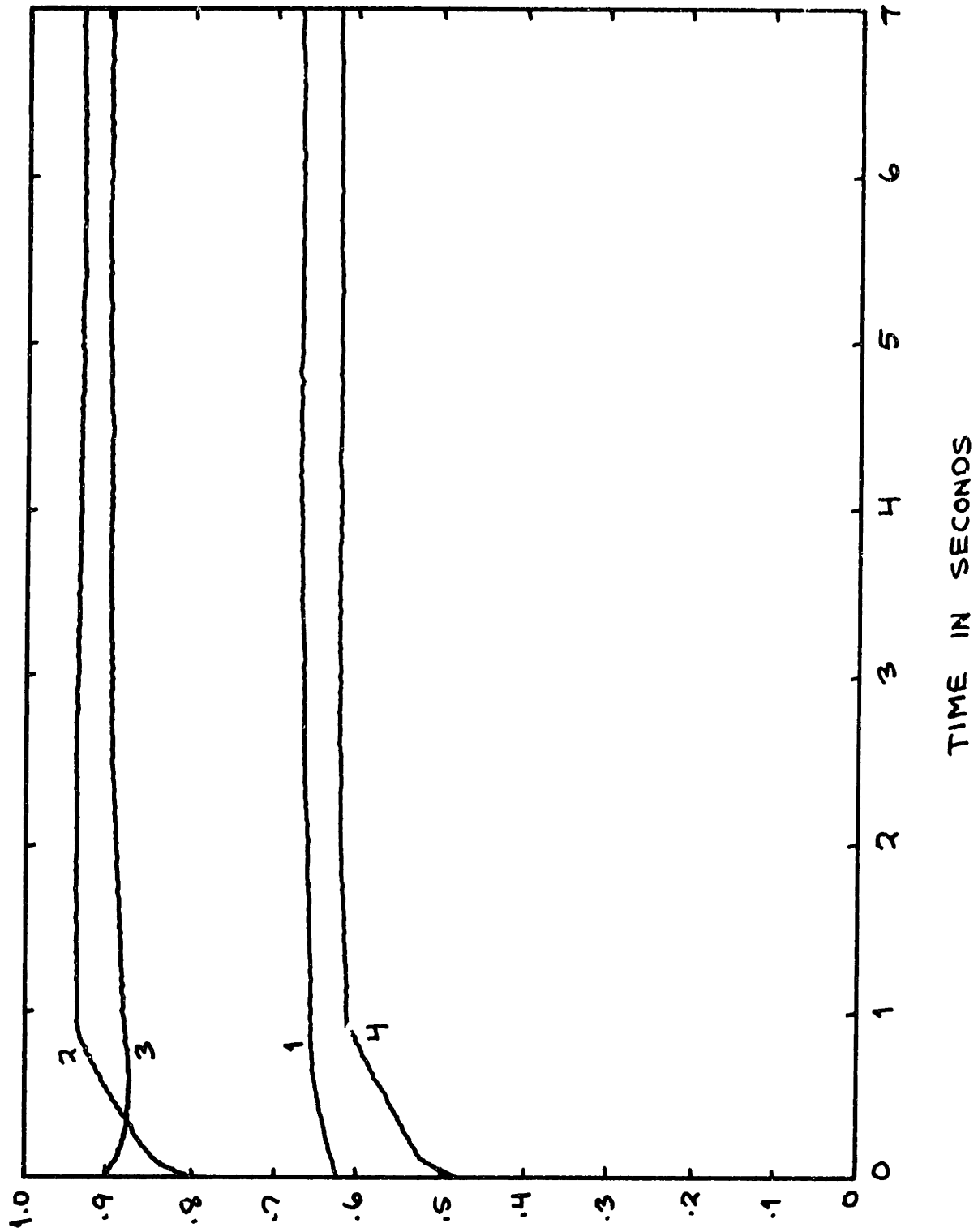

Figure 36.

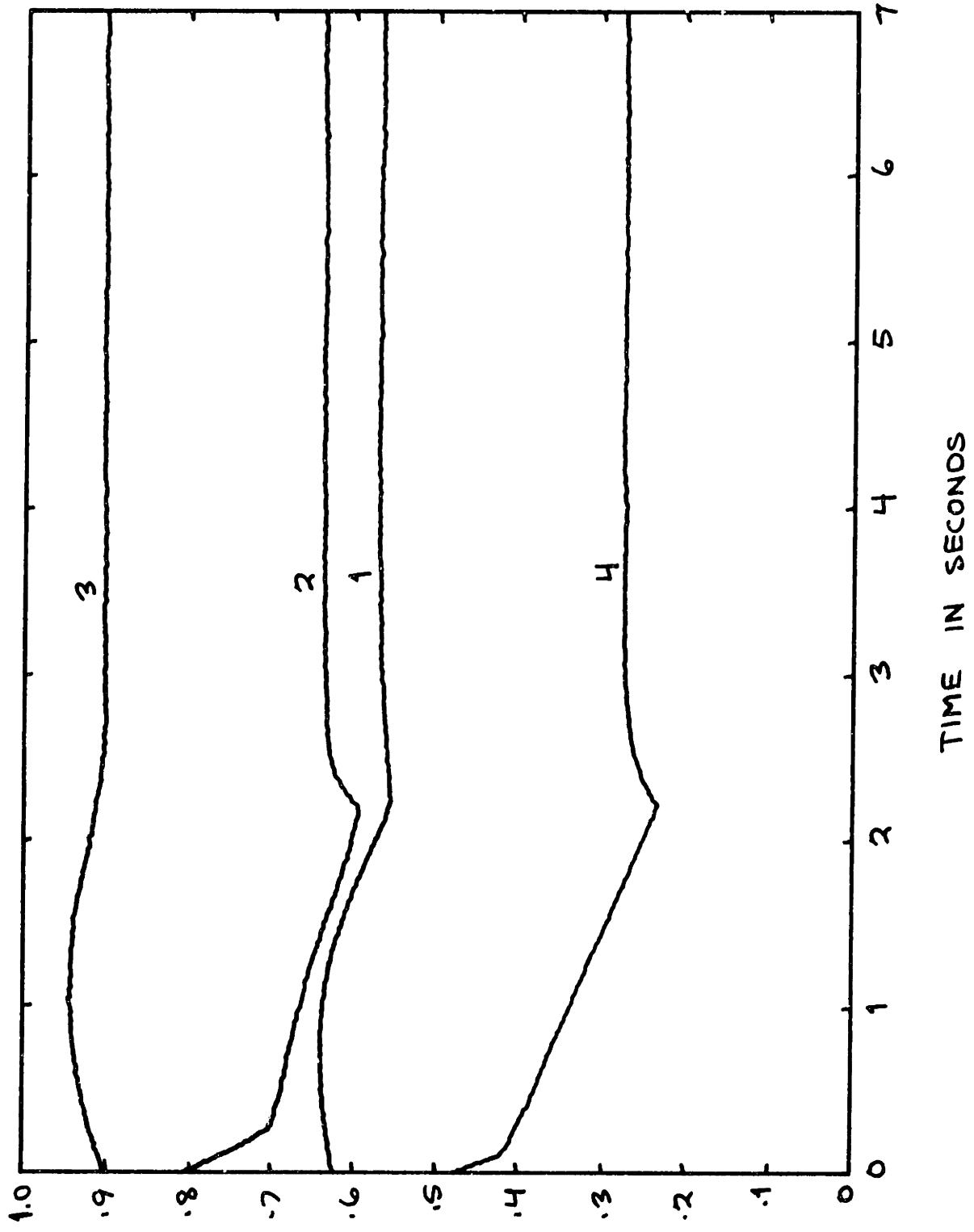

Figure 37.

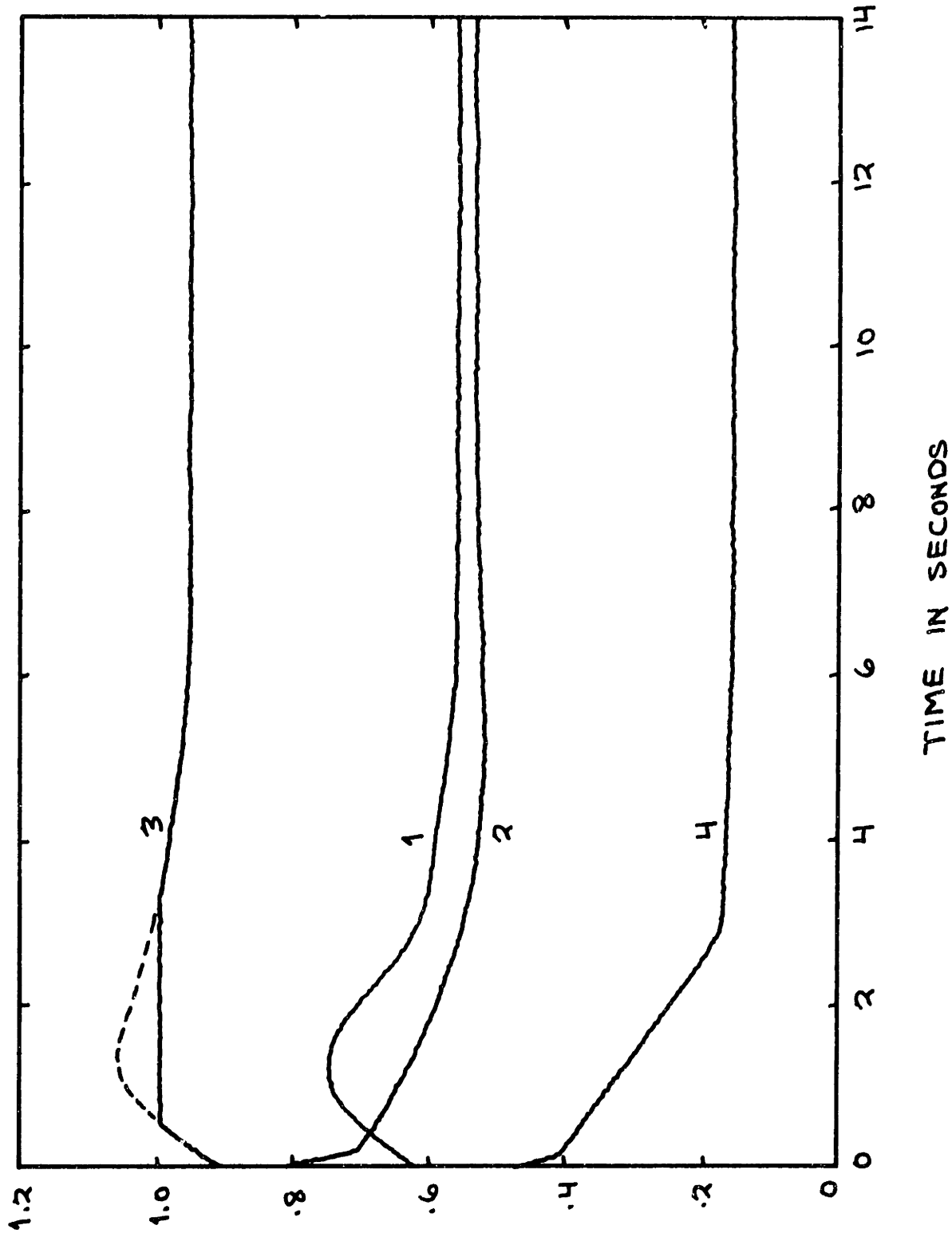

Figure 38.

quite reached steady state after 7 seconds elapsed time.

Figure 38 shows very definitely that the fuel control configuration used does not have the ability to prevent a rotor overspeed if the load torque is lost completely, such as would happen in the event of a drive train failure. The dashed line represents the estimate of the amount of overspeed based on visual observation of the output on the DVM (digital volt meter) on the analog computer. This estimation is necessary since the ADC's will not transmit any signal larger than 1.0 machine units. This failure to prevent overspeed is due to the large amount of fluid mechanical energy stored in the volume between the compressor and turbine. Two effective means of preventing an overspeed in such a situation are to throttle the exhaust flow by means of variable nozzles or to bleed the compressor discharge air to atmosphere.

CHAPTER V. CONCLUSIONS AND RECOMMENDATIONS

The overall result of this thesis is to give some insights into the types of problems associated with the analysis and control of gas turbine systems and to provide the basic groundwork necessary for future work in this area.

The modeling techniques presented do not contain any techniques that have not been used in the past. What is presented is a textbook type of treatment that should enable the reader, who has a reasonable knowledge of basic system dynamics and control principles, to learn state of the art gas turbine modeling techniques. The presentation starts from fundamental physical principles and uses energy considerations to develop a unified treatment of gas turbine modeling. The modeling techniques presented can be applied with relative ease to almost any type of gas turbine configuration conceivable.

Due to the high costs associated with pure analog and pure digital computer simulation of gas turbines it is felt that hybrid simulation will provide the best approach to gas turbine performance evaluation and control systems design in the near future. The hybrid simulation presented in this analysis is a somewhat crude, first-cut approach to the simulation problem,

developed within the present limits of the Mechanical Engineering computer facility. The problems encountered here could provide some valuable information to be used in the development of future hybrid simulations.

The chapter on control in a very limited manner presents some aspects of basic gas turbine fuel control philosophy. Again, nothing new is presented, and the development of the case study fuel control serves merely as an illustration, and as a means of closing the fundamental control loop. Since the case study engine is a fabrication it can not be stated with any certainty that the fuel control designed in this thesis would work on an actual engine.

The numerous engine responses, both open and closed loop, give a good description of the general dynamic characteristics of the single shaft gas turbine. The gas turbine dynamics are essentially those of the rotor, while the pressure and temperature state variables respond very quickly to any input disturbance and then follow the speed in a quasi-steady state fashion. The pressure and temperature state variables are included under the assumption that more efficient control of gas turbines will be possible if more state variables are sensed and used in the fundamental control loops.

The possibilities for future work are numerous to say the least. However, the first and by far the most important area that has to be explored is the accurate representation of the full scale nonlinear turbomachine characteristics. This is the limiting factor in any type of computer simulation of the large scale nonlinear dynamics of gas turbines. If an efficient, low cost method of accurately representing these characteristics were made available this would allow for new approaches to the solutions of many of the design problems associated with gas turbines and their control systems. New types of engine configurations and applications could then be investigated for improvements in performance and efficiency, and new concepts in fuel control philosophy could be explored for the possibility of providing more efficient, low cost gas turbine control systems.

The second major area that has to be investigated is that of developing better and more accurate methods of modeling gas turbines, i.e., better representing the distributed nature of the gas turbine and introducing two-dimensional effects. While such analyses would of necessity be limited to sophisticated computer facilities, they are necessary if some

of the problems associated with compressor surge in high performance aircraft type gas turbines are to be solved.

If these two major problem areas can be adequately solved, then the gas turbine may begin to more fully realize its potential as a source of power and propulsion.

BIBLIOGRAPHY

Specific References

1. H. M. Paynter, "System Dynamic Analysis - Experimental Supercritical Steam Generator", Internal Report, Pi-Square Engineering Company, 1957 (unpublished)

2. H. M. Paynter, "First Interim Technical Report - Computer Simulation of the Power Conversion System for Nike-X Power Plants", DA-49-129-ENG-542, Arthur D. Little, Inc.

3. D. F. Flowers, "Some Transient Aspects of Gas Turbine Operation and Control", MIT Thesis, Sc.D., 1949

4. R. Oldenburger, "Regulators", Control Engineers Handbook, J. G. Truxal, Editor, McGraw-Hill, 1958

5. D. R. Ahlbeck, "Simulating a Jet Gas Turbine with an Analog Computer", Simulation, September, 1966

6. W. F. Marscher, "Linear Analysis of Aircraft Gas Turbine Control Systems Dynamics", MIT Thesis, S.M., 1960

7. L. B. Sarantsev, "Analysis of the Dynamics of Gas Turbines and Their Control Systems", ASME Paper 70-GT-76

8. V. L. Larrowe and M. M. Spencer, "Analog Computer Simulation of Gas Turbines for Control Study", Gas Turbine Fuel Controls, Analysis and Design, SAE Progress in Technology, Vol. 9, 1965

9. H. I. H. Saravanamuttoo and A. J. Fawke, "Simulation of Gas Turbine Dynamic Performance", ASME Paper 70-GT-50

10. R. G. Willoh and K. Seldner, "Multistage Compressor Simulation Applied to the Prediction of Axial Flow Instabilities", NASA TM X-1880, 1969

11. K. Seldner and H. Gold, "Computer and Engine Performance Study of a Generalized Parameter Fuel Control for Jet Engines", NASA TN D-5871, 1970

12. C. J. Rubis and A. Bodnaruk, "Acceleration Performance Analysis of a Gas Turbine Destroyer Escort", ASME Paper 70-GT-77

13. D. Karnopp and R. Rosenberg, Analysis and Simulation of Multiport Systems, MIT Press, 1968

14. J. H. Horlock, Axial Flow Compressors, Butterworths Scientific Publications, 1958

15. D. Gabriel, L. Wallner, R. Lubick and G. Vasu, "Some Effects of Inlet Pressure and Temperature Transients on Turbojet Engines", Aero. Eng. Rev., Vol. 16, No. 9, Sept. 1957, pp. 54-57

16. D. H. Mallinson and W. G. E. Lewis, "The Part-Load Performance of Various Gas Turbine Engine Schemes", Internal Combustion Turbines, Lectures Sponsored by the Institution of Mechanical Engineers, Reprinted for Distribution in U.S.A. by ASME

17. D. G. Shepherd, Introduction to the Gas Turbine, Constable and Co., Ltd., 1960

18. P. D. Hansen, "The Dynamics of Heat Exchange Processes", MIT Thesis, Sc.D., 1960

19. London, Sampsell and McGowan, "The Transient Response of Gas Turbine Plant Heat Exchangers - Additional Solutions for Generators of the Periodic Flow AN Direct Transfer Types", ASME Paper 63-AHGT-15

20. London, Biancardi, and Mitchell, "The Transient Response of Gas Turbine Plant Heat Exchangers - Regenerators, Intercoolers, Precoolers, and Ducting", ASME Paper 59-GTP-5

21. B. E. G. Forsling, "Main Propulsion Gas Turbine Set for the Oil Tanker Auris", Proceedings of the Institution of Mechanical Engineers, 1954, Vol. 168, No. 5

22. D. G. Ainley, "Performance of Axial Flow Turbines", Internal Combustion Turbines, Lectures Sponsored by the Institution of Mechanical Engineers, Reprinted

for Distribution in U.S.A. by ASME

23. B. H. Jennings and W. L. Rogers, Gas Turbine Analysis and Practice, Dover, 1969

24. D. G. Shepherd, Principles of Turbomachinery, Macmillan, 1956

25. F. D. Jordan, M. R. Hum and A. N. Carras, "An Analog Computer Simulation of a Closed Brayton Cycle System", ASME Paper 69-GT-50

26. S. J. Przybylko, L. Hutcheson, B. Suder and T. R. Warwick, "Advanced Integrated Digital Engine Simulation - A Step Forward for Propulsion System Testing", AIAA Paper 70-633, AIAA 6th Propulsion Joint Specialist Conference, San Diego, June 1970

27. D. A. Evens, "Control Concepts for a High Bypass Aircraft Turbofan Engine", SAE Paper 690403, National Air Transportation Meeting, New York, 1969

28. D. A. Prue and T. L. Soule, "Advanced Control System Considerations for Small Shaft-Type Aircraft Gas Turbines", ASME Paper 70-GT-132

29. W. I. Rowen, "Controlling the Gas Turbine in a Shipboard Environment - A Study in Propulsion Dynamics", ASME Paper 70-GT-121

30. D. A. O'Neil, "Governing Gas Turbine Engines for Marine Propulsion - Power vrs. Speed Control", ASME Paper 68-GT-54

31. N. G. Alvis, "Electric Hydraulic Governor Control for Industrial and Commercial Gas Turbine Use", ASME Paper 66-GT-118

32. L. Andreoni, "Industrial Gas Turbine Fuel Controls", SAE Paper 650499

33. L. A. Zalmanzon and B. A. Cherkasov, "Control of Gas Turbine and Ramjet Engines", NASA TT F-41, 1961

General References

34. B. P. Bichayev, Analog and Digital Models of Marine Gas Turbines, Russian Publication Available for Distribution in U.S.A. from Victor Kamkin Bookstore

35. H. P. Durland, "Simulation of Jet Engine Transient Performance", ASME Paper 65-WA/MD-16

36. W. E. Reed and J. H. Murray, "Use of Electronic Model to Evaluate Control Concepts for a Regenerative Gas Turbine", Gas Turbine Fuel Controls, Analysis and Design, SAE Progress in Technology, Vol. 9, 1965

37. G. E. Ferre and D. C. Lenkaitis, "Gas Turbine Engine Analog Simulation for Acceleration Sensing Fuel Control Studies", Gas Turbine Fuel Controls, Analysis and Design, SAE Progress in Technology, Vol. 9, 1965

38. M. C. Steele and F. Weber, "Control of Regenerative Gas Turbine Auxiliary Power Units", Gas Turbine Fuel Controls, Analysis and Design, SAE Progress in Technology, Vol. 9, 1965

39. R. P. Cande and R. P. McCabe, "The Fuel Flow Reset Approach to Gas Turbine Governing", Gas Turbine Fuel Controls, Analysis and Design, SAE Progress in Technology, Vol. 9, 1965

40. U. Floor, "Control of Speed and Power", Gas Turbine Engineering Handbook, J. W. Sawyer, Editor, Gas Turbine Publications, Inc., 1966

41. T. Shang, "Governing and Overspeed of Steam Turbines", MIT Thesis, S.M., 1963

42. G. T. Csanady , Theory of Turbomachines, McGraw-Hill, 1964

43. G. F. Wislicenus, Fluid Mechanics of Turbomachinery, Vol. 1 & 2, Dover, 1965

44. J. H. Horlock, Axial Flow Turbines, Butterworths Scientific Publications, 1966

45. F. J. Evans and G. Sheard, "Transient Torque of Steam Turbines in Power Systems", Proceedings of the Institution of Mechanical Engineers, Steam Plant Group, Vol. 185, 27/71, 1970-71

46. J. C. McMillan, "Gas Turbine Inlet Temperature Sensor", Diesel and Gas Turbine Progress, Feb., 1972

47. R. Scott and G. B. Manning, "The Redesign and Simulated Test of a Small Closed Brayton Cycle Turbine-Compressor Set for Nuclear Application", ASME Paper 69-GT-62

48. J. I. Black, "Feasibility Study of Fluidic Turbine Temperature Sensors in Gas Turbine Engines", ASME Paper 69-GT-70

49. G. M. Babic and L. A. Urban, "Engine Vane Control", ASME Paper 69-GT-14

50. E. G. Johnson, "Fluidic Gas Turbine Controls", Fluidics Quarterly, Vol. 2, No. 1

APPENDIX I

Compressor and Turbine Characteristics

Compressor:

$$PRC = \frac{P_{03}}{P_{02}}$$

$$TRT = \frac{T_{03}}{T_{02}}$$

$$XWC = \frac{\dot{m}_3\sqrt{T_{02}}}{P_{02}} \Bigg/ \left(\frac{\dot{m}_3\sqrt{T_{02}}}{P_{02}}\right)_{Design}$$

$$XNT = \frac{N_G}{\sqrt{T_{02}}} \Bigg/ \left(\frac{N_G}{\sqrt{T_{02}}}\right)_{Design}$$

$$AC = .75\,(XNC) + .27\,(XNC)^3$$

$$BC = 3.0\,(XNC)^{1.5} + 3.0\,(XNC)^7$$

$$CC = .018\,(2 - XNC)^{5.8}$$

$$DC = .891\sqrt{.9 - (XNC - .9)^2}$$

$$EC = 1.0 + XNC + 3.6\,(XNC)^{4.1}$$

$$FC = 4.0 \quad \text{if} \quad PRC \leq EC$$

$$FC = 2.0 \quad \text{if} \quad PRC > EC$$

$$GEC = \left(\frac{\gamma-1}{\gamma}\right)_{COMPRESSOR}$$

$$XWC = AC\left[1 - \frac{(PRC-1)}{BC}\right]^{CC}$$

$$EFFC = OC\left[1 - \left(\frac{EC-PRC}{EC-1}\right)^{FC}\right]$$

$$TRC = 1. + \left[\frac{(PRC)^{GEC} - 1.}{EFFC}\right]$$

Turbine:

$$PRT = \frac{P_{OS}}{P_{O4}}$$

$$TRT = \frac{T_{OS}}{T_{O4}}$$

$$XWT = \frac{\dot{m}_4^0\sqrt{T_{O4}}}{P_{O4}} \Big/ \left(\frac{\dot{m}_4^0\sqrt{T_{O4}}}{P_{O4}}\right)_{Design}$$

$$XNT = \frac{N_G}{\sqrt{T_{O4}}} \Big/ \left(\frac{N_G}{\sqrt{T_{O4}}}\right)_{Design}$$

$$AT = 1.0006$$

$$BT = 3.1 + \left(\frac{1.62}{XNT + .26}\right)$$

$$CT = .7$$

$$DT = .88\left[1 - (1-XNT)^4\right]^{.65}$$

$$ET = 1. - .8(XNT)^{1.25}$$

$$GET = \left.\frac{\gamma-1}{\gamma}\right)_{TURBINE}$$

$$XWT = AT\left[1 - (PRT)^{BT}\right]^{CT}$$

$$EFFT = 1. - \left[1 - \sqrt{\frac{1-ET}{1-PRT}}\right]^2$$

$$TRT = 1 - EFFT \cdot \left[1 - (PRT)^{GET}\right]$$

The subscript notation used is consistent with that used in figure 10.

APPENDIX II

Digital Portion of Hybrid Simulation

```
// FOR GTSIM
*IOCS(CARD,1403 PRINTER,DISK)
*LIST SCURCE PROGRAM
      INTEGER SFIX
      REAL NG,NGT,NGTL,NGTLM,MU11,MU21,MU12,MU22
      DIMENSION IX(4),F(12),X(4,151),FMAX(12),XSCL(4),FILT(3)
      READ(2,15) NPTS,ION,ICFF
      READ(2,16) P3TLM,T4TLM,NGTLM,FTIME,XSCL(4)
      READ(2,16)(FMAX(I),I=1,12)
      GEC=.283151
      GET=.2536441
      XSCL(1)=0.0
      XSCL(2)=FTIME
      XSCL(3)=0.0
      FILT(1)=.5
      FILT(2)=.625
      FILT(3)=.75
      CALL HINT
      CALL CLR
      CALL RUN
      I=1
      CALL PP
      CALL JCL(0,.T.)
      CALL WAIT(2)
      CALL JCL(0,.F.)
      P3T=AC(0)
      T4T=AC(1)
      NGT=AC(2)
      WFT=AC(3)
      X(1,1)=P3T
      X(2,1)=T4T
      X(3,1)=NGT
      X(4,1)=WFT
      GC TO 4
    2 CALL JCL(1,.T.)
      CALL JCL(1,.F.)
```

```
      CALL RBADX(IX,0,3,1)
      P3T=FLOTS(IX(1))
      T4T=FLOTS(IX(2))
      NGT=FLOTS(IX(3))
      WFT=FLOTS(IX(4))
      I=I+1
      X(1,I)=P3T
      X(2,I)=T4T
      X(3,I)=NGT
      X(4,I)=WFT
      IF(I.EQ.ICN) CALL JCL(5,.T.)
      IF(I.EQ.ICFF) CALL JCL(5,.F.)
      IF(I.EQ.NPTS) GO TO 6
      IF(ABS(P3T-P3TL).LE.P3TLM.AND.ABS(T4T-T4TL).LE.T4TLM.AND.ABS(NGT-N
     1GTL).LE.NGTLM) GO TO 2
4     P3TL=P3T
      T4TL=T4T
      NGTL=NGT
      P3=P3T*16329.6
      T4=T4T*2159.69
      NG=NGT*8000.0
      PRC=P3/2041.2
      PRT=1./PRC
      XNC=NG/7200.0
      XNT=NG/(SQRT(T4)*172.622)
      AC=.75*XNC+.27*XNC*XNC*XNC
      BC=3.*XNC**1.5+3.*XNC**7.
      CC=.0180251*(2.-XNC)**5.794
      DC=.8906561*SQRT(.9-(XNC-.9)*(XNC-.9))
      EC=1.+XNC+3.6*XNC**4.1
      IF(PRC.LE.EC) FC=4.
      IF(PRC.GT.EC) FC=2.
      XWC=AC*(1.-(PRC-1.)/BC)**CC
      EFFC=DC*(1.-((EC-PRC)/(EC-1.))**FC)
      TRC=1.+(PRC**GEC-1.)/EFFC
      AT=1.0006C27
```

```
 BT=3.1+1.62/(XNT+.26)
 CT=.7
 DT=.88*(1.-(1.-XNT)**4.)**.65
 ET=1.-.8*XNT**1.25
 XWT=AT*(1.-PRT**BT)**CT
 EFFT=DT*(1.-(1.-SQRT((1.-ET)/(1.-PRT)))*(1.-SQRT((1.-ET)/(1.-PRT))
1))
 TRT=1.-EFFT*(1.-PRT**GET)
 PHI11=-CC*PRC/(BC+1.-PRC)
 DADNC=.75+.81*XNC*XNC
 DBDNC=4.5*SQRT(XNC)+21.*XNC**6.
 DCDNC=-.1044*(2.-XNC)**4.8
 PHI21=XNC*DADNC/AC+XNC*CC*(PRC-1.)*DBDNC/(BC*(BC+1.-PRC))+XNC*ALOG
1(1.-(PRC-1.)/BC)*DCDNC
 DNDPC=DC*FC*(EC-PRC)**(FC-1.)/(EC-1.)**FC
 PSI11=(PRC/TRC)*(GEC/(EFFC*PRC**(1.-GEC))-(PRC**GEC-1.)*DNDPC/(EFF
1C*EFFC))
 DNDDC=EFFC/DC
 DNDEC=-FC*DC*((EC-PRC)/(EC-1.))**(FC-1.)*(PRC-1.)/((EC-1.)*(EC-1.)
1)
 DCDNC=-DC*(XNC-.9)/(.9-(XNC-.9)*(XNC-.9))
 DEDNC=1.+14.76*XNC**3.1
 DNDNC=DNDDC*DCDNC+DNDEC*DEDNC
 PSI21=-(PRC**GEC-1.)*XNC*DNDNC/(TRC*EFFC*EFFC)
 PHI12=-BT*CT*PRT**BT/(1.-PRT**BT)
 DBDNT=-1.62/((XNT+.26)*(XNT+.26))
 PHI22=-CT*PRT**BT*ALOG(PRT)*XNT*DBDNT/(1.-PRT**BT)
 DNDPT=-DT*(SQRT(1.-PRT)-SQRT(1.-ET))*SQRT(1.-ET)/((1.-PRT)*(1.-PRT
1))
 PSI12=(PRT/TRT)*(EFFT*GET/PRT**(1.-GET)-(1.-PRT**GET)*DNDPT)
 DCDNT=2.288*(1.-XNT)*(1.-XNT)*(1.-XNT)/(1.-(1.-XNT)**4.)**.35
 DEDNT=-XNT**.25
 DNDDT=EFFT/DT
 DNDET=-DT*(1.-SQRT((1.-ET)/(1.-PRT)))/SQRT((1.-ET)*(1.-PRT))
 DNDNT=DNDDT*DCDNT+DNDET*DEDNT
 PSI22=(XNT/TRT)*(PRT**GET-1.)*DNDNT
```

```
      MU11=PHI11+(1./(1.-1./TRC))*PSI11
      MU21=PHI21+(1./(1.-1./TRC))*PSI21-1.
      MU12=PHI12+(1./(1.-1./TRT))*PSI12
      MU22=PHI22+(1./(1.-1./TRT))*PSI22-1.
      WCT=XWC*.8
      TCT=TRC*.2498
      WTT=XWT*P3*.003269/SQRT(T4)
      TET=TRT*T4T
      TQCT=3.026*WCT*(TCT-.2498)/NGT
      TQTT=3.397*WTT*(T4T-TET)/NGT
      F(1)=41.6700*(PHI11*WCT/P3T-(1.-PHI12)*WTT/P3T)/FMAX(1)
      F(2)=41.670*(.5*(1.+PHI22)*WTT/T4T)/FMAX(2)
      F(3)=41.6700*(PHI21*WCT/NGT-PHI22*WTT/NGT)/FMAX(3)
      F(4)=96.8500*((PHI11+PSI11)*WCT*TCT/P3T-(1.-PHI12)*WTT*T4T/P3T)/FM
     1AX(4)
      F(5)=96.8500*.5*(PHI22-1.)*WTT/FMAX(5)
      F(6)=96.8500*((PHI21+PSI21)*WCT*TCT/NGT-PHI22*WTT*T4T/NGT)/FMAX(6)
      F(7)=0.95490*((1.-MU12)*TQTT/P3T-MU11*TQCT/P3T)/FMAX(7)
      F(8)=(-.9549*.5*MU22*TQTT/T4T)/FMAX(8)
      F(9)=0.95490*(MU22*TQTT/NGT-MU21*TQCT/NGT)/FMAX(9)
      F(10)=41.6700*(WCT*(1.-PHI11-PHI21)-WTT*(.5+PHI12-.5*PHI22))/FMAX(
     110)
      F(11)=96.8500*(WCT*TCT*(1.-PHI11-PHI21-PSI11-PSI21)-WTT*T4T*(PHI12
     1-.5-.5*PHI22))/FMAX(11)
      F(12)=0.95490*(TQTT*(MU12-.5*MU22)-TQCT*(1.-MU11-MU21))/FMAX(12)
      DO 75 IF=1,12
      IF1=IF-1
75    CALL HWDAS(IF1,SFIX(F(IF)),IER)
      GO TO 2
6     CALL PC
      LOOK=1
      CALL DATSW(0,JS)
      IF(JS.EQ.1) LOOK=0
      CALL PICTR(X,4,XLAB,XSCL,4,NPTS,0,1,2,-2,FTIME,LOOK)
      PAUSE 1111
      LOOK=1
```

```
      CALL DATSW(0,JS)
      IF(JS.EQ.1) LOOK=0
      IFILT=1
      CALL DATSW(1,JS)
      IF(JS.EQ.1) IFILT=2
      CALL DATSW(2,JS)
      IF(JS.EQ.1) IFILT=3
      DO 7 J=2,NPTS
      X(1,J)=FILT(IFILT)*X(1,J)+(1.-FILT(IFILT))*X(1,J-1)
7     X(2,J)=FILT(IFILT)*X(2,J)+(1.-FILT(IFILT))*X(2,J-1)
      CALL PICTR(X,4,XLAB,XSCL,4,NPTS,0,1,2,-2,FTIME,LOOK)
15    FORMAT(3I5)
16    FORMAT(8F10.5)
      CALL EXIT
      END
// DUP
*DELETE              GTSIM
*STORECI   XWS  UA  GTSIM           1131
// XEQ GTSIM
     C   DATA CARDS
  141    5  200
     C   NPTS, ION, IOFF      NO. OF TIME INTERVALS  NO. OF TIME INTERVALS UNTIL
     C   DISTURBANCE IS TURNED ON  NO. OF TIME INTERVALS UNTIL DISTURBANCE IS
     C   TURNED OFF
.02       .02       .02       14.0      1.0
     C   P3TLM, T4TLM, NGTLM, FTIME, XSCL(4)       P3T LINEAR RANGE  T4T
     C   LINEAR RANGE  NGT LINEAR RANGE  FINAL TIME  MAX. Y VALUE ON PLOT
243.0     35.0      309.0     283.0     54.0      295.0     4.71      .61
5.2       140.0     105.0     1.92
     C   FMAX(I),I=1,12      MAXIMUM VALUES OF COEFFICIENTS, USED TO SCALE DAM'S
// *
// END
```

APPENDIX III

Digital Simulation

```
// FOR
*EXTENDED PRECISION
*LIST SOURCE PROGRAM
      SUBROUTINE EQSIM
      DIMENSION IDATA(8),DATA(4)
      COMMON T,CT,Y(20),F(20),STIME,FTIME,NEWDT,IFWRT,N
      IF(NEWDT.NE.-1) GO TO 2
      DATA(1)=STIME
      DATA(2)=FTIME
      DATA(3)=0.0
      DATA(4)=1.0
      CALL R3TR2(DATA,IDATA,4)
      WRITE(1'7)IDATA
      Y(4)=.48975
      GEC=.283151
      GET=.2536441
      XX2=Y(1)/53.37
      XX1=XX2/Y(2)
      Y(1)=XX1
      Y(2)=XX2
      ICNT=0
      INDEX=10
      GO TO 4
    2 IF(NEWDT.EQ.0) GO TO 1
      ICNT=ICNT+1
      IFWRT=1
      IF(ICNT.NE.INCEX) GO TO 4
      IF(ICNT.EQ.10) DT=.028
      INDEX=INDEX+5
      IFWRT=0
    4 P3=Y(2)*53.37
      T4=Y(2)/Y(1)
      NG=Y(3)
      Y(6)=P3/16329.6
      Y(7)=T4/2159.69
      Y(8)=NG/8000.
```

```
      Y(9)=Y(4)/2.5
      PRC=P3/2041.2
      PRT=1./PRC
      XNC=NG/7200.
      XNT=NG/(SQRT(T4)*172.6221927)
      AC=.75*XNC+.27*XNC*XNC*XNC
      BC=3.*XNC**1.5+3.*XNC**7.
      CC=.0180251*(2.-XNC)**5.794
      DC=.8906561*SQRT(.9-(XNC-.9)*(XNC-.9))
      EC=1.+XNC+3.6*XNC**4.1
      IF(PRC.LE.EC) FC=4.
      IF(PRC.GT.EC) FC=2.
      XWC=AC*(1.-(PRC-1.)/BC)**CC
      EFFC=DC*(1.-((EC-PRC)/(EC-1.))**FC)
      TRC=1.+(PRC**GEC-1.)/EFFC
      AT=1.0006027
      BT=3.1+1.62/(XNT+.26)
      CT=.7
      TT=.88*(1.-(1.-XNT)**4.)**.65
      ET=1.-.8*XNT**1.25
      XWT=AT*(1.-PRT**BT)**CT
      EFFT=TT*(1.-(1.-SQRT((1.-ET)/(1.-PRT)))*(1.-SQRT((1.-ET)/(1.-PRT))
     1))
      TRT=1.-EFFT*(1.-PRT**GET)
      WC=100.*XWC
      TC=539.69*TRC
      WT=.4086772*P3/SQRT(T4)
      TE=T4*TRT
      TQC=1798.31323*WC*(TC-539.69)/NG
      TQT=2011.04077*WT*(T4-TE)/NG
1     F(1)=.05*(WC-WT)
      F(2)=.068370935*(WC*TC+70225.8752*Y(4)-WT*Y(2)/Y(1))
      F(3)=.381971896*(TQT-TQC-9.77632882E-05*Y(3)*Y(3))
      RETURN
      END
// DUP
```

```
*STORE      WS  UA  EQSIM
// XEQ DYSYS
     C   DATA CARDS
 3        14.0       .014       0.0
     C   SYSTEM DEFINITION CARD      N, FTIME, DT, STIME
10206.6    1739.69   7200.
     C   INITIAL CONDITIONS      P3, T4, NG AT  =0
060708
     C   PRINTER CONTROL CARD
                       111             1011
     C   PLOTTER CONTROL CARD

     C   PLOTTER LABEL CARD
// *
// END
```